



Project Title:

Qualifying and **I**mplementing a user-centric designed and **E**fficient **T** electric vehicle

Project Acronym: **QUIET**

GA: **769826**

Topic: **Electric vehicle user-centric design for optimized energy efficiency**

Topic identifier: **GV-05-2017**

Type of action: **RIA Research and Innovation action**

Deliverable No.	QUIET D4.2	
Deliverable Title	Assessment report for enhanced energy efficiency and comfort	
Scheduled Deliverable Date	2019-09	
Actual (granted) Deliverable Date	2020-02 (for preliminary version) For final version: when complete (agreed with the Project Officer)	
Deliverable Type	Report	
Dissemination level	Public	
Written by	Harald Grantner (AVL) Götz Lindenberg / Esther Kieseritzky (RUB) Daniel Habenbacher (ATT) Daniele Basciotti / Hansjörg Kapeller (AIT) Philipp Stegmüller (OBR) Christoph Pucher / Daniel Biernatzki (VEN)	2020-06-19 2020-02-21 2020-02-25 2020-04-17 2020-05-20 2020-05-20
Checked by	Jürgen Roither (AIT) Leo Götz (STS)	2020-06-25 2020-06-25
Approved by	WP Leader (AVL) Coordinator (AIT) Quality Coordinator (HRE-G)	2020-06-02 2020-06-25 2020-07-10
Status	Final version	2020-07-21

This project has received funding from the European Union's Horizon 2020 research and innovation programme under grant agreement No. 769826. The content of this publication is the sole responsibility of the Consortium partners listed herein and does not necessarily represent the view of the European Commission or its services.

D4.2: ASSESSMENT REPORT FOR ENHANCED ENERGY EFFICIENCY AND COMFORT (PU)



Publishable Executive Summary

The objectives of QUIET are to reduce the energy needed for cooling and heating the cabin of an electric vehicle under different driving conditions, by at least 30 % compared to the Honda baseline 2017 and a weight reduction of about 20 % of vehicle components (e.g. doors, windshields, seats, heating and air conditioning) is also addressed. These efforts will finally lead to a minimum of 25 % driving range increase under both hot (+40 °C) and cold (-10 °C) weather conditions.

This is achieved by exploiting the synergies of a technology portfolio in the areas of:

- user centric design with enhanced passenger comfort and safety,
- lightweight materials with enhanced thermal insulation properties, and
- optimized vehicle energy management

The developed technologies will be integrated and qualified in a Honda B-segment electric vehicle validator.

Among these, a novel refrigerant for cooling, combined with an energy-saving heat pump operation for heating, advanced thermal storages based on phase change materials and powerfilms for infrared radiative heating of the cabin was developed and will be investigated. This new concept promises a smart and efficient energy supply of the all related powertrain components and the cabin, a fast mode change between heating and cooling with the use of low amounts of refrigerant. All the here mentioned components and the entire thermal management system, which are used in this smart concept are part of work package WP4, the actual status and development parameters are described in the present report D4.2.

Detailed analysis and assessment of the present status of the donator vehicle (Honda FIT EV) and derivation of reasonable options for re-design of the vehicle thermal management system (VTMS) was done as first step. Extensive tests incl. data analysis and assessment were done for the entire vehicle, the passenger compartment and single components like particular heat exchangers, HVAC blower, AC compressor, etc. Additionally, development, layout, design and first simulations of a new HVAC / vehicle thermal management system incl. heat pump, and the choice of suitable components were done. An investigation of the donator vehicle geometrical situation, for later integration of the new VTMS system was performed as well.

Based on the geometrical investigation / packaging assessment, the status evaluation of the donator vehicle and on the results of the system simulation, the AC circuit and the coolant circuits incl. all heat exchangers, valves, hoses etc. were designed, specified and parts were ordered for build-up at the AC system testbed.

Special developed components are necessary for an efficient usage of the alternative refrigerant, which allows to heat up the cabin via an energy-efficient heat pump also for really cold conditions. Within the previous reporting period the special compressor and a special electronic expansion valve (EXV) went through a detailed component testing phase. For the used refrigerant, a special safety / security concept, which is required, were developed. This safety / security concept includes a new and a safe way for the passenger and the environment in case of a security alert.

For storage of heat / energy by means of phase change materials (PCM), and later usage of this heat for e.g. defrosting of the vehicle front end condenser a thermal storage tank is planned for the vehicle set-up. Within the reporting period the extended tests with PCM-aluminium foam composites were done. The gained results are also presented in the present report.

This project has received funding from the European Union's Horizon 2020 research and innovation programme under grant agreement No. 769826. The content of this publication is the sole responsibility of the Consortium partners listed herein and does not necessarily represent the view of the European Commission or its services.

D4.2: ASSESSMENT REPORT FOR ENHANCED ENERGY EFFICIENCY AND COMFORT (PU)



The radiation heating elements and their control units were already designed in the previous reporting period. In the present period they were manufactured and adapted for installation to in the demonstrator vehicle. Currently, the process of covering these elements with fabric material and preparing them for installation in the demonstrator vehicle is going on. So, the influence on overall energy consumption for vehicle heating will be considered and analysed during the planned vehicle tests.

To be able to judge the energy savings and efficiency improvements possible by application of the described measures the system architecture for an efficient energy distribution network was modelled. This was done based on the subsequent simulation models of the different technological approaches. The simulation results and the overall thermal energy distribution concept are presented in the present report.

In the current reporting period, all these newly developed VTMS components were build-up at the AC-System testbed. The workflow was divided into two work packages. The first, so-called “Step-1”, contained only the R290 refrigerant circuit, including all corresponding components. The components implemented in this build-up were refrigerant compressor, condenser, receiver, PRV, EXV, chiller / evaporator, IWT, piping and hoses. For industrial use a refrigerant filter should be included as well. This component was not used here because it was not seen to be necessary for the testbed system. These components were specifically designed or selected for usage with the new refrigerant R290 (Propane). The build-up, instrumentation and commissioning for Step-1 were done. The measurements were performed, and the corresponding results are depicted in the present report.

The system for “Step-2” included the complete Step-1 build-up and additionally all the coolant circuits incl. pumps, switching valves, radiators, fan, HVAC unit, piping etc. It was build-up, instrumented and commissioned as well. To test its thermal behaviour and energy efficiency was the second measurement campaign after Step-1. The aim of these measurements was to prove the new systems ability to improve the overall system efficiency with alternative refrigerant. The measurements were done, corresponding results and findings are depicted in the present report.

This project has received funding from the European Union’s Horizon 2020 research and innovation programme under grant agreement No. 769826. The content of this publication is the sole responsibility of the Consortium partners listed herein and does not necessarily represent the view of the European Commission or its services.



Table of Contents

Abbreviations and Nomenclature	9
1. Introduction.....	10
1.1. Description of the deliverable -- Goals	11
2. Powerfilms for infrared radiative and convective heating (ATT).....	12
2.1. PMV- Index.....	12
2.2. Local Comfort Index	13
2.3. Zhang Thermal Sensation Index	13
2.4. Energy consumption of powerfilms	14
2.5. Heating system efficiency	14
2.6. Production of heating foils.....	15
2.7. Application of heating foils on GFRP parts.....	17
2.8. ECU.....	24
2.8.1. DC/DC – converter modules	24
2.8.2. Auxiliary power supply	26
2.8.3. Control unit arrangement.....	27
3. Thermal storage tank using PCM (RUB/IFAM)	28
3.1. Specifications for PCM thermal storage tank:	28
3.2. Challenge:	28
3.3. Status:.....	28
3.4. Technological Implementation.....	31
3.5. Conclusions on thermal storage tank	31
4. Thermal management network - energy distribution – simulation (AIT).....	32
4.1. Introduction to thermal comfort assessment	32
4.2. Thermal comfort evaluations	33
4.2.1. Scenario 1	33
4.2.2. Scenario 2	34
4.2.3. Scenario 3	35
4.2.4. Scenario 4.....	36
4.2.5. Scenario 5.....	37
4.2.6. Scenario 6.....	38
4.2.7. Scenario 7	39
4.3. Use case: energy reduction through heating panels	40
4.4. Conclusions on thermal comfort simulations.....	41
5. Build-up of the R290 refrigerant circuit and the VTMS at the AC system testbed (AVL)	42
5.1. Set-up and measurements of the R290 refrigerant circuit (Step-1).....	42
5.2. Determination of correct amount of refrigerant and oil in the system	44

This project has received funding from the European Union’s Horizon 2020 research and innovation programme under grant agreement No. 769826. The content of this publication is the sole responsibility of the Consortium partners listed herein and does not necessarily represent the view of the European Commission or its services.



5.3. Measurement of reference points to make sure compressor works correctly	45
5.4. Generation of measurement matrix for Step-1	46
5.5. Measurement of air conditioning modes.....	47
5.6. Measurement of heat pump modes	49
5.6.1. Failure of EXV no. 2	49
5.6.2. Failure of compressor no. 1	50
5.6.3. Analysis of oil drained from system after failure of compressor no. 1 (AVL)	52
5.6.4. Failure Analysis of compressor no. 1 (OBR)	54
5.6.5. Failure Analysis of compressor no. 2 (OBR)	55
5.6.6. Compatibility check of materials used in refrigerant circuit	58
5.6.7. Re-commissioning of R290 refrigerant circuit after compressor failures	59
5.6.8. Second failure of EXV no. 2	60
5.6.9. Continuation of heat pump modes measurement	62
6. Set-up, instrumentation and commissioning of the entire VTMS (Step-2) (AVL).....	64
7. Development of control strategy for entire VTMS (AVL).....	67
8. Commissioning of the control board for the entire VTMS (Step-2) on testbed.....	69
9. Measurements of the entire VTMS (Step-2) (AVL).....	70
9.1. Measurements of summer load case	70
9.2. Second failure of compressor no. 2.....	72
9.3. Third failure of EXV no.1	73
9.4. Measurements of winter load case	74
10. Conclusions.....	77
11. Bibliography	79
12. Acknowledgment.....	80

This project has received funding from the European Union’s Horizon 2020 research and innovation programme under grant agreement No. 769826. The content of this publication is the sole responsibility of the Consortium partners listed herein and does not necessarily represent the view of the European Commission or its services.



List of Figures

Figure 1: PMV Index for driver and passenger with and without heating elements13

Figure 2: ISO Local Comfort for driver and passenger with and without heating elements13

Figure 3: Thermal Sensation Index for driver and passenger with and without heating elements14

Figure 4: Power consumption over time14

Figure 5: Efficiency over time.....15

Figure 6: Layer structure of heating foil.....16

Figure 7: Substrate after etching- (left) and screen-printing process (right)17

Figure 8: Infrared picture of sunvisor at 80°C.....24

Figure 9: three DC/DC converters.....25

Figure 10: Heatsink with cooling fans.....25

Figure 11: Infrared image of DC/DC converters in idle state26

Figure 12: 24 VDC auxiliary power supply26

Figure 13: Arrangement of control unit.....27

Figure 14: Arrangement of control unit.....27

Figure 15: Apparatus for measurement of thermal conductivity.....29

Figure 16: Thermal conductivity of the samples delivered to RUB.....29

Figure 17: Measured data of thermal storage (Heat-up / Charging case @ \dot{v} coolant = 1.9 l/min).....30

Figure 18: Measured data of thermal storage (Cool-down / Discharging case @ \dot{v} coolant = 1.9 l/min)..30

Figure 19: Thermal comfort model dependencies and scale32

Figure 20: HMI settings for scenario 1.....34

Figure 21: PMV results for scenario 134

Figure 22: HMI settings for scenario 2.....35

Figure 23: PMV results for scenario 235

Figure 24: HMI settings for scenario 3.....36

Figure 25: PMV results for scenario 336

Figure 26: HMI settings for scenario 4.....37

Figure 27: PMV results for scenario 437

Figure 28: HMI settings for scenario 5.....38

Figure 29: PMV results for scenario 538

Figure 30: HMI settings for scenario 6.....39

Figure 31: PMV results for scenario 639

Figure 32: HMI settings for scenario 7.....40

This project has received funding from the European Union’s Horizon 2020 research and innovation programme under grant agreement No. 769826. The content of this publication is the sole responsibility of the Consortium partners listed herein and does not necessarily represent the view of the European Commission or its services.



Figure 33: PMV results for scenario 7	40
Figure 34: PMV results for the use case.....	41
Figure 35: PMV over time for the use case.....	41
Figure 36: Energy consumption comparison.....	41
Figure 37: Build-up and instrumentation of Step-1 (R290 Micro-AC circuit) at AC system testbed.....	42
Figure 38: Instrumentation of testbed build-up Step-1 (R290 Micro-AC circuit).....	43
Figure 39: WAECO service station for flushing the entire refrigerant circuit	44
Figure 40: Determination of necessary amount of refrigerant for the R290 Micro-AC circuit.....	45
Figure 41: Reference point measurement data	46
Figure 42: Measurement matrix used for step 1 (R290 Micro-AC circuit only).....	47
Figure 43: Measurement results of air conditioning modes for step 1	48
Figure 44: Contamination of EXV no. 2	49
Figure 45: Oil drained from refrigerant circuit after failure of compressor no. 1	51
Figure 46: Contamination of the refrigerant filter after failure of compressor no. 1.....	51
Figure 47: Oil drained from refrigerant circuit after 30 min of operation of compressor no. 2	52
Figure 48: Soot and water content of oil drained from refrigerant circuit.....	52
Figure 49: Material fractions found in oil after failure of compressor no. 1	53
Figure 50: Results of gas-chromatography analysis of oil - excerpt	54
Figure 51: Compressor no. 1 - Bearings after failure	54
Figure 52: Compressor no. 1 - Scrolls after failure	55
Figure 53: Compressor no. 1 – Conclusions on failure reasons	55
Figure 54: Compressor no. 2 – Wear marks at scroll after 30 min operation.....	56
Figure 55: Compressor no. 2 – Indication for external particles at scroll inlet after 30 min operation.....	56
Figure 56: Compressor no. 2 –External particles at scroll inlet after 30 min of operation	57
Figure 57: Refrigerant filter installed before the compressor on testbed	57
Figure 58: Materials used in the R290 micro AC refrigerant circuit of QUIET (Step-1)	59
Figure 59: Reference measurement data for rebuilt compressor no. 2 (Step-1).....	60
Figure 60: 2 nd failure of EXV no. 2 – particles in EXV no. 2	61
Figure 61: 2 nd failure of EXV no. 2 – particles found	61
Figure 62: Comparison of AC measurement point before and after the failures.....	62
Figure 63: Result for different operational conditions in heat pump mode measurements.....	63
Figure 64: COP values achieved during heat pump mode measurements for different operational conditions	63

This project has received funding from the European Union’s Horizon 2020 research and innovation programme under grant agreement No. 769826. The content of this publication is the sole responsibility of the Consortium partners listed herein and does not necessarily represent the view of the European Commission or its services.



Figure 65: Build-up and instrumentation of Step-2 (entire VTMS) at AC system testbed	64
Figure 66: Build-up and instrumentation of Step-2 (entire VTMS) at AC system testbed	65
Figure 67: Instrumentation of testbed build-up for Step-2 (entire VTMS)	66
Figure 68: Control strategy for entire VTMS.....	67
Figure 69: Boundary conditions for control strategy of entire VTMS	68
Figure 70: Commissioning of control board for entire VTMS at AC system testbed	69
Figure 71: Control board for entire VTMS	69
Figure 72: Exemplary results of Step-2 summer case measurements (S_WP1 to S_WP3)	71
Figure 73: Exemplary results of Step-2 summer case measurements (S_WP4 to S_WP6)	71
Figure 74: Damage of compressor no. 2 (Source OBR).....	73
Figure 75: Exemplary results of Step-2 winter case measurements (W_WP1 to W_WP3).....	75
Figure 76: Exemplary results of Step-2 winter case measurements (W_WP4 to W_WP6).....	75

List of Tables

Table 1: List of Abbreviations and Nomenclature.....	9
Table 2: Layer structure, materials and thickness.....	17
Table 3: Applied heating foils and infrared pictures	18
Table 4: Thermal comfort scale based on the predicted mean vote index.....	32
Table 5: PMV Index factors overview.....	33
Table 6: HVAC System settings, Scenario 1	33
Table 7: HVAC System settings, Scenario 2.....	34
Table 8: HVAC System settings, Scenario 3.....	35
Table 9: HVAC System settings, Scenario 4.....	36
Table 10: HVAC System settings, Scenario 5.....	37
Table 11: HVAC System settings, Scenario 6.....	38
Table 12: HVAC System settings, Scenario 7.....	39
Table 13: Summer load case, boundary conditions	70
Table 14: Parameters gained from summer case measurement.....	71
Table 15: Winter load case, boundary conditions	74
Table 16: Parameters gained from winter case measurement.....	75

This project has received funding from the European Union’s Horizon 2020 research and innovation programme under grant agreement No. 769826. The content of this publication is the sole responsibility of the Consortium partners listed herein and does not necessarily represent the view of the European Commission or its services.



Abbreviations and Nomenclature

Table 1: List of Abbreviations and Nomenclature.

Symbol or Shortname	Description
EV	Electric Vehicle
WP	Work Package
HVAC	Heating, Ventilation and Air Conditioning
GFRP	glass-fibre reinforced plastic
RHS	Radiation Heating System
CU	Control unit
PCM	Phase Change Material
PMV	Predicted Mean Vote
HMI	Human Machine Interface
EXV	Electric Expansion Valve
PRV	Pressure Relief Valve
IWT	Internal Heat Exchanger
VTMS	Vehicle Thermal Management System
Coriolis	Measurement device for mass flow (refrigerant / oil mixture) in the AC circuit
OCR	Measurement device for oil concentration rate in the AC circuit
COP	Coefficient of Performance
EER	Energy Efficiency Ratio

This project has received funding from the European Union's Horizon 2020 research and innovation programme under grant agreement No. 769826. The content of this publication is the sole responsibility of the Consortium partners listed herein and does not necessarily represent the view of the European Commission or its services.

D4.2: ASSESSMENT REPORT FOR ENHANCED ENERGY EFFICIENCY AND COMFORT (PU)



1. Introduction

The objectives of QUIET are to reduce the energy needed for cooling and heating the cabin of an electric vehicle under different driving conditions, by at least 30 % compared to the Honda baseline 2017 and a weight reduction of about 20 % of vehicle components (e.g. doors, windshields, seats, heating and air conditioning) is also addressed. These efforts will finally lead to a minimum of 25 % driving range increase under both hot (+40 °C) and cold (-10 °C) weather conditions.

This is achieved by exploiting the synergies of a technology portfolio in the areas of:

- user centric design with enhanced passenger comfort and safety,
- lightweight materials with enhanced thermal insulation properties, and
- optimized vehicle energy management

The developed technologies will be integrated and qualified in a Honda B-segment electric vehicle validator.

Among these, a novel refrigerant for cooling, combined with an energy-saving heat pump operation for heating, advanced thermal storages based on phase change materials and *powerfilms* for infrared radiative heating of the cabin was developed and will be investigated. This new concept promises a smart and efficient energy supply of the all related powertrain components and the cabin, a fast mode change between heating and cooling with the use of low amounts of refrigerant. All the here mentioned components and the entire thermal management system, which are used in this smart concept are part of work package WP4, the actual status and development parameters are described in the present report D4.2.

Detailed analysis and assessment of the present status of the donator vehicle (Honda FIT EV) and derivation of reasonable options for re-design of the vehicle thermal management system (VTMS) was done as first step. Extensive tests incl. data analysis and assessment were done for the entire vehicle, the passenger compartment and single components like particular heat exchangers, HVAC blower, AC compressor, etc. Additionally, development, layout, design and first simulations of a new HVAC / vehicle thermal management system incl. heat pump, and the choice of suitable components were done. An investigation of the donator vehicle geometrical situation, for later integration of the new VTMS system was performed as well.

Based on the geometrical investigation / packaging assessment, the status evaluation of the donator vehicle and on the results of the system simulation, the AC circuit and the coolant circuits incl. all heat exchangers, valves, hoses etc. were designed, specified and parts were ordered for build-up at the AC system testbed.

Specially developed components are necessary for an efficient usage of the alternative refrigerant, which allows to heat up the cabin via an energy-efficient heat pump also for really cold conditions. Within the previous reporting period the special compressor and a special electronic expansion valve (EXV) went through a detailed component testing phase. For the used refrigerant, a special safety / security concept, which is required, were developed. This safety / security concept includes a new and a safe way for the passenger and the environment in case of a security alert.

For storage of heat / energy by means of phase change materials (PCM), and later usage of this heat for e.g. defrosting of the vehicle front end condenser a thermal storage tank is planned for the vehicle set-up. Within the reporting period the extended tests with PCM-aluminium foam composites were done. The gained results are also presented in the present report.

This project has received funding from the European Union's Horizon 2020 research and innovation programme under grant agreement No. 769826. The content of this publication is the sole responsibility of the Consortium partners listed herein and does not necessarily represent the view of the European Commission or its services.

D4.2: ASSESSMENT REPORT FOR ENHANCED ENERGY EFFICIENCY AND COMFORT (PU)



The radiation heating elements and their control units were already designed in the previous reporting period. In the present period they were manufactured and adapted to the conditions present in the demonstrator vehicle. Currently, the process of covering these elements with fabric material and preparing them for installation in the demonstrator vehicle is going on. The control units were developed and produced. Currently they are prepared to be built into the demonstrator vehicle as soon as the radiation elements are ready for installation. So their influence on overall energy consumption for vehicle heating will be considered and analysed during the planned vehicle tests.

To be able to judge the energy savings and efficiency improvements possible by application of the described measures the system architecture for an efficient energy distribution network was modelled. This was done based on the simulation models of the different technological approaches. The simulation results and the overall thermal energy distribution concept are presented in the present report.

In the present reporting period, all these newly developed VTMS components were build-up at the AC-System testbed. The workflow was divided into two steps. Step-1 contained just the pure refrigerant circuit and all the included components. The components implemented in this build-up were refrigerant compressor, condenser, receiver, PRV, EXV, chiller / evaporator, IWT, piping and hoses. For industrial use a refrigerant filter should be included as well. This component was not used here because it was not seen to be necessary for the testbed system. These components were specifically designed or selected for usage with the new refrigerant R290 (Propane).

The system for Step-2 included all the coolant circuits incl. pumps, switching valves, thermal storage, radiators, fan, HVAC unit, piping etc. It was build-up, instrumented and commissioned as well. Testing its thermal behaviour and energy efficiency was the second measurement and analysis campaign after Step-1. The aim of these measurements was to proof the new systems ability to improve the overall system efficiency with alternative refrigerant.

1.1. Description of the deliverable -- Goals

The deliverable deals with the system simulation results and measured data of the newly developed VTMS. It shows the proposed energy distribution and the savings derived from energy distribution network simulations, as well as the efficiency of the entire VTMS, which was proved at the AC system testbed. It is associated with task: T4.5. This report describes the measurement set-up, execution and gained results. For energy distribution simulations the model and the derived results are presented as well.

This project has received funding from the European Union's Horizon 2020 research and innovation programme under grant agreement No. 769826. The content of this publication is the sole responsibility of the Consortium partners listed herein and does not necessarily represent the view of the European Commission or its services.



2. Powerfilms for infrared radiative and convective heating (ATT)

The ATT related part in this project is the development of an energy saving interior heating concept that supports the other heating components (heat pump etc.). Here, radiative heating elements should be placed inside the vehicle on suitable interior parts to obtain the same level of comfort while convective heating power is reduced.

The radiation heating elements and their control units were already designed in the previous reporting period. In the present period they were manufactured and adapted to the conditions present in the demonstrator vehicle. Currently the process of covering these heating elements with fabric material and preparing them for installation in the demonstrator vehicle is going on. The control unit development was finished and the units themselves were produced. Currently they are prepared to be built into the demonstrator vehicle as soon as the radiation elements are ready for installation. Therefore, the influence of these heating elements on overall energy consumption for vehicle heating will be considered and analysed during the planned vehicle tests.

A simulation on passenger comfort and energy efficiency for the radiation heating elements was already presented in the previous deliverable D4.1. A short repetition of the results is given in Figure 1 to Figure 5. For detailed information on used boundary conditions, model settings, analysis approaches and further results please refer to deliverable D4.1.

2.1. PMV- Index

The first simulated value is the PMV-Index [1] for both, driver and passenger with and without radiant heating system. The PMV, i.e. Predicted mean vote Index, is a global Index referring to the whole body. Following numbers describe the PMV – Index:

- +3 hot
- +2 warm
- +1 slightly warm
- 0 neutral
- -1 slightly cool
- -2 cool
- -3 cold

The PMV target value is 0 which means enjoyable. The graph for the PMV Index is depicted in Figure 1. The simulation with the Powerfilm reaches the target value faster than the one without heating elements.

This project has received funding from the European Union's Horizon 2020 research and innovation programme under grant agreement No. 769826. The content of this publication is the sole responsibility of the Consortium partners listed herein and does not necessarily represent the view of the European Commission or its services.

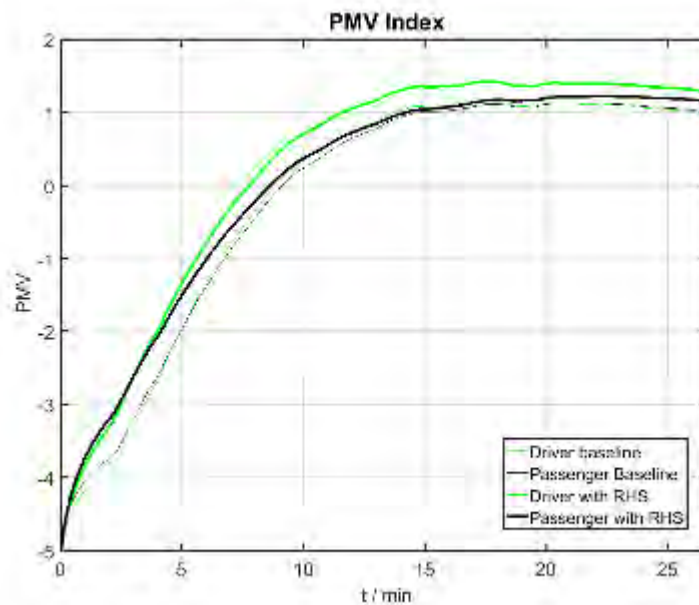


Figure 1: PMV Index for driver and passenger with and without heating elements

2.2. Local Comfort Index

The Local Comfort Index [1] is like the PMV a global index. The target value is 3, which means neutral. In Figure 2 the ISO Local Comfort is displayed. The simulation with the radiant heating system reaches the neutral level faster than the one without.

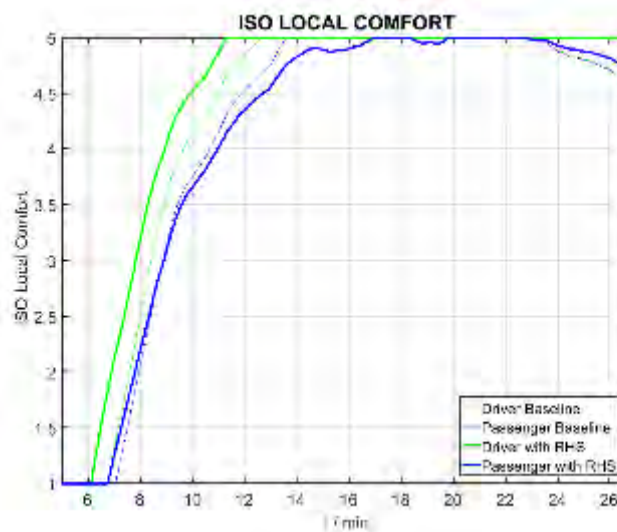


Figure 2: ISO Local Comfort for driver and passenger with and without heating elements

2.3. Zhang Thermal Sensation Index

Zhang’s local thermal comfort prediction is based on a huge number of human climate chamber tests at the University of Berkley, California. Based on regression analysis Hui Zhang developed in [2] a powerful mathematical framework for the prediction of the local thermal sensation and comfort.

This project has received funding from the European Union’s Horizon 2020 research and innovation programme under grant agreement No. 769826. The content of this publication is the sole responsibility of the Consortium partners listed herein and does not necessarily represent the view of the European Commission or its services.

In Figure 3 the Zhang Thermal Sensation Index is displayed. The target value is 0. There cannot be seen any bigger differences between the versions.

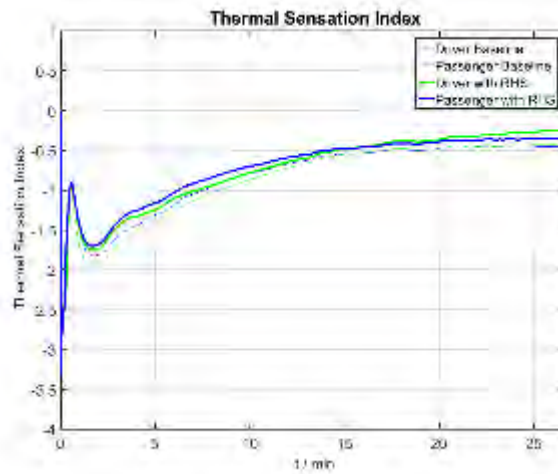


Figure 3: Thermal Sensation Index for driver and passenger with and without heating elements

2.4. Energy consumption of powerfilms

In Figure 4 the energy consumption of the baseline and the RHS is displayed. After 10 minutes the RHS has an energetical advantage. The energy calculation is given in (1)

$$E_x(t) = \int_0^t P_x(\tau) d\tau \tag{1}$$

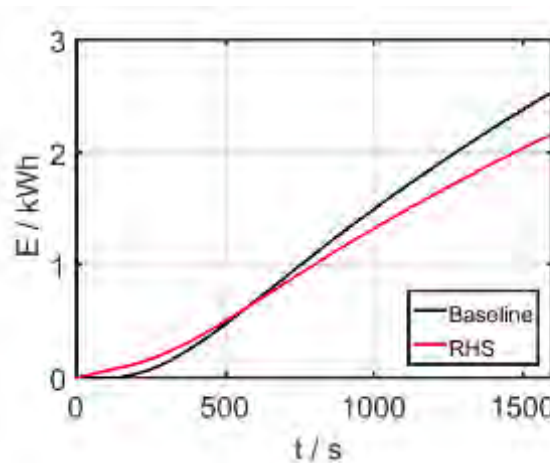


Figure 4: Power consumption over time

2.5. Heating system efficiency

For the efficiency calculation the inlet energy as well as the outlet energy are considered, since these quantities are time dependent also the efficiency is time dependent. Especially in the first 10 minutes the gap in efficiency

This project has received funding from the European Union's Horizon 2020 research and innovation programme under grant agreement No. 769826. The content of this publication is the sole responsibility of the Consortium partners listed herein and does not necessarily represent the view of the European Commission or its services.

is big, after this time the gap stays constant, the efficiency of the RHS is always better than the conventional heating system. The time dependent efficiencies can be seen in Figure 5, the calculation of the efficiency is given in (2).

$$\eta = \frac{E_{IN} - E_{OUT}}{E_{IN}} \quad (2)$$

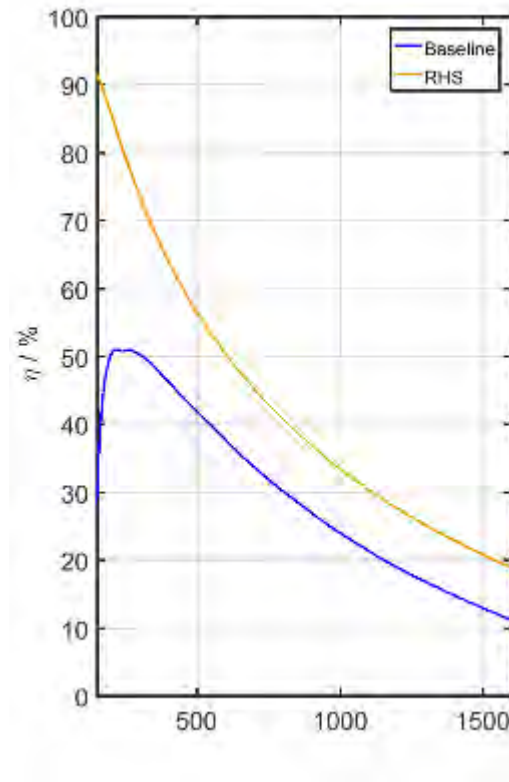


Figure 5: Efficiency over time

As a conclusion to these simulations it can be said that the application of radiation heating elements inside the passenger compartment will support the passenger comfort by at the same time leading to energy savings after approx. 10 minutes. Whereby the efficiency of this heating system is always better than of a standard heating system.

2.6. Production of heating foils

The layer structure of a heating foil is shown in Figure 6. Polyimid (PI) with a thickness of 25 μm is used as substrate. This material is not only stable at high temperatures, with this low thickness it is also very flexible. The substrate is produced via a double-sided etching process, where the copper is reduced on the area between the electrodes. The carbon ink is applied on the substrate and electrodes through a screen-printing process. For

This project has received funding from the European Union's Horizon 2020 research and innovation programme under grant agreement No. 769826. The content of this publication is the sole responsibility of the Consortium partners listed herein and does not necessarily represent the view of the European Commission or its services.

the protection of the carbon ink on the top side, a thermal curing protective coating is also applied through a screen-printing process. With a special adhesive, the heating foils can be attached easily on the desired interior parts.

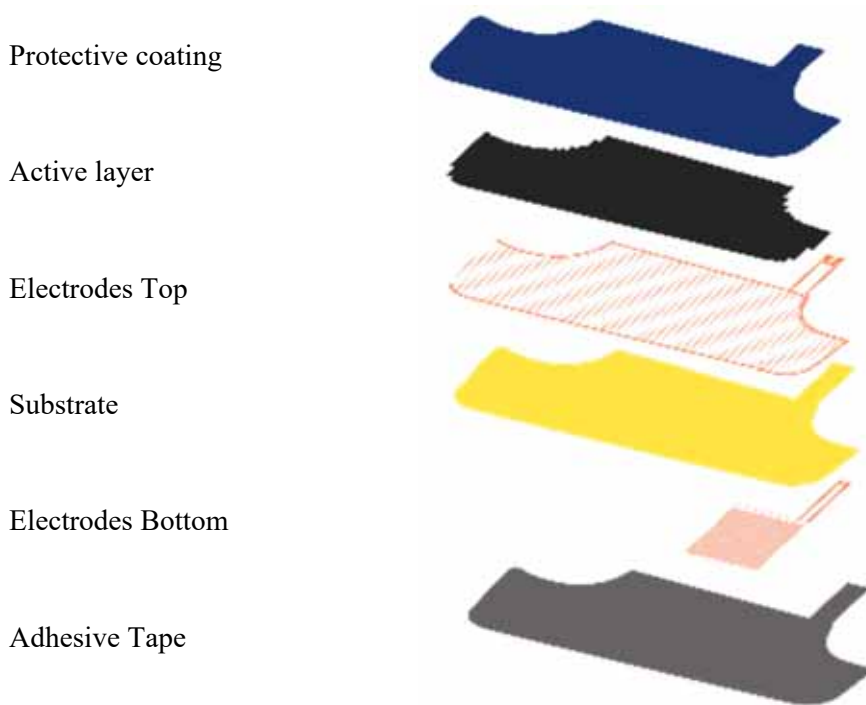


Figure 6: Layer structure of heating foil



Figure 7: Substrate after etching- (left) and screen-printing process (right)

Table 2: Layer structure, materials and thickness

2.7. Application of heating foils on GFRP parts

The produced heating foils are attached on 3D GFRP (glass-fibre reinforced plastic) parts. The GFRP parts get


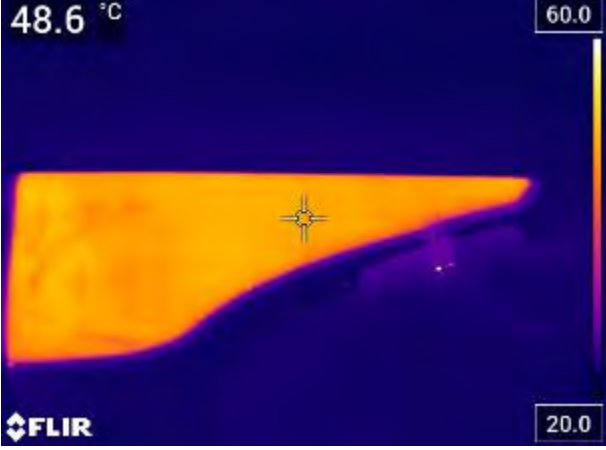

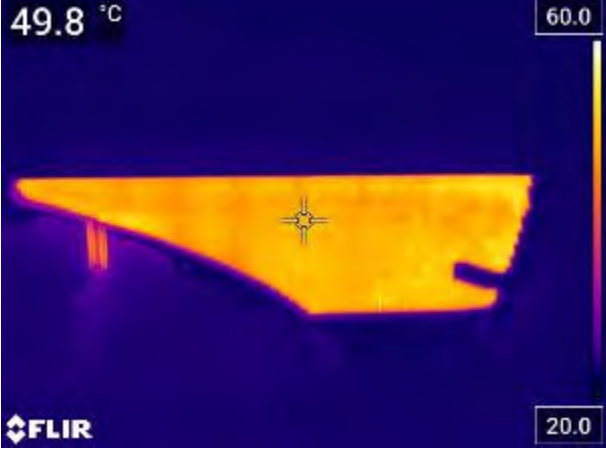
Layer	Material	Thickness [μm]
Protective Coating	Thermic curing, solvent based lacquer	6
Active Layer	Carbon ink	8
Electrodes Top	Copper (etched)	18
Substrate	Polyimid (PI)	25
Electrodes Bottom	Copper (etched)	18
Adhesive Tape	Fleece with double-sided polyacrylate adhesive	160

fully covered by a fabric.

In Table 3 the applied heating foils on the GFRP parts as well as infrared pictures, are shown. Here, a supply voltage of 48 V was applied until the heating foils had a temperature between 45 and 60°C.

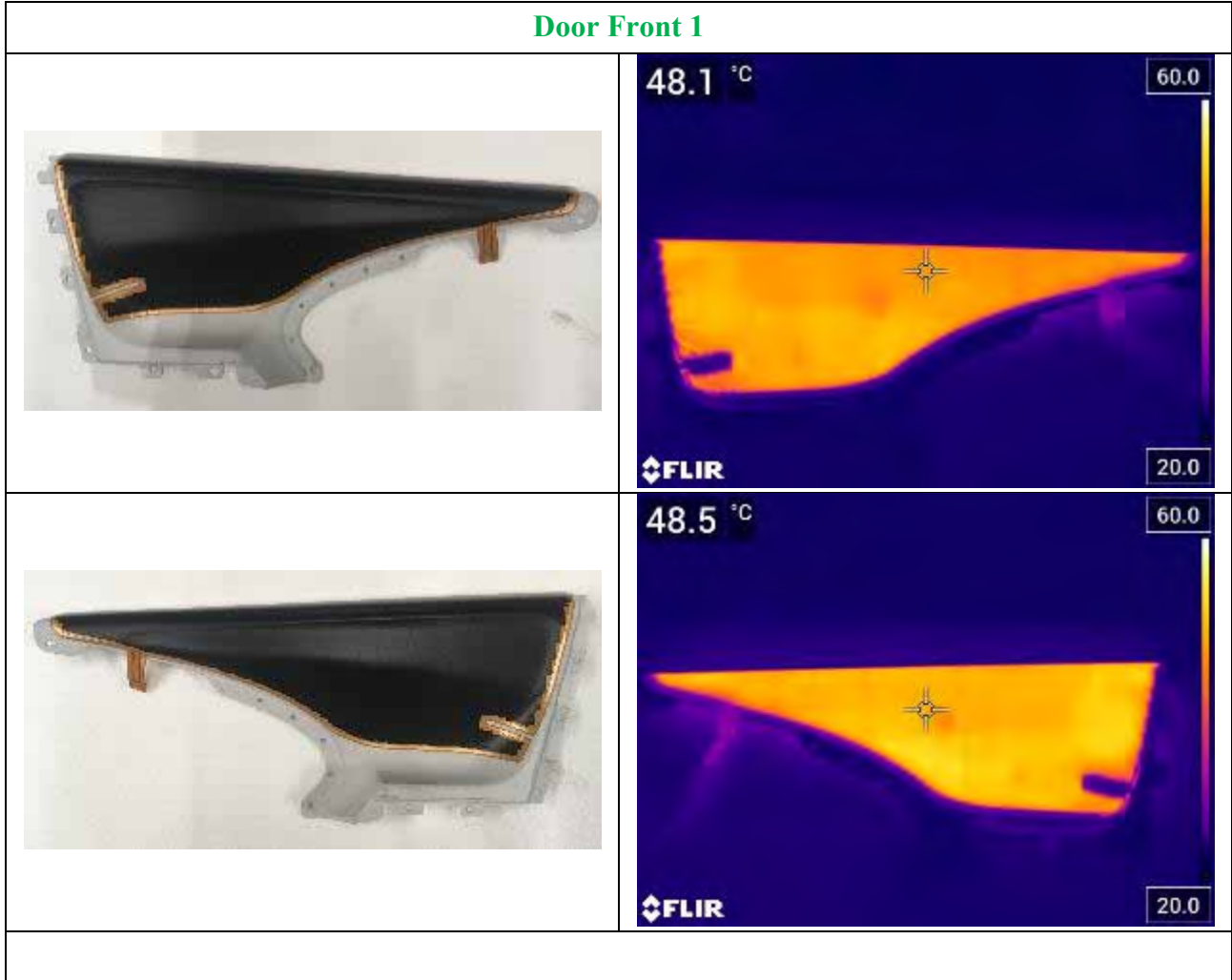
This project has received funding from the European Union’s Horizon 2020 research and innovation programme under grant agreement No. 769826. The content of this publication is the sole responsibility of the Consortium partners listed herein and does not necessarily represent the view of the European Commission or its services.

Table 3: Applied heating foils and infrared pictures

Applied heating foil	Infrared picture
Door Back 1	
	
	

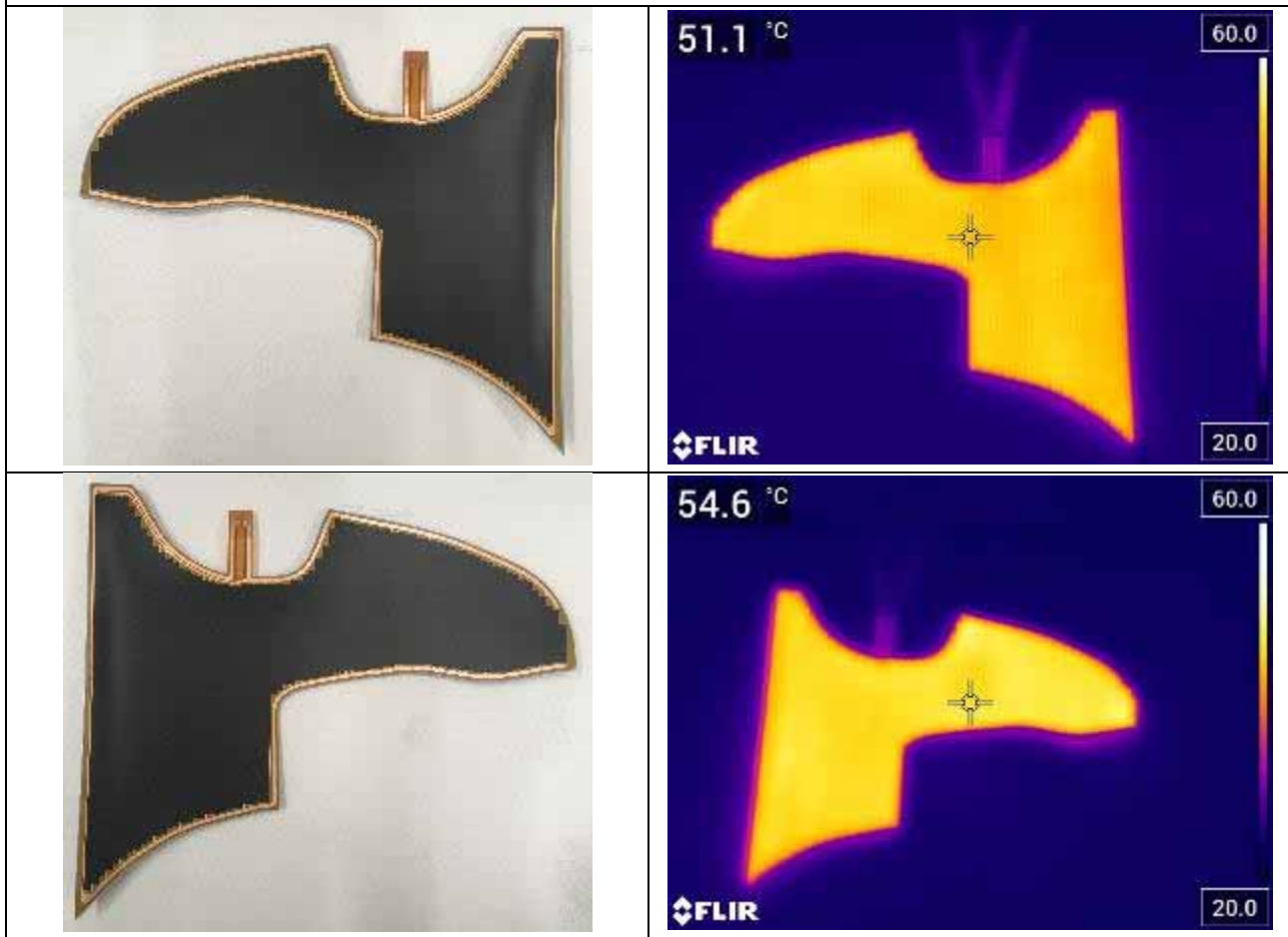
This project has received funding from the European Union’s Horizon 2020 research and innovation programme under grant agreement No. 769826. The content of this publication is the sole responsibility of the Consortium partners listed herein and does not necessarily represent the view of the European Commission or its services.

Door Front 1



This project has received funding from the European Union's Horizon 2020 research and innovation programme under grant agreement No. 769826. The content of this publication is the sole responsibility of the Consortium partners listed herein and does not necessarily represent the view of the European Commission or its services.

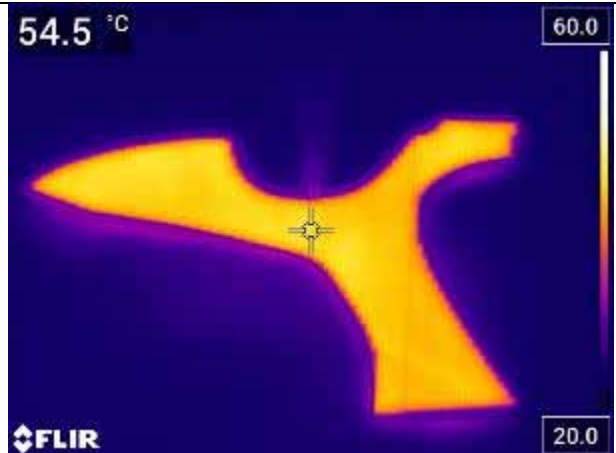
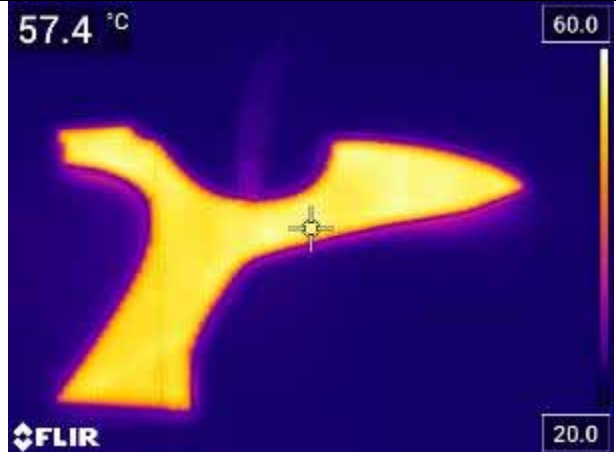
Door Back 2



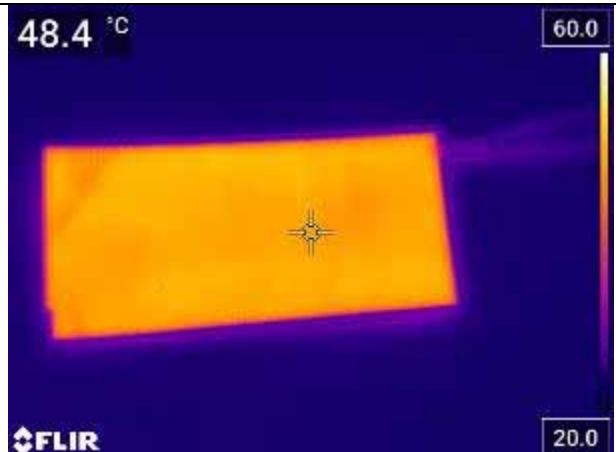
This project has received funding from the European Union's Horizon 2020 research and innovation programme under grant agreement No. 769826. The content of this publication is the sole responsibility of the Consortium partners listed herein and does not necessarily represent the view of the European Commission or its services.

D4.2: ASSESSMENT REPORT FOR ENHANCED ENERGY EFFICIENCY AND COMFORT (PU)

Door Front 2

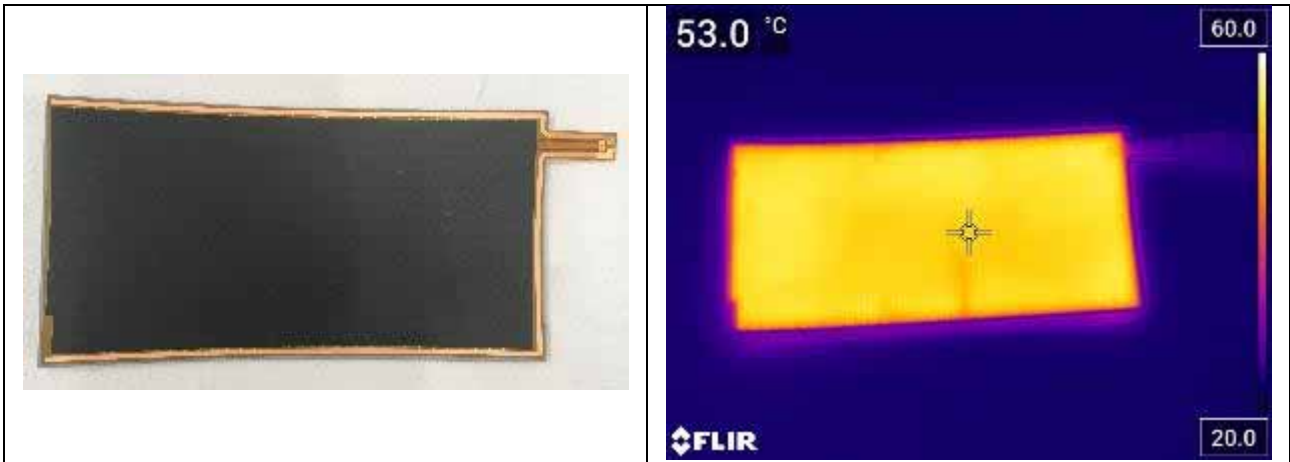


Roof Back

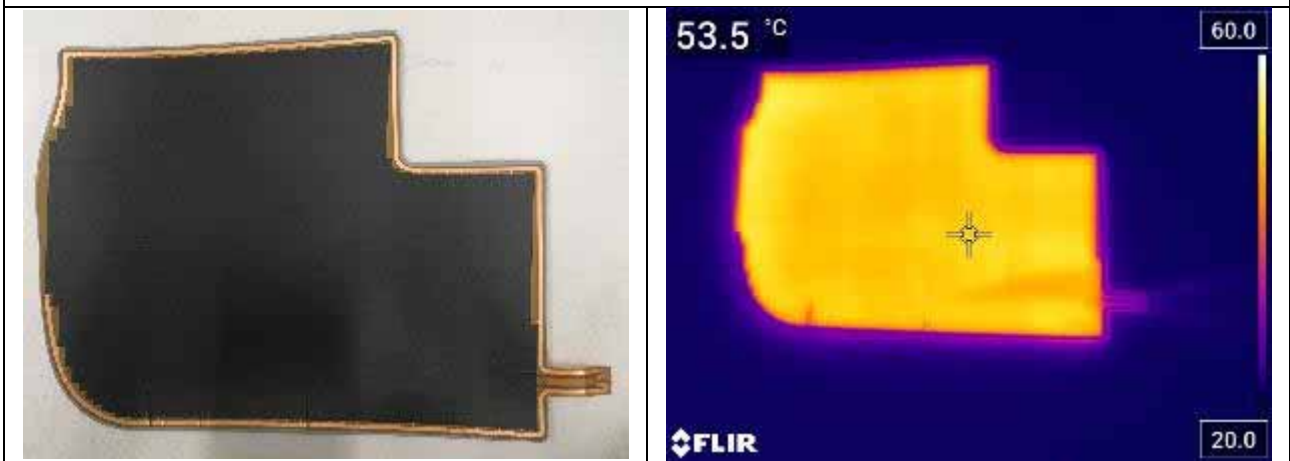


This project has received funding from the European Union's Horizon 2020 research and innovation programme under grant agreement No. 769826. The content of this publication is the sole responsibility of the Consortium partners listed herein and does not necessarily represent the view of the European Commission or its services.

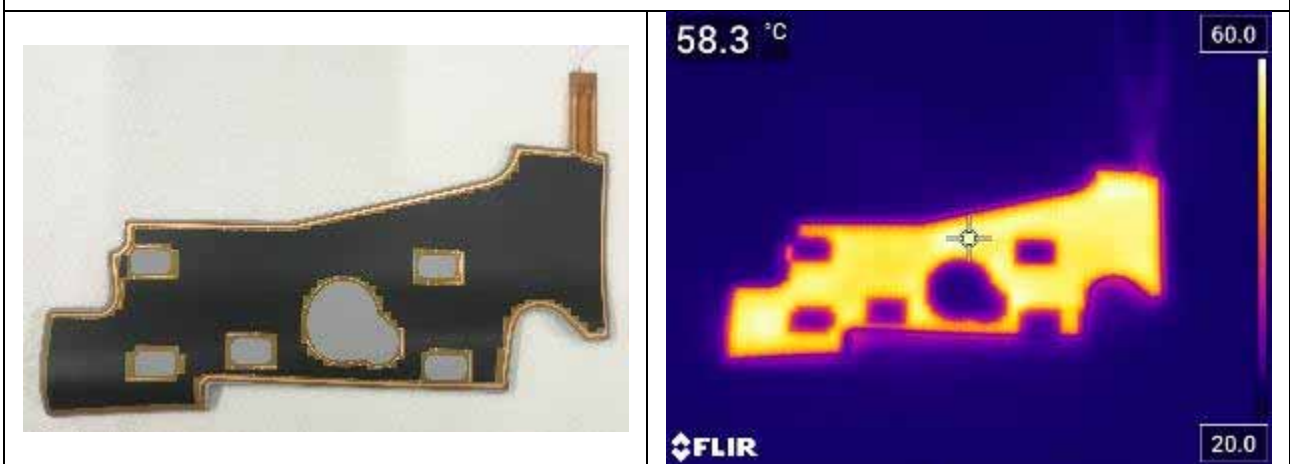
D4.2: ASSESSMENT REPORT FOR ENHANCED ENERGY EFFICIENCY AND COMFORT (PU)



Roof Front

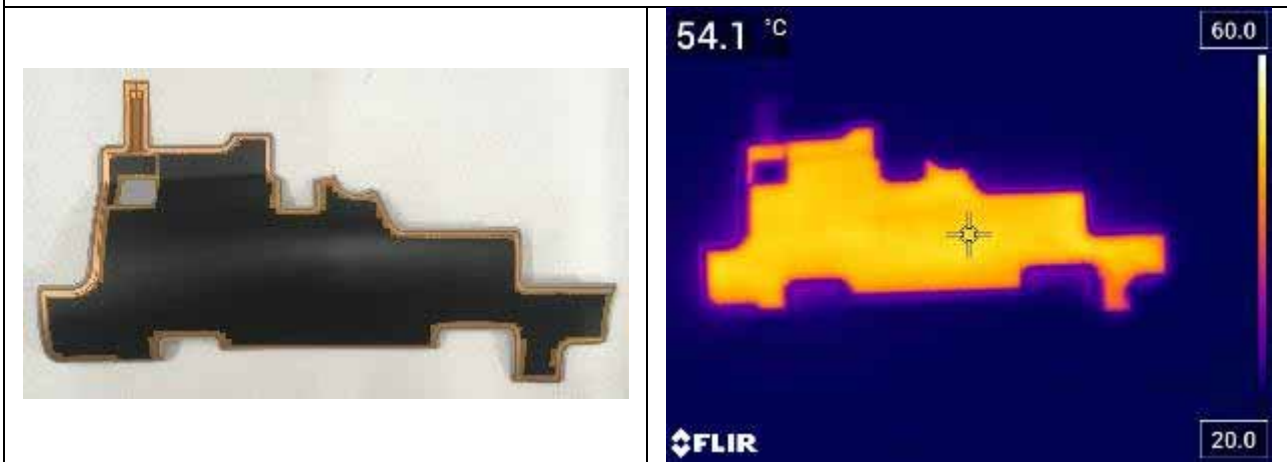


Footwell Driver

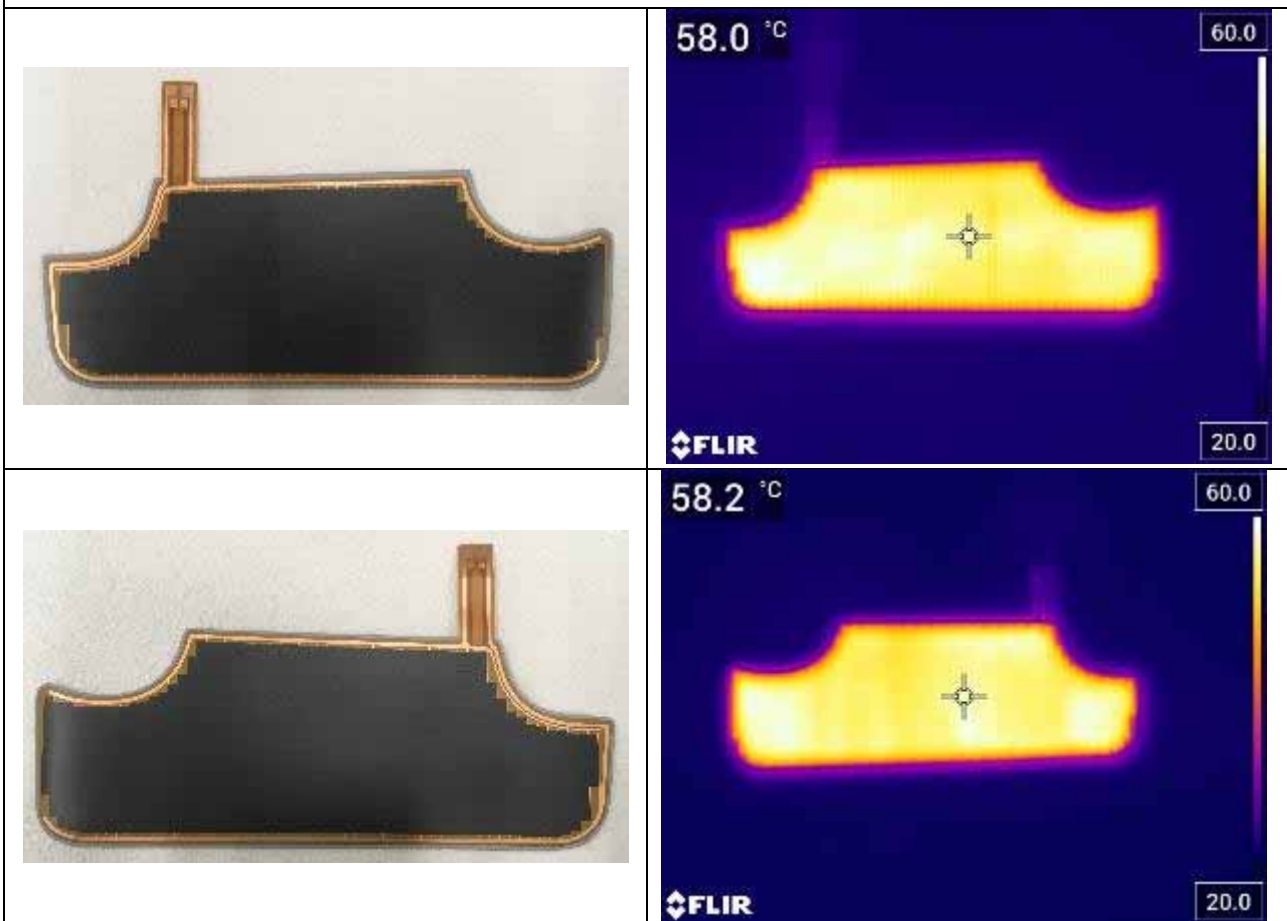


This project has received funding from the European Union's Horizon 2020 research and innovation programme under grant agreement No. 769826. The content of this publication is the sole responsibility of the Consortium partners listed herein and does not necessarily represent the view of the European Commission or its services.

Footwell Passenger



Sunvisor



Since the sunvisor has the biggest distance between heating foil and user, the temperature of this heating foil will be higher than the others. Therefore, it was tested at higher temperatures. This is shown in Figure 8. It can be seen that the temperature distribution is homogeneous over the whole area.

This project has received funding from the European Union's Horizon 2020 research and innovation programme under grant agreement No. 769826. The content of this publication is the sole responsibility of the Consortium partners listed herein and does not necessarily represent the view of the European Commission or its services.

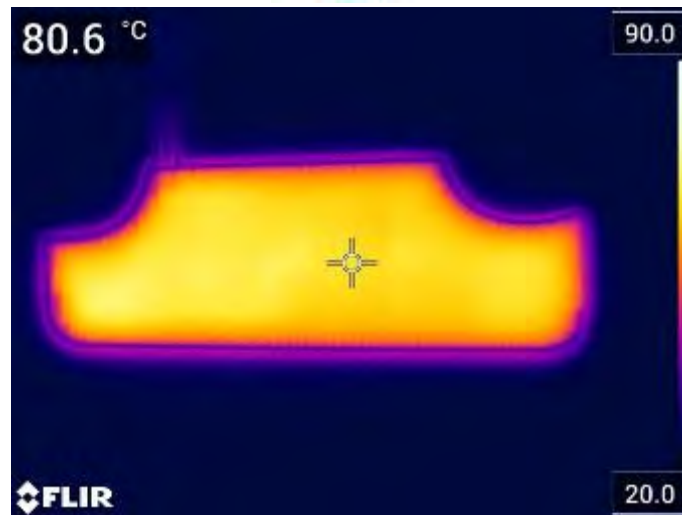


Figure 8: Infrared picture of sunvisor at 80°C

2.8. ECU

2.8.1.DC/DC – converter modules

There are three independent DC/DC- converter modules used. Each module has the following characteristics:

- Maximum output power: 750 W
- Output Voltage: 48 V
- Maximum output current: 15,6 A
- Minimum Input current: 200 VDC
- Maximum Input current: 400 VDC
- Maximum Input current: 4,5 A
- Converter module: QHL750300S48
- Efficiency: 90%

At the core of each DC/DC converter board is a QHL750 – series DC/DC converter module. It offers high efficiency and sophisticated safety features, such as overcurrent and overtemperature protection.

Each of the three DC/DC – converter modules, supplies up to three power modules. Each power module has two independent output channels. Therefore, each DC/DC converter is used to supply up to six heating foils.



Figure 9: three DC/DC converters

To dissipate the waste heat generated by the DC/DC converters, the modules themselves are mounted onto a 3 mm steel mounting plate of the used electrical cabinet. To increase thermal performance, a thermal conductive paste is used. In addition, a heatsink, including a cooling fan, is placed onto each power module to improve its thermal performance even more.



Figure 10: Heatsink with cooling fans

This project has received funding from the European Union’s Horizon 2020 research and innovation programme under grant agreement No. 769826. The content of this publication is the sole responsibility of the Consortium partners listed herein and does not necessarily represent the view of the European Commission or its services.



Figure 11: Infrared image of DC/DC converters in idle state

In the above thermal image, the heating of the DC/DC converter modules in idle state can be observed. This image is taken without the heatsinks and the cooling fan attached. An adequate test with maximum power output must be made.

2.8.2. Auxiliary power supply

A 24 VDC auxiliary power supply is needed to supply the digital circuitry and the cooling fans with power. It can be seen in the middle of the picture. On the right side, the housing for the control circuitry for the three cooling fans of the DC/DC converter can be seen.



Figure 12: 24 VDC auxiliary power supply

2.8.3. Control unit arrangement

The arrangement of the control unit (CU) is shown in Figure 13. It can be seen that the CU is divided into three sections. Each section contains two or three power boards, which are those PCBs with the yellow connectors on top of them.

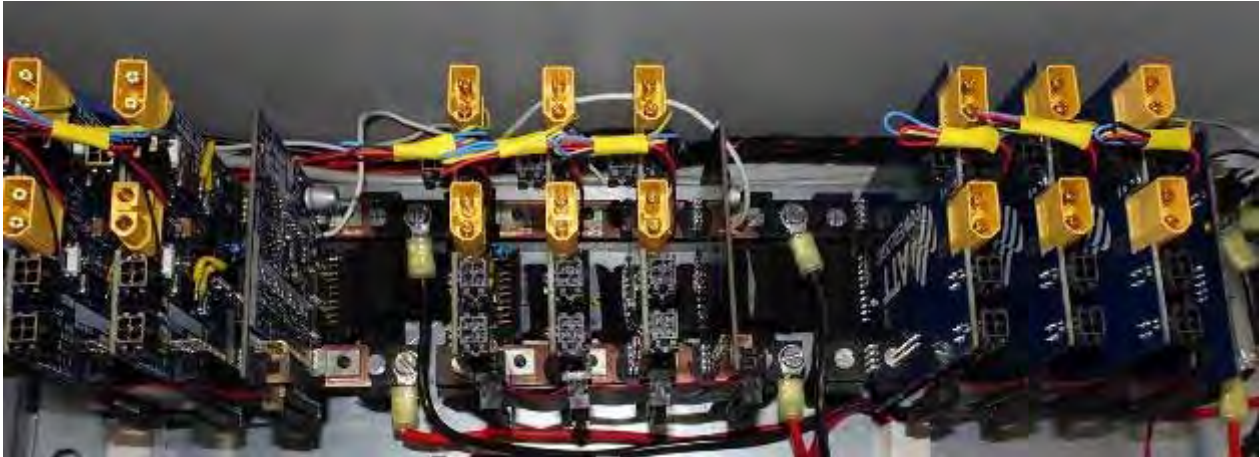


Figure 13: Arrangement of control unit

Each section also has a sensor – frontend board which connects to the power boards using ribbon cable. The connectors for the sensors are therefore located on the power board.

All the board of the CU are securely bolted onto copper busbars (Figure 14), which also function as the power delivery system. The system voltage is 48 VDC.

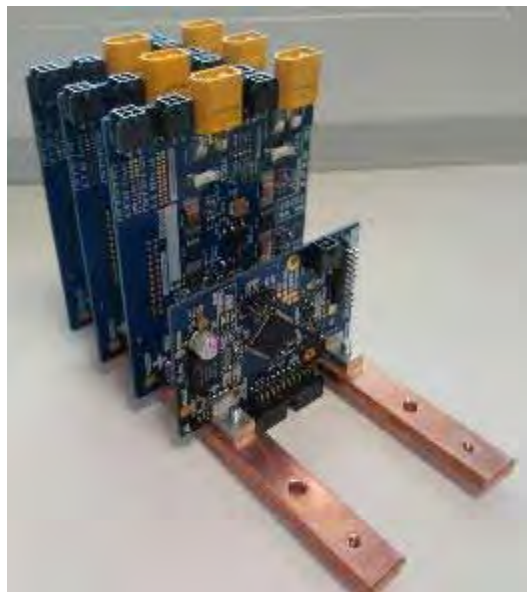


Figure 14: Arrangement of control unit

This project has received funding from the European Union's Horizon 2020 research and innovation programme under grant agreement No. 769826. The content of this publication is the sole responsibility of the Consortium partners listed herein and does not necessarily represent the view of the European Commission or its services.



3. Thermal storage tank using PCM (RUB/IFAM)

The thermal storage was built by RUB based on Al-foam provided by IFAM as carrier matrix for the PCM. The part will be implemented into the demonstrator vehicle to be tested onto its ability to store and emit the desired heat. IFAM / RUB did approval testbed measurements before the part was handed over to AVL for implementation into the demonstrator vehicle. The test results look promising (see Figure 17 and Figure 18 for an excerpt), but the final assessment of the potential of this component will be only possible after the tests in the demonstrator vehicle were done.

3.1. Specifications for PCM thermal storage tank:

Around 500W of heat should be dissipated for a time period of 5 minutes (42Wh minimum capacity).

The maximum storage size including insulation is: 490x275x80 mm.

The temperature range of the storage medium has to be between 15°C and 20°C.

3.2. Challenge:

The paraffin-based PCM RT18HC with a latent heat of approx. 230kJ/kg (64Wh/kg) and a narrow melting / solidification range around 18°C is suitable to store 42Wh of heat between 15 and 20°C.

Previous applications for PCM in air- or water-guided heat exchangers allow charging and discharging times between 2h and 8h. The heat transfer rate of these systems is between 0.1 and 0.5W output per Wh heat storage capacity. Due to the specifications of the project, the heat transfer must be increased to 12W per Wh (factor 25-100!).

3.3. Status:

The PCM storage built by RUBITHERM based on Al Foams provided by IFAM as carrier matrix for the PCM reaches unprecedented power to stored energy ratios for PCM storages. In 5 to 10 minutes, specific outputs are achieved for which conventional storage tanks need 2 to 12 hours. A mathematical comparison with a directly mixable water storage tank shows that 4 to 5 times the amount of water would be required.

The storage prototype has been delivered to AVL for implementation into the vehicle. Data of charging/discharging cycles have been provided to AIT for incorporation into the control unit of the HVAC system.

The Al foam were investigated in terms of thermal conductivity by IFAM. To be able to do so, samples of the Al foams were cut from a specimen, they were machined to obtain defined and parallel surfaces and the porosity was determined from sample weight and dimensions. A porosity value of 77.5% was found. The samples were measured three times, in between of the measurements they were completely removed, turned upside down and measured again. This was done to avoid problems with poor thermal contact. The used apparatus and the resulting thermal conductivity are shown in [Figure 15](#) and [Figure 16](#).

This project has received funding from the European Union's Horizon 2020 research and innovation programme under grant agreement No. 769826. The content of this publication is the sole responsibility of the Consortium partners listed herein and does not necessarily represent the view of the European Commission or its services.

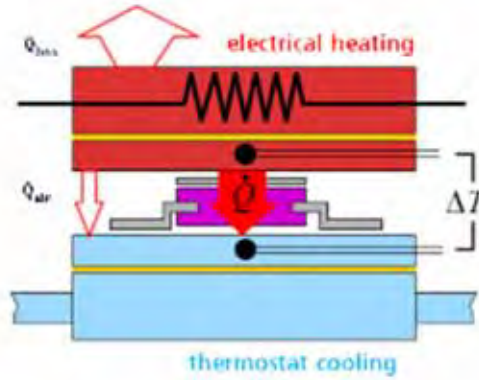
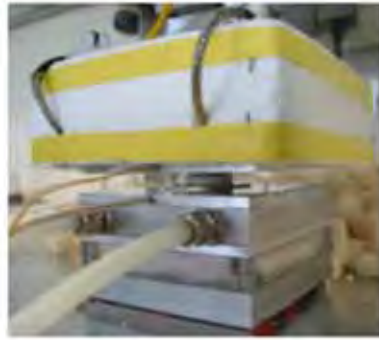


Figure 15: Apparatus for measurement of thermal conductivity

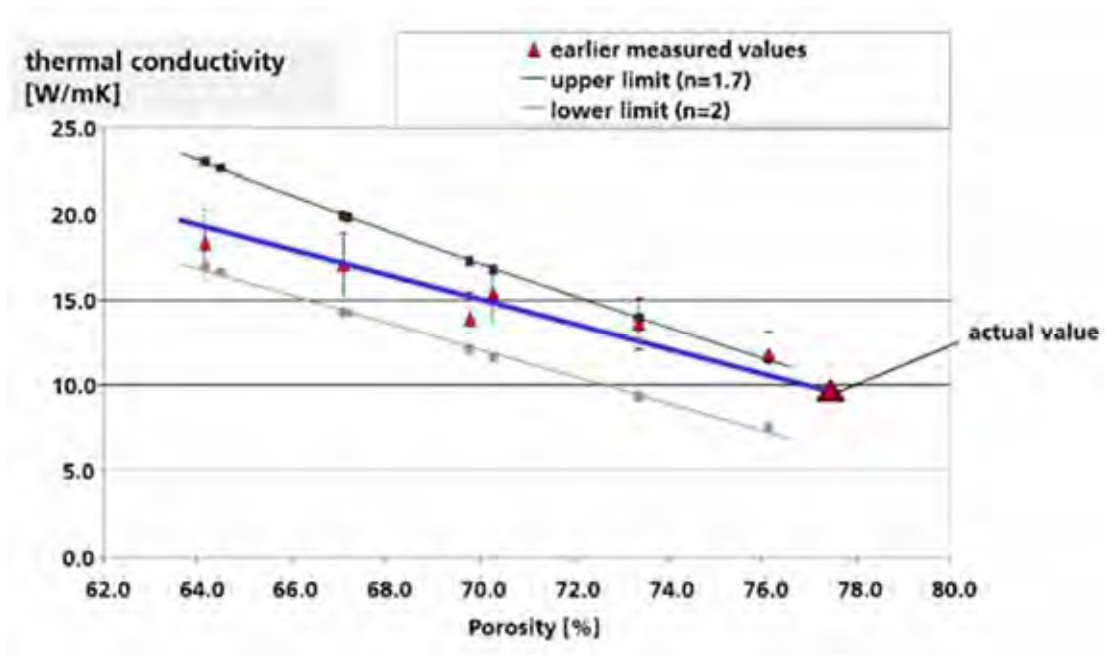


Figure 16: Thermal conductivity of the samples delivered to RUB

The calculation of the thermal conductivity is given in (3)

$$\lambda_S = \lambda_{bulk} \cdot (1 - P_s)^{\frac{\cos^2 \alpha \cdot (3F - 1) - 2F}{(2F) \cdot F - 1}}$$

λ —thermal conductivity; P —porosity; F —form factor; α —orientation of pores

simplified: $\lambda_S = \lambda_{bulk} \cdot (1 - P_s)^n$

(3)

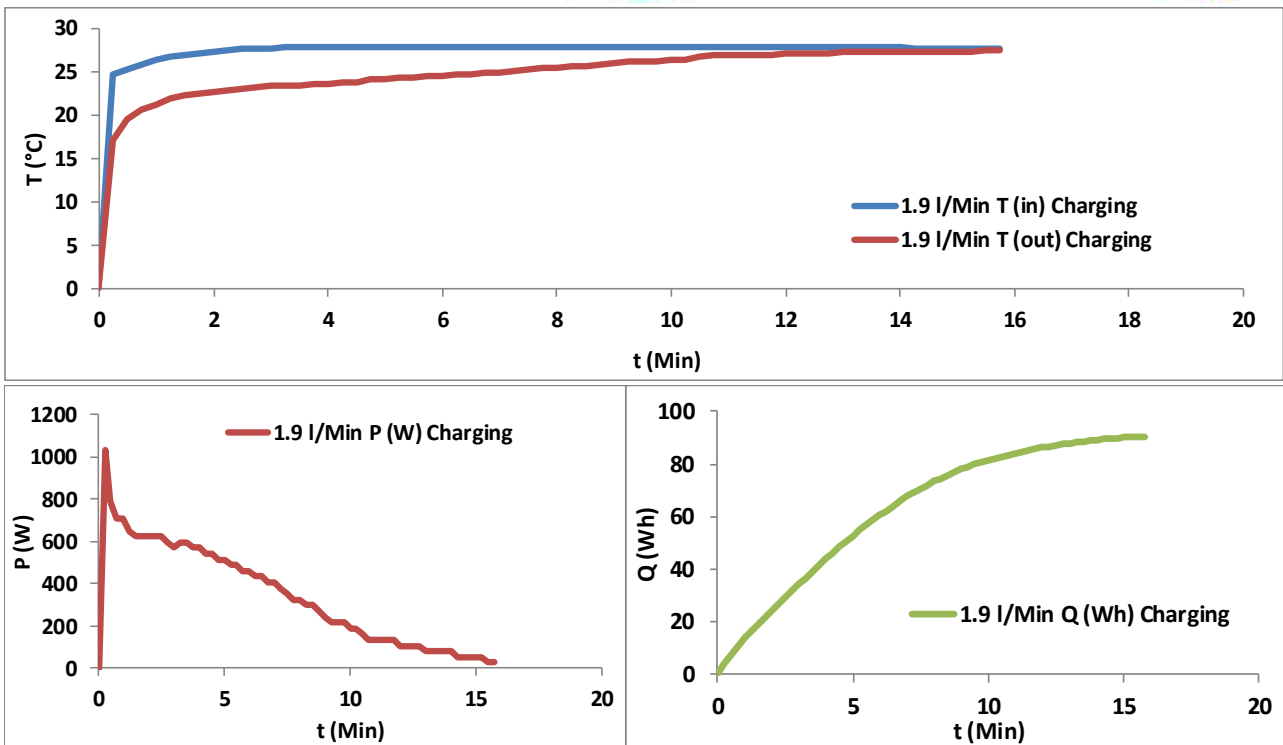


Figure 17: Measured data of thermal storage (Heat-up / Charging case @ \dot{v} coolant = 1.9 l/min)

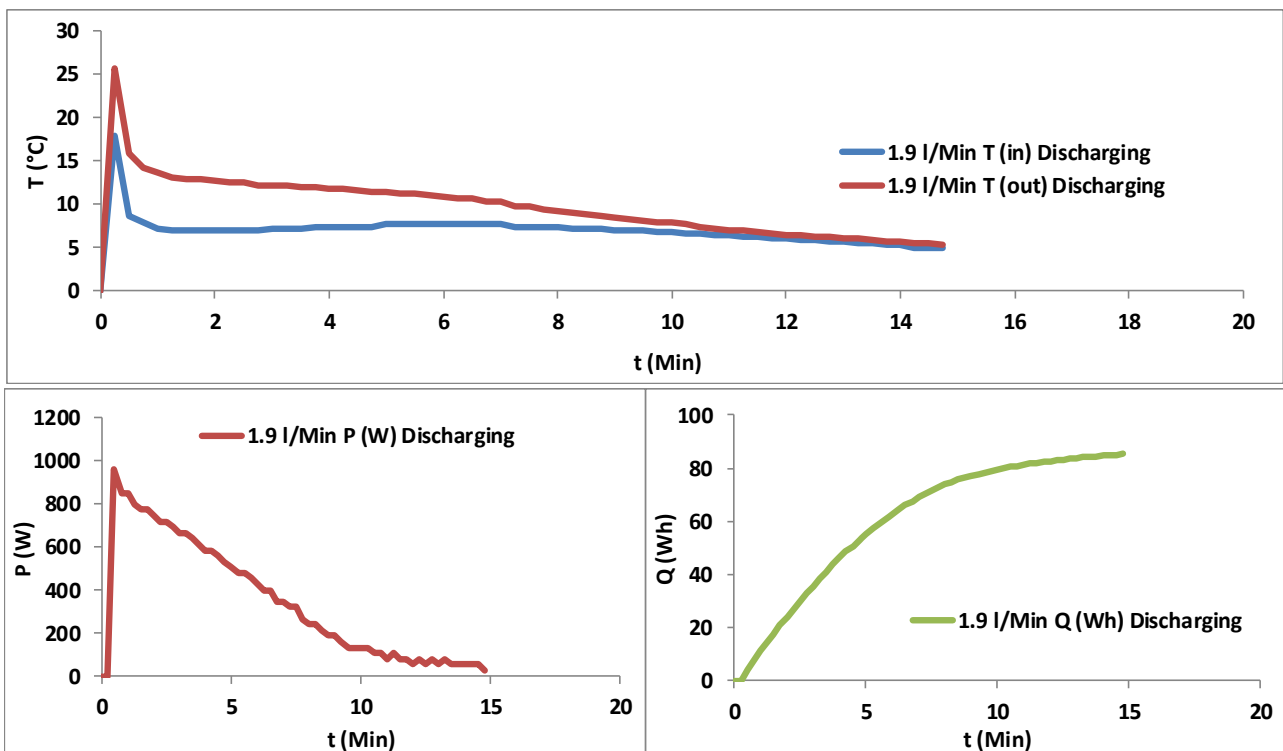


Figure 18: Measured data of thermal storage (Cool-down / Discharging case @ \dot{v} coolant = 1.9 l/min)

This project has received funding from the European Union’s Horizon 2020 research and innovation programme under grant agreement No. 769826. The content of this publication is the sole responsibility of the Consortium partners listed herein and does not necessarily represent the view of the European Commission or its services.



3.4. Technological Implementation

While waiting for feedback about the performance in the vehicle RUBITHERM is investigating the technological steps necessary for producing this kind of storages on larger scale.

3.4.1. Status on Production Capabilities

On a laboratory scale, the high-performance PCM RT18HC could be converted into a leak-proof variant relatively easily. In a production process this requires new equipment solutions that can deal with the increased viscosity at the elevated temperature necessary for the polymerisation of the PCM. Furthermore components are added at temperatures near the flash point of the pure PCM requiring precautions regarding fire protection of the setup. A further challenge is the incorporation of the highly viscous product into a porous Al foam structure. In the laboratory this was done by means of multi-stage vacuum infiltration.

3.4.2. Preparation of the special PCM

The components that are added to the RT18HC are inert polymers with a softening range of 100°C. The challenge is to get the mixture homogeneous at high viscosity where normal stirrers become ineffective. Experiments with extruders have often resulted in fires. Therefore, a solution is sought in which an agitator in a thermally controlled mixing vessel constantly changes its position horizontally and vertically. These movements of the entire agitator require a completely new design of a production line.

Emptying a reactor filled with the highly viscous PCM is another challenge, as the produced substance can be pumped, but our existing transfer pumps reach their performance limit by overheating and cannot be cleaned without complete disassembly. Here too, a new system that can only be used for this product must be set up.

3.4.3. Infiltration of the Al Foams

Infiltration requires multiple changes of pressure and vacuum, as air bubbles in the Al-foam structure migrate only extremely slowly. One can observe here clearly that the PCM is not a liquid anymore. How this process can be automatized still needs to be researched.

3.5. Conclusions on thermal storage tank

RUB is in the experimental and planning phase to create conditions for the production of high-performance PCM storages. The specifications of the components place high demands on the new systems, which require considerable investment.

This project has received funding from the European Union's Horizon 2020 research and innovation programme under grant agreement No. 769826. The content of this publication is the sole responsibility of the Consortium partners listed herein and does not necessarily represent the view of the European Commission or its services.

4. Thermal management network - energy distribution – simulation (AIT)

In order to gain insight into the energy distribution and the energy savings to be expected a thermal management network simulation model was built-up by AIT. It is based on the simulation models of the particular components and combines them to an overall thermal management simulation model. In the following this model is described and results are presented.

4.1. Introduction to thermal comfort assessment

The assessment of the thermal comfort in confined space, such as a vehicle cabin, is a complex task involving the evaluation of both the physiological and the psychological states of the person under consideration. A well-known index used to estimate global thermal comfort of people is the Predicted Mean Vote (PMV) Index (see [3]), which gives the thermal comfort response in steady-state for airconditioned environment (see Table 4).

Table 4: Thermal comfort scale based on the predicted mean vote index

-3	-2	-1	0	+1	+2	3
cold	cool	slightly cool	thermal neutral state	slightly warm	warm	hot

The index has been developed based on a large statistical research on a group of individuals, and it defines ranges that should result in thermal satisfaction for most of the occupants in a space. A PMV value of zero represents the ideal value considered as the thermal neutrality. However, values of the PMV Index in the range between -1.0 and +1.0 are considered acceptable and recommended (see Table 4).

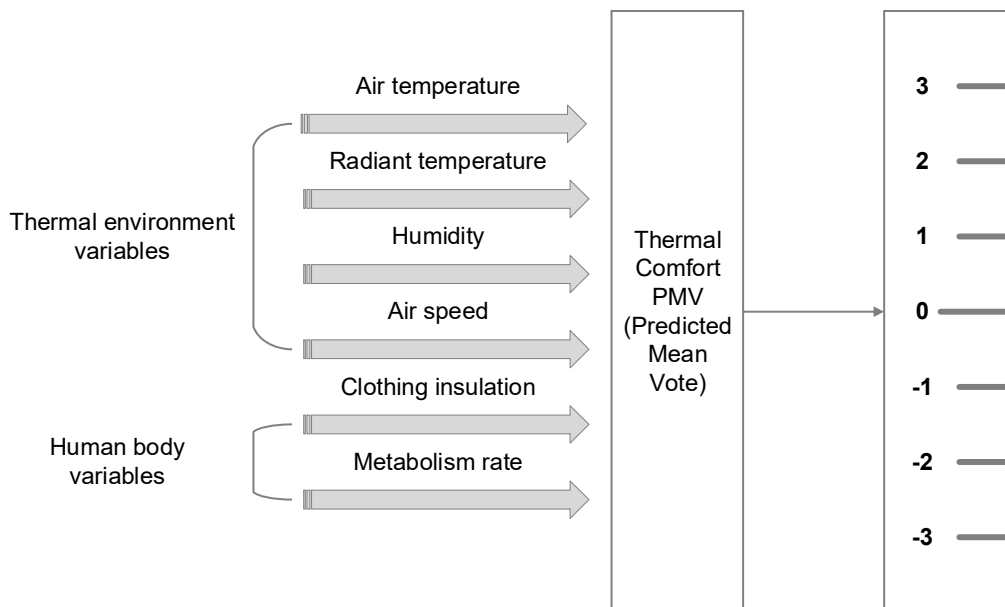


Figure 19: Thermal comfort model dependencies and scale

PMV Index factors are reported in (4). The PMV Index is a function of four thermal environment variables and two human body factors, see Figure 19. The PMV index includes the factors related with thermal comfort,

This project has received funding from the European Union’s Horizon 2020 research and innovation programme under grant agreement No. 769826. The content of this publication is the sole responsibility of the Consortium partners listed herein and does not necessarily represent the view of the European Commission or its services.



such as metabolic heat generation (M), clothing insulation (f_{cl}), air humidity (RH), air temperature (T_{air}), radiant temperature (T_{rad}) and air velocity (v_{air}).

$$PMV = f(M, I_{cl}, RH, T_{air}, T_{rad}, v_{air}) \quad (4)$$

Table 5 gives an overview of PMV factors and provides typical ranges as well as the values used for the case study. The models and the parameters of the HVAC systems have been previously described in deliverable D2.2 (Multi-physical entire vehicle model; control units for energy management system) and are therefore not reported in this deliverable.

Table 5: PMV Index factors overview

	Typical ranges
M	46 to 232 W/m ² (0.8 to 4 met)
I_{cl}	0 to 0.310 m ² .K/W (0 to 2 clo)
T_{air}	-10 to 30°C
v_{air}	0 to 2 m/s
RH	20-80 %

Following in the chapter 4.2 the developed scenarios and the assessment of them within the framework of the proposed design for the HMI. Additionally, in chapter 4.3 an investigation of the system performance for two configurations and namely the standard heating system and the concept using heating panels is presented and assessed.

4.2. Thermal comfort evaluations

4.2.1.Scenario 1

An overview of the settings for the HVAC system (mode, flaps and panels) and the HMI configuration (initial status of the cabin and selected actions from the user) is shown respectively in Table 6 and Figure 20. The Scenario 1 refers to the initial cabin thermal condition for which all passengers feel hot (e.g. entering the car after park conditions in summer). The HVAC system is set to cool down everybody in the cabin and the flaps are selected in position “HEAT-DEF”. Heating panels are turned off.

Table 6: HVAC System settings, Scenario 1

Mode	Flaps settings	Heating panels settings
Cooling	HEAT-DEF	OFF (all passengers feel hot)

This project has received funding from the European Union’s Horizon 2020 research and innovation programme under grant agreement No. 769826. The content of this publication is the sole responsibility of the Consortium partners listed herein and does not necessarily represent the view of the European Commission or its services.

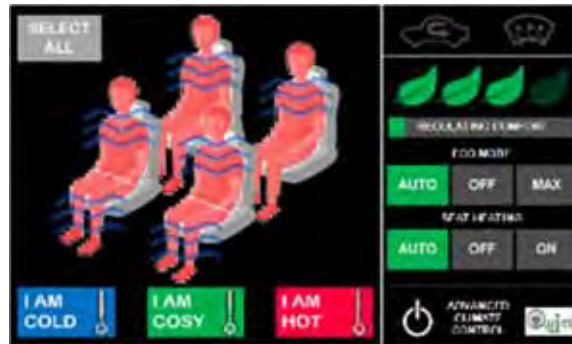


Figure 20: HMI settings for scenario 1

The evaluation of the results is presented in terms of PMV value in steady-state conditions (that is after 1h of cabin conditioning) and is shown in Figure 21. Six PMV values are presented and namely: one average PMV value for the passenger behind the driver and one for the codriver, and two separate PMV values both for the driver and the co-driver related to the legs area and the average value of heat and chest position.

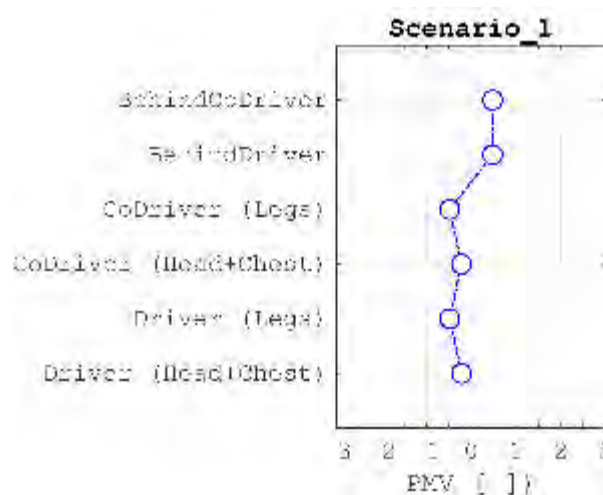


Figure 21: PMV results for scenario 1

The results from the scenario 1 show that in steady state conditions the HVAC system is able to give to the passengers a comfortable thermal state, with all position in a neutral driver and co-driver legs area slightly cold (PMV ~ -0.5) and passengers on the back side feeling slightly warmer (PMV ~ +0.5).

4.2.2.Scenario 2

An overview of the settings for the HVAC system (mode, flaps and panels) and the HMI configuration (initial status of the cabin and selected actions from the user) is shown respectively in Table 7 and Figure 22. The Scenario 2 refers to the initial cabin thermal condition for which all passengers feel cold (e.g. entering the car after park conditions in winter). The HVAC system is set to heat up everybody in the cabin and the flaps are selected in position “BI-LEV”. Heating panels are turned on to ensure a faster thermal comfort response.

Table 7: HVAC System settings, Scenario 2

Mode	Flaps settings	Panels settings
Heat-pump	BI-LEV	ON (for passengers that feel cold)

This project has received funding from the European Union’s Horizon 2020 research and innovation programme under grant agreement No. 769826. The content of this publication is the sole responsibility of the Consortium partners listed herein and does not necessarily represent the view of the European Commission or its services.

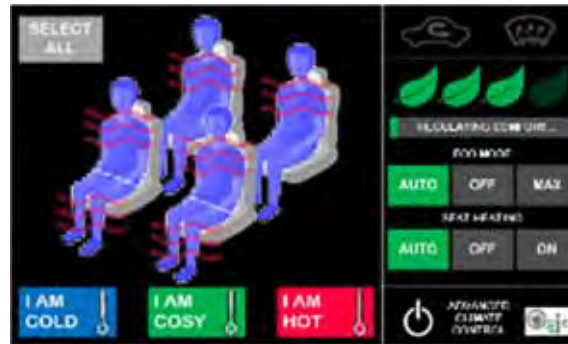


Figure 22: HMI settings for scenario 2

The evaluation of the results is presented in terms of PMV value in steady-state conditions (that is after 1h of cabin conditioning) and is shown in Figure 23. Six PMV values are presented and namely: one average PMV value for the passenger behind the driver and one for the codriver, and two separate PMV values both for the driver and the co-driver related to the legs area and the average value of heat and chest position.

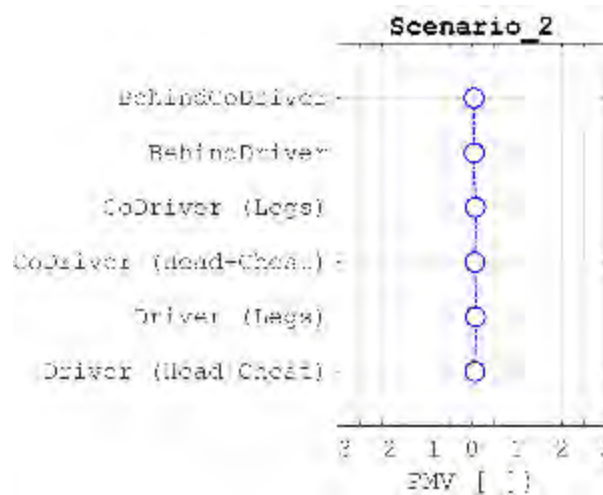


Figure 23: PMV results for scenario 2

The results from the scenario 2 show that in steady state conditions the HVAC system is able to give to the passengers a comfortable thermal state, with all position in a neutral thermal state (PMV ~ 0).

4.2.3.Scenario 3

An overview of the settings for the HVAC system (mode, flaps and panels) and the HMI configuration (initial status of the cabin and selected actions from the user) is shown respectively in Table 8 and Figure 24. The Scenario 3 refers to the initial cabin thermal condition for which all passengers feel cold (e.g. entering the car after park conditions in winter). The HVAC system is set to heat up everybody in the cabin (except for the driver) and the flaps are selected in position “BI-LEV”. Heating panels are turned on except for the driver.

Table 8: HVAC System settings, Scenario 3

Mode	Flaps settings	Panels settings
Heat-pump	BI-LEV	ON (for passengers that feel cold)

This project has received funding from the European Union’s Horizon 2020 research and innovation programme under grant agreement No. 769826. The content of this publication is the sole responsibility of the Consortium partners listed herein and does not necessarily represent the view of the European Commission or its services.



Figure 24: HMI settings for scenario 3

The evaluation of the results is presented in terms of PMV value in steady-state conditions (that is after 1h of cabin conditioning) and is shown in Figure 25. Six PMV values are presented and namely: one average PMV value for the passenger behind the driver and one for the codriver, and two separate PMV values both for the driver and the co-driver related to the legs area and the average value of heat and chest position.

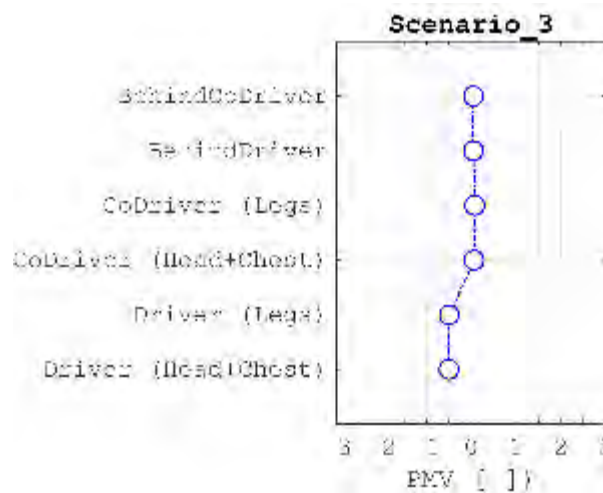


Figure 25: PMV results for scenario 3

The results from the scenario 3 show that in steady state conditions the HVAC system is able to give to the passengers a comfortable thermal state, with driver feeling slightly cold (PMV ~ -0.5) and for the rest of the passengers a thermal neutral state (PMV ~ 0).

4.2.4.Scenario 4

An overview of the settings for the HVAC system (mode, flaps and panels) and the HMI configuration (initial status of the cabin and selected actions from the user) is shown respectively in Table 9 and Figure 26. The Scenario 4 refers to the initial cabin thermal condition for which all passengers feel hot (e.g. entering the car after park conditions in summer) except for the co-driver. The HVAC system is set to cool down the cabin and the flaps are selected in position “HEAT -DEF”. Heating panels are turned off.

Table 9: HVAC System settings, Scenario 4

Mode	Flaps settings	Panels settings
Cooling	HEAT -DEF	OFF

This project has received funding from the European Union’s Horizon 2020 research and innovation programme under grant agreement No. 769826. The content of this publication is the sole responsibility of the Consortium partners listed herein and does not necessarily represent the view of the European Commission or its services.



Figure 26: HMI settings for scenario 4

The evaluation of the results is presented in terms of PMV value in steady-state conditions (that is after 1h of cabin conditioning) and is shown in Figure 27. Six PMV values are presented and namely: one average PMV value for the passenger behind the driver and one for the codriver, and two separate PMV values both for the driver and the co-driver related to the legs area and the average value of heat and chest position.

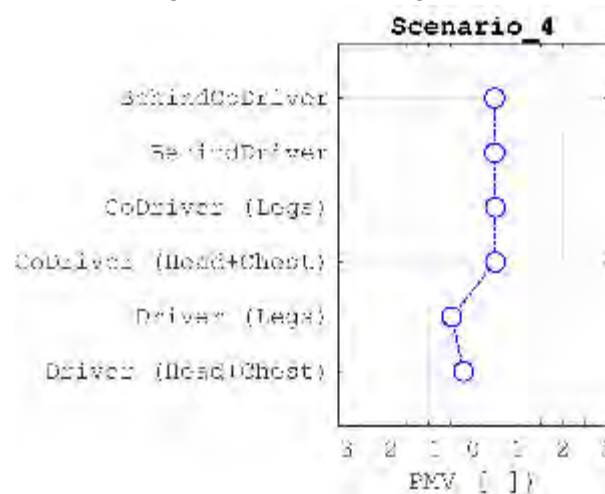


Figure 27: PMV results for scenario 4

The results from the scenario 3 show that in steady state conditions the HVAC system is able to give to the passengers a comfortable thermal state, with driver legs position feeling slightly cold (PMV ~ -0.5) and for the rest of the body and rest of the passengers a thermal neutral state (PMV ~ 0).

4.2.5.Scenario 5

An overview of the settings for the HVAC system (mode, flaps and panels) and the HMI configuration (initial status of the cabin and selected actions from the user) is shown respectively in Table 10 and Figure 28. The Scenario 5 refers to the initial cabin thermal condition for which all passengers feels in neutral condition (e.g. entering the car after park conditions in winter) and the driver feels in the upper part of the body warm and the bottom part cold. The HVAC system is set to cool down the cabin and the flaps are selected in position “VENT”. Heating panels are turned on for the driver in the legs area.

Table 10: HVAC System settings, Scenario 5

Mode	Flaps settings	Panels settings
Cooling	VENT	ON (for passengers that feel cold)

This project has received funding from the European Union’s Horizon 2020 research and innovation programme under grant agreement No. 769826. The content of this publication is the sole responsibility of the Consortium partners listed herein and does not necessarily represent the view of the European Commission or its services.



Figure 28: HMI settings for scenario 5

The evaluation of the results is presented in terms of PMV value in steady-state conditions (that is after 1h of cabin conditioning) and is shown in Figure 29. Six PMV values are presented and namely: one average PMV value for the passenger behind the driver and one for the codriver, and two separate PMV values both for the driver and the co-driver related to the legs area and the average value of heat and chest position.

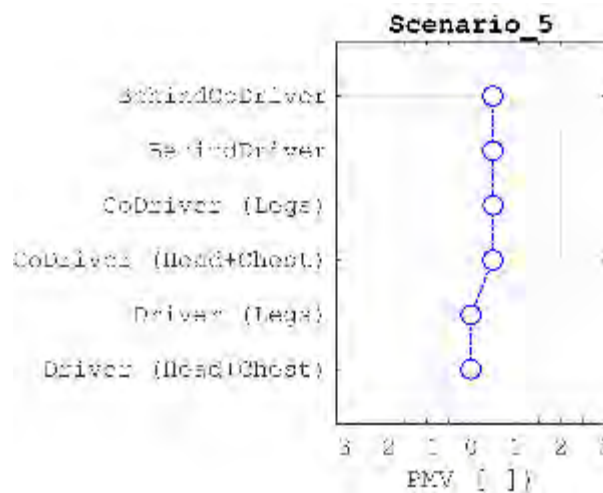


Figure 29: PMV results for scenario 5

The results from the scenario 1 show that in steady state conditions the HVAC system is able to give to the passengers a comfortable thermal state, with the driver in a neutral thermal state (PMV ~ 0) and the rest of the passengers slightly warmer (PMV ~ +0.5).

4.2.6.Scenario 6

An overview of the settings for the HVAC system (mode, flaps and panels) and the HMI configuration (initial status of the cabin and selected actions from the user) is shown respectively in Table 11 and Figure 30. The Scenario 6 refers to the initial cabin thermal condition for which all back passengers feel warm. The HVAC system is set to cool down the cabin and the flaps are selected in position “HEAT-DEF”. Heating panels are turned off.

Table 11: HVAC System settings, Scenario 6

Mode	Flaps settings	Panels settings
Cooling	HEAT-DEF	OFF

This project has received funding from the European Union’s Horizon 2020 research and innovation programme under grant agreement No. 769826. The content of this publication is the sole responsibility of the Consortium partners listed herein and does not necessarily represent the view of the European Commission or its services.



Figure 30: HMI settings for scenario 6

The evaluation of the results is presented in terms of PMV value in steady-state conditions (that is after 1h of cabin conditioning) and is shown in Figure 31. Six PMV values are presented and namely: one average PMV value for the passenger behind the driver and one for the codriver, and two separate PMV values both for the driver and the co-driver related to the legs area and the average value of heat and chest position.

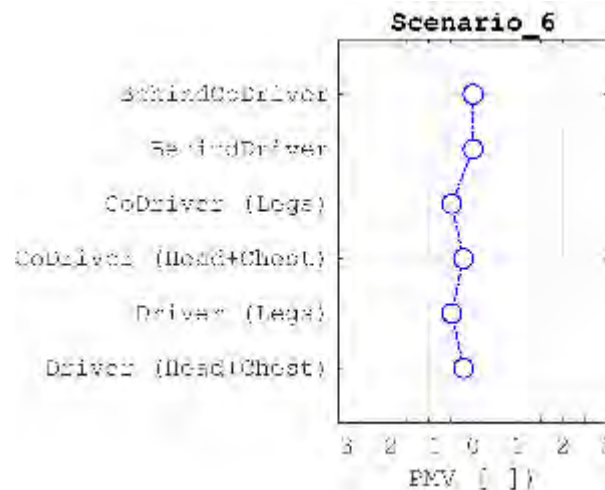


Figure 31: PMV results for scenario 6

The results from the scenario 6 show that in steady state conditions the HVAC system is able to give to the passengers a comfortable thermal state, with values of PMV between -0.5 and 0.

4.2.7.Scenario 7

An overview of the settings for the HVAC system (mode, flaps and panels) and the HMI configuration (initial status of the cabin and selected actions from the user) is shown respectively in Table 12 and Figure 32. The Scenario 7 refers to the initial cabin thermal condition for which there is a mixture of thermal state between feeling warm and cold. The HVAC system is set to cool down the cabin and the flaps are selected in position “HEAT-DEF”. Heating panels are turned on to ensure a thermal comfort state for the passengers that feel cold.

Table 12: HVAC System settings, Scenario 7

Mode	Flaps settings	Panels settings
Cooling	HEAT-DEF	ON (for passengers that feel cold)

This project has received funding from the European Union’s Horizon 2020 research and innovation programme under grant agreement No. 769826. The content of this publication is the sole responsibility of the Consortium partners listed herein and does not necessarily represent the view of the European Commission or its services.



Figure 32: HMI settings for scenario 7

The evaluation of the results is presented in terms of PMV value in steady-state conditions (that is after 1h of cabin conditioning) and is shown in Figure 33. Six PMV values are presented and namely: one average PMV value for the passenger behind the driver and one for the codriver, and two separate PMV values both for the driver and the co-driver related to the legs area and the average value of heat and chest position.

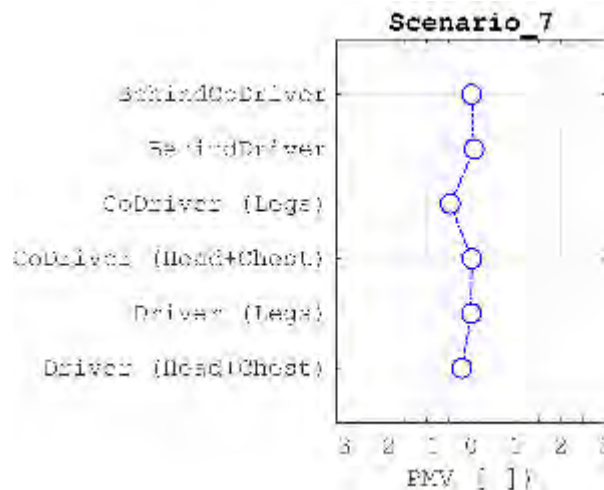


Figure 33: PMV results for scenario 7

The results from the scenario 7 show that in steady state conditions the HVAC system is able to give to the passengers a comfortable thermal state, with values of PMV between -0.5 and 0.

4.3. Use case: energy reduction through heating panels

The use case describes the comparison of two solutions and namely: a) the standard concept with the heating system keeping the cabin temperature to 20°C and b) the alternative solution for which the cabin temperature is reduce to 15°C and the heating panels and turned on to achieve a neutral thermal state. The scenario with the heating panels has the aim of reducing the heat losses and therefore reduce the energy consumption. Both scenarios have been compared for one cycle of 1h in which the cabin starting from the initial condition of -10°C (PMV -5) is heated up to the required temperature level.

As it can be seen in Figure 34, the steady state conditions for both solutions are very similar. On the other hand the solution with the heating panels is able both: 1) to achieve energy reduction of about 11% (see Figure 36) and increase the thermal comfort (PMV -0.5 is reached 7 min faster).

This project has received funding from the European Union’s Horizon 2020 research and innovation programme under grant agreement No. 769826. The content of this publication is the sole responsibility of the Consortium partners listed herein and does not necessarily represent the view of the European Commission or its services.

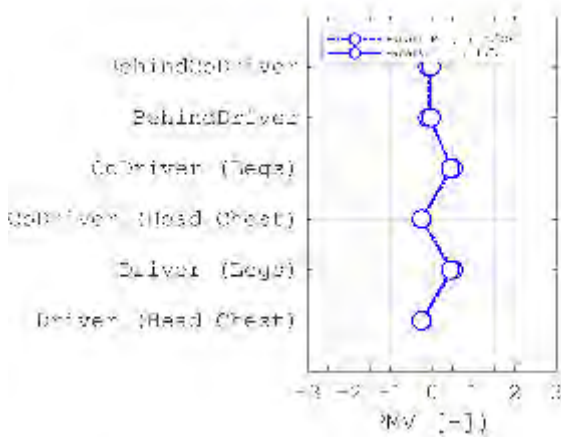


Figure 34: PMV results for the use case

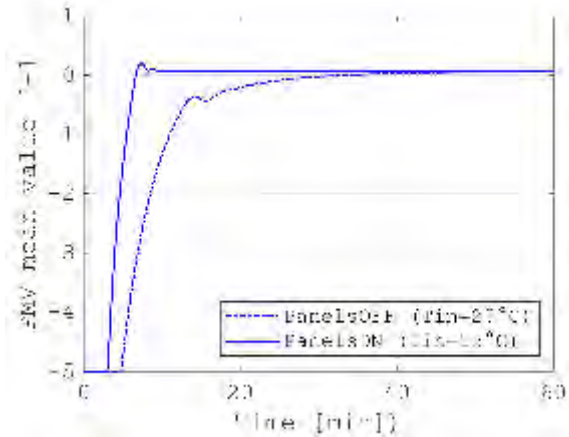


Figure 35: PMV over time for the use case

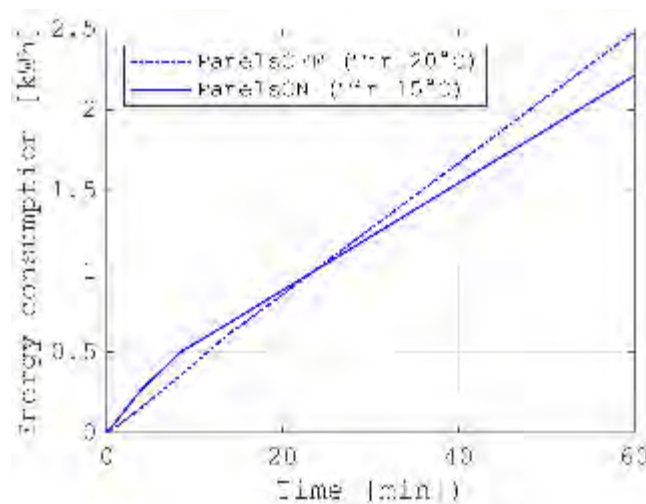


Figure 36: Energy consumption comparison

4.4. Conclusions on thermal comfort simulations

The activities within WP4 have been focusing on the assessment of the different technological solutions as well as the assessment of the HMI framework with respect to the thermal comfort. The assessment of the thermal comfort in confined space, such as a vehicle cabin, is a complex task and a well-known index used to estimate global thermal comfort of people is the Predicted Mean Vote (PMV) Index is used.

Various realistic scenarios have been developed and evaluated with the simulation approach described in deliverable D2.2. The results from the scenarios show that in steady state conditions the HVAC system and the heating panels are able to give to the passengers a comfortable thermal state, with small differences between passengers which space between slightly cold thermal state (PMV ~ -0.5) and a slightly warmer thermal state (PMV ~ +0.5).

Additionally, a use case has been developed to compare the heating panel solution with the standard HVAC system solution. The standard concept consists of the HVAC system keeping the cabin temperature to 20°C while in the alternative solution the cabin temperature is reduced to 15°C and the heating panels are turned on to achieve a neutral thermal state. The heating panel solution is able to achieve at steady state similar thermal state conditions. Moreover, the solution with the heating panels is able both: 1) to achieve energy reduction of about 11% and increase the thermal comfort (faster heat up response).

This project has received funding from the European Union's Horizon 2020 research and innovation programme under grant agreement No. 769826. The content of this publication is the sole responsibility of the Consortium partners listed herein and does not necessarily represent the view of the European Commission or its services.

5. Build-up of the R290 refrigerant circuit and the VTMS at the AC system testbed (AVL)

In order to prove the ability of the newly developed VTMS to reach higher efficiency and energy savings, it was necessary to build-up, instrument and commission the entire system incl. the R290 refrigerant circuit at the AC system testbed. Subsequently detailed measurements of AC and heat pump modes, of COP etc. were the next step.

The build-up and measurements were split into two work packages to reduce complexity. The first was the R290 refrigerant circuit only, including all corresponding components. This work package was called *Step-1*. Here two coolant circuits connected via refrigerant-coolant plate heat exchanger were represented by two separate conditioning units.

The second work package, called *Step-2*, consisted of the entire VTMS system incl. R290 refrigerant circuit and the two coolant circuits. It represented the full VTMS as it will be implemented into the demonstrator vehicle.

5.1. Set-up and measurements of the R290 refrigerant circuit (Step-1)

In step-1 the entire R290 refrigerant circuit was build up at the AC system testbed (see Figure 37), the two coolant circuits connected via refrigerant-coolant plate heat exchanger were represented by two separate conditioning units.

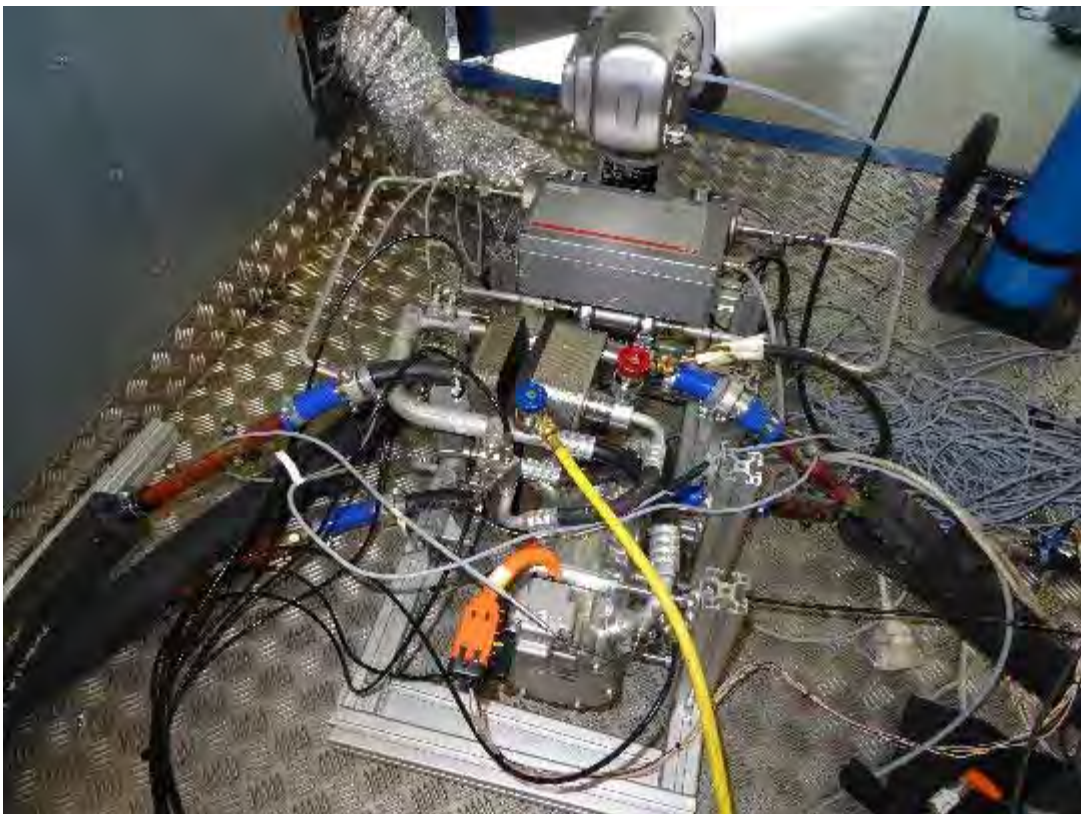


Figure 37: Build-up and instrumentation of Step-1 (R290 Micro-AC circuit) at AC system testbed

This project has received funding from the European Union's Horizon 2020 research and innovation programme under grant agreement No. 769826. The content of this publication is the sole responsibility of the Consortium partners listed herein and does not necessarily represent the view of the European Commission or its services.

The instrumentation was done by means of a high number of pressure and temperature sensors implemented into the refrigerant circuit and coolant circuits (see Figure 38). In the AC circuit a *Coriolis* device was used for measurement of refrigerant mass flow. The oil concentration present in the system was measured by means of an *OCR device* (supplier *Anton Paar*). In order to deliver correct data the OCR needed to be calibrated to the present combination of Propane and the particular compressor oil (Fuchs POE-236). The type of oil to be used was defined by OBR based on their compressor tests. According to this definition provision of necessary calibration curve was done. This calibration curve was delivered in late June 2019 and implemented into the OCR device of the testbed system.

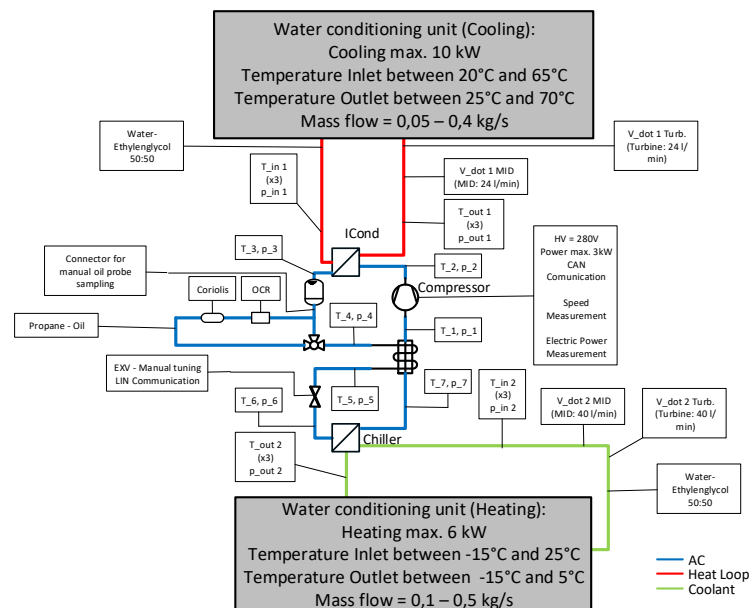


Figure 38: Instrumentation of testbed build-up Step-1 (R290 Micro-AC circuit)

After the build-up and instrumentation of the AC circuit it was connected to the AC system testbed and the test set-up was commissioned. This process was done very carefully to make sure that EXV and compressor control worked as desired, all implemented measurement devices work properly and deliver reasonable measurement values. In agreement with OBR, AVL implemented several stopping criteria into its testbed control and operating system to ensure the compressor cannot be operated outside of its determined load and speed range.

The system was flushed with refrigerant several times to make sure that it is clean and no particles are inside. For flushing a WAECO service station was used, flushing with approx. 8 kg of R134a until the oil is seen to be clean. All commissioning tests were passed and so as a next step the derivation of the necessary amount of refrigerant was done.



Figure 39: WAECO service station for flushing the entire refrigerant circuit

5.2. Determination of correct amount of refrigerant and oil in the system

After the refrigerant circuit (Step-1) and the corresponding instrumentation was successfully commissioned at the AC system testbed, it was necessary to determine the necessary amount of refrigerant inside the refrigerant circuit.

The determination of the correct amount of refrigerant in the system was done under consideration of the receiver size for the extreme operational conditions for AC and HP modes. Ideal pressure levels were applied for these investigations. The correct amount of Propane was determined to be 270 g. This includes the additional amount of Propane necessary for the included measurement devices like Coriolis measurement device, OCR measurement device, all additional piping etc. Without all these devices installed on the testbed, the desired amount of 150 g Propane (see Deliverable D4.1) for the refrigerant circuit seems to be reachable.

After deriving the correct amount of refrigerant, the correct amount of oil inside the system (oil concentration rate OCR) was determined together with OBR. 84 g *Fuchs POE-236* were agreed to be the correct amount for safe operation of the compressor and an OCR of approx. 3% to 5%.

In Figure 40 the diagram depicting the correct amount of refrigerant is given.

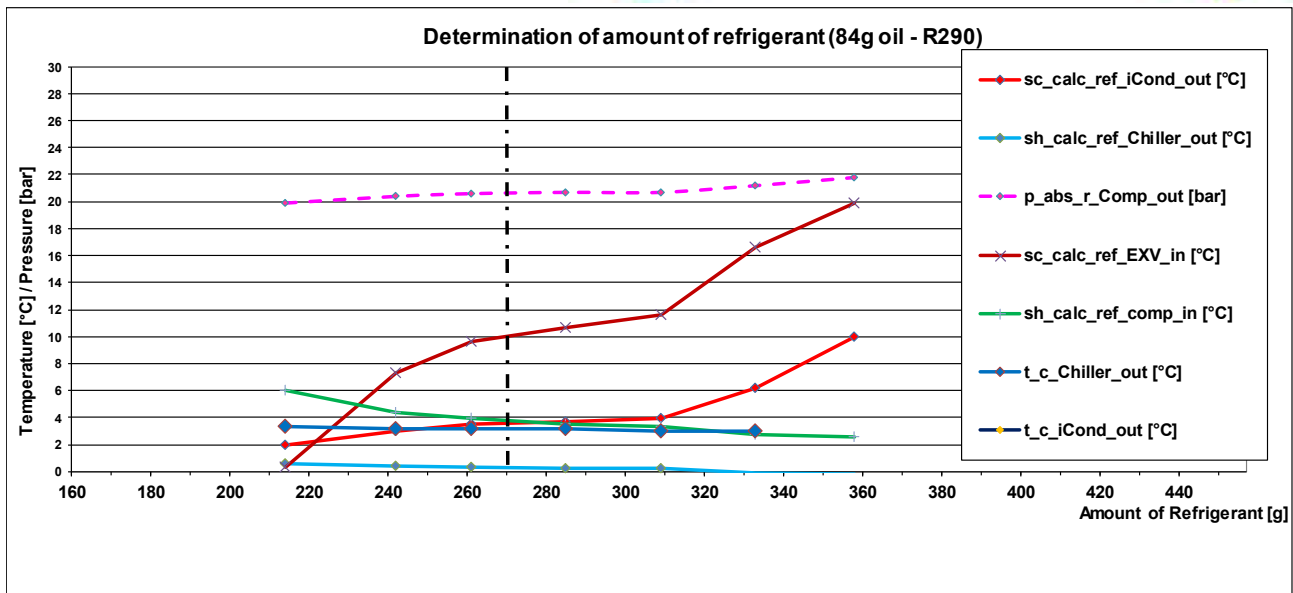


Figure 40: Determination of necessary amount of refrigerant for the R290 Micro-AC circuit (incl. all measurement devices and additional piping included in testbed set-up)

While the measurements for the derivation of the necessary amount of refrigerant and oil were done, the EXV, named no. 1, led to issues. It did not respond correctly to control signals, sometimes led to wrong positioning / wrong opening cross section and finally got stuck. In agreement with VEN, the supplier of this part, it was decided to unmount and replace it by the second supplied EXV, named no. 2. Since the system was flushed several times before start of testbed operation the reason was seen in the prototype status of the EXV no. 1. Before installation of the EXV no. 2 the system was again flushed several times.

5.3. Measurement of reference points to make sure compressor works correctly

After the necessary amount of refrigerant was determined several reference points were measured to make sure that the prototype R290 compressor works correctly in the system build-up. Therefore, measurement points which were already measured at OBR while their approval tests were also applied at the AC system testbed. The results were handed over to OBR to be checked and assessed (see Figure 41). Since the results seen at the AC system testbed corresponded very well to the OBR results, approval for start of the measurements was given by OBR.

This project has received funding from the European Union's Horizon 2020 research and innovation programme under grant agreement No. 769826. The content of this publication is the sole responsibility of the Consortium partners listed herein and does not necessarily represent the view of the European Commission or its services.

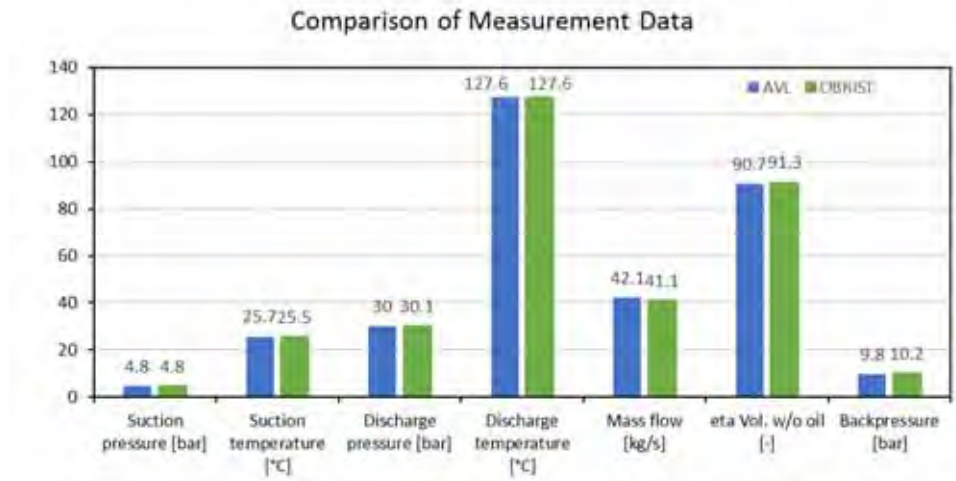


Figure 41: Reference point measurement data

5.4. Generation of measurement matrix for Step-1

The measurement matrix (list of measurement points to be investigated) was defined in order to first investigate different air-conditioning modes. After that several heat pump mode measurement points were defined to be analyzed as well. In Figure 42 the measurement matrix for Step-1 is given. Whereby measurement points 19 to 54 represent AC modes and measurement points 1 to 18 represent heat pump modes.

This project has received funding from the European Union’s Horizon 2020 research and innovation programme under grant agreement No. 769826. The content of this publication is the sole responsibility of the Consortium partners listed herein and does not necessarily represent the view of the European Commission or its services.

MP No.	vdot_c_ICond_in [l/min]	t_c_ICond_in [°C]	vdot_c_Chiller_in [l/min]	t_c_Chiller_in [°C]	sh_calc_r290_chiller_out [K]	Compr speed [rpm]
1	15	65	5	-20	5	8000 (max.)
2	15	65	10	-20	5	8000 (max.)
3	15	65	15	-20	5	8000 (max.)
4	20	65	5	-20	5	8000 (max.)
5	20	65	10	-20	5	8000 (max.)
6	20	65	15	-20	5	8000 (max.)
7	15	65	5	-20	5	4000
8	15	65	10	-20	5	4000
9	15	65	15	-20	5	4000
10	20	65	5	-20	5	4000
11	20	65	10	-20	5	4000
12	20	65	15	-20	5	4000
13	15	65	5	-20	5	2000
14	15	65	10	-20	5	2000
15	15	65	15	-20	5	2000
16	20	65	5	-20	5	2000
17	20	65	10	-20	5	2000
18	20	65	15	-20	5	2000
19	15	30	5	8	5	8000 (max.)
20	15	30	10	8	5	8000 (max.)
21	15	30	15	8	5	8000 (max.)
22	15	50	5	8	5	8000 (max.)
23	15	50	10	8	5	8000 (max.)
24	15	50	15	8	5	8000 (max.)
25	20	30	5	8	5	8000 (max.)
26	20	30	10	8	5	8000 (max.)
27	20	30	15	8	5	8000 (max.)
28	20	50	5	8	5	8000 (max.)
29	20	50	10	8	5	8000 (max.)
30	20	50	15	8	5	8000 (max.)
31	15	30	5	8	5	4000
32	15	30	10	8	5	4000
33	15	30	15	8	5	4000
34	15	50	5	8	5	4000
35	15	50	10	8	5	4000
36	15	50	15	8	5	4000
37	20	30	5	8	5	4000
38	20	30	10	8	5	4000
39	20	30	15	8	5	4000
40	20	50	5	8	5	4000
41	20	50	10	8	5	4000
42	20	50	15	8	5	4000
43	15	30	5	8	5	2000
44	15	30	10	8	5	2000
45	15	30	15	8	5	2000
46	15	50	5	8	5	2000
47	15	50	10	8	5	2000
48	15	50	15	8	5	2000
49	20	30	5	8	5	2000
50	20	30	10	8	5	2000
51	20	30	15	8	5	2000
52	20	50	5	8	5	2000
53	20	50	10	8	5	2000
54	20	50	15	8	5	2000

Figure 42: Measurement matrix used for step 1 (R290 Micro-AC circuit only)

5.5. Measurement of air conditioning modes

When the determination of the correct amounts of refrigerant and oil was finished, and it was made sure that the compressor and the system work correctly the measurement of the air conditioning modes was started.

While the measurements of the air conditioning modes were performed no anomalies happened. Exemplary results of these measurements are depicted in Figure 43.

This project has received funding from the European Union's Horizon 2020 research and innovation programme under grant agreement No. 769826. The content of this publication is the sole responsibility of the Consortium partners listed herein and does not necessarily represent the view of the European Commission or its services.

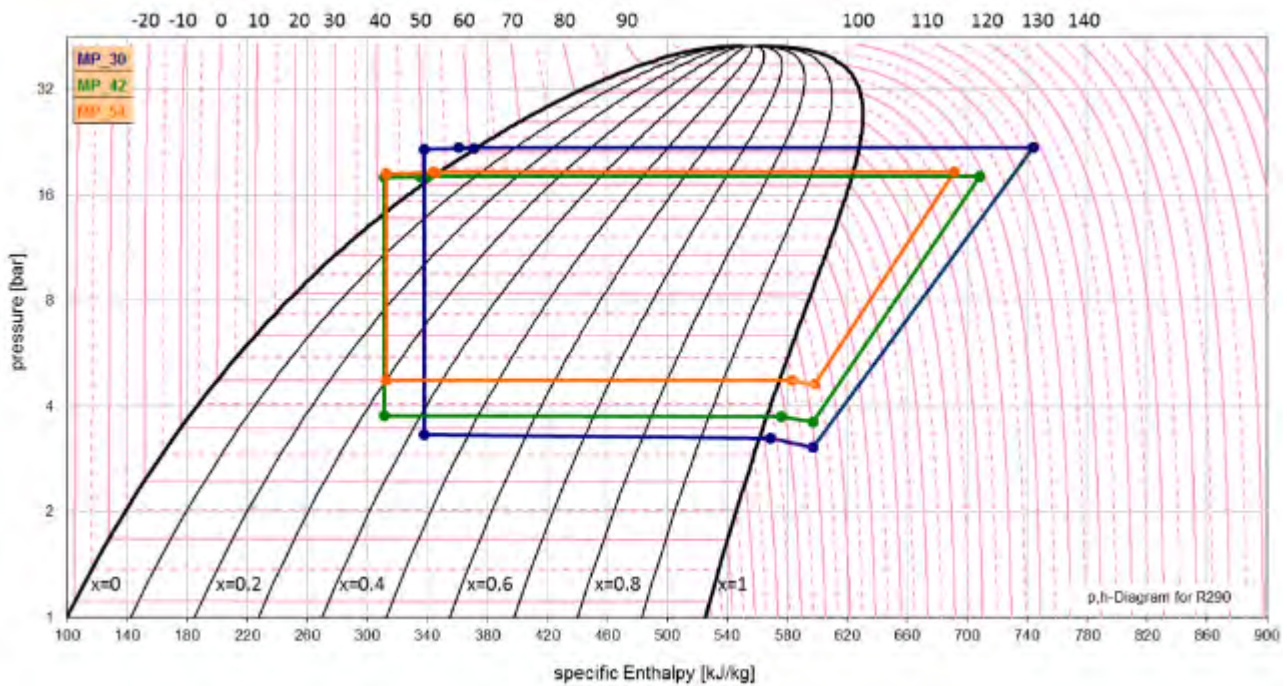


Figure 43: Measurement results of air conditioning modes for step 1

The measurements of the air conditioning modes showed a good performance of the R290 AC system. The targets for cooling performance were reached without experiencing problems. In terms of cooling the passenger compartment the used R290 AC system is suited to be used in future electric vehicle applications to save energy and increase driving range.

This project has received funding from the European Union’s Horizon 2020 research and innovation programme under grant agreement No. 769826. The content of this publication is the sole responsibility of the Consortium partners listed herein and does not necessarily represent the view of the European Commission or its services.

5.6. Measurement of heat pump modes

Within this chapter the measurement of the system working in the heat pump mode are discussed. However, regarding the high-promising targets the solution of the issues for the commissioning are described.

5.6.1. Failure of EXV no. 2

At the very beginning of measuring the heat pump modes the EXV no. 2 also led to problems. Like EXV no. 1 during determination of necessary amount of refrigerant it did not respond correctly to control signals, sometimes led to wrong positioning / wrong opening cross section and finally got stuck. Very slight blackening was seen in the oil drained from the system. In agreement with VEN, the supplier of this prototype part, it was decided to unmount it and to send it to VEN for detailed inspection.

VEN carefully inspected the EXV no. 2, the following reasons for the failure were found:

- Inside the EXV no. 2, in the valve mechanics and the bearing a contamination with small particles was examined (see Figure 44). Due to the build-up of this contamination in the valve mechanics the mechanical friction increased. This led to blocking / standstill of the EXV. The reason for the contamination was not found, but according to VEN it was not to see in the EXV itself.

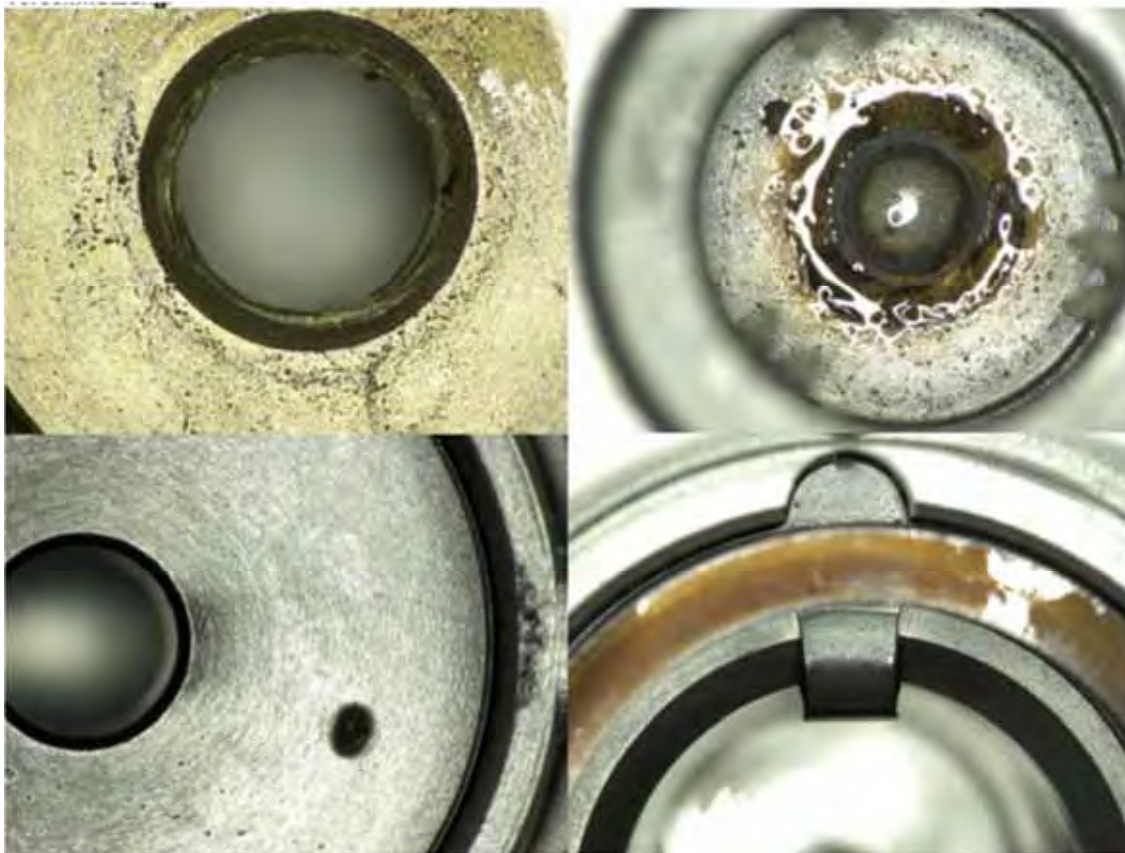


Figure 44: Contamination of EXV no. 2

This project has received funding from the European Union's Horizon 2020 research and innovation programme under grant agreement No. 769826. The content of this publication is the sole responsibility of the Consortium partners listed herein and does not necessarily represent the view of the European Commission or its services.



In agreement with AVL the EXV internal gearbox was replaced by VEN by a version less critical to particles. The entire EXV was carefully cleaned, tested, approved and sent back to AVL for reassembling it into the testbed set-up. VEN also recommended to use a refrigerant filter in front of the EXV.

While the EXV was in inspection the refrigerant circuit was cleaned carefully and again flushed several times, the compressor was unmounted for this process. A refrigerant filter (*HyLok FI3H-10mm-15my*) was installed in front of the EXV, as recommended by VEN, and the repaired EXV no. 2 was reassembled into the testbed set-up.

While the EXV no. 2 was in inspection VEN performed storage tests of the EXV with the used oil *Fuchs POE-236*. The tests were done as follows:

- EXVs were washed / cleaned and lubricated with *Fuchs POE-236* oil
- Functional test was passed
- EXVs were stored @ -40°C and @ +130°C. in a climate chamber (dry air) for 100 hours. Connections of EXVs were not closed.
- Functional test after storage was not passed
- EXVs were dismantled and parts analysed
- The lubrication oil was resinified

The findings of this storage tests were handed over to OBR, who had chosen and tested the used *Fuchs POE-236* with the used compressor. OBR discussed them with *Fuchs* the oil supplier, they answered that the reason for this process is to see in the hygroscopic characteristic of the POE oil. But in mixture with the refrigerant, no matter if Propane, or e.g. R1234yf, this effect is not present. Additionally, the refrigerant circuit is sealed and therefore it is impossible for the R290 - POE-236 mixture to get in contact with the humidity of the ambience. According to this statement of *Fuchs* this topic was seen not to be relevant for the present problems.

The process of inspection, repair, procurement and installation of the filter, reassembling the EXV, refilling the refrigerant circuit and re-commissioning led to a time delay of approx. 4 weeks.

5.6.2. Failure of compressor no. 1

After EXV no. 2 was re-installed and the system was re-commissioned etc., the measurements of the heat pump modes were started. Already after the first measurements, the results led to the assumption that the compressor must be damaged. There was no remarkable pressure build-up seen over the compressor, even when running it at higher speeds.

After discussions on the possible root causes of these problems AVL and OBR agreed to unmount the compressor, named no.1, and to send it to OBR for inspection. The oil drained from the system in the course of unmounting the compressor was blackened, but no solid particles were found (see Figure 45).

This project has received funding from the European Union's Horizon 2020 research and innovation programme under grant agreement No. 769826. The content of this publication is the sole responsibility of the Consortium partners listed herein and does not necessarily represent the view of the European Commission or its services.



Figure 45: Oil drained from refrigerant circuit after failure of compressor no. 1

Additionally, the refrigerant filter in front of the EXV was contaminated with a sludge- / slush-like substance (see Figure 46). No solid particles were present in this substance, so the filter was cleaned and prepared for re-installation.

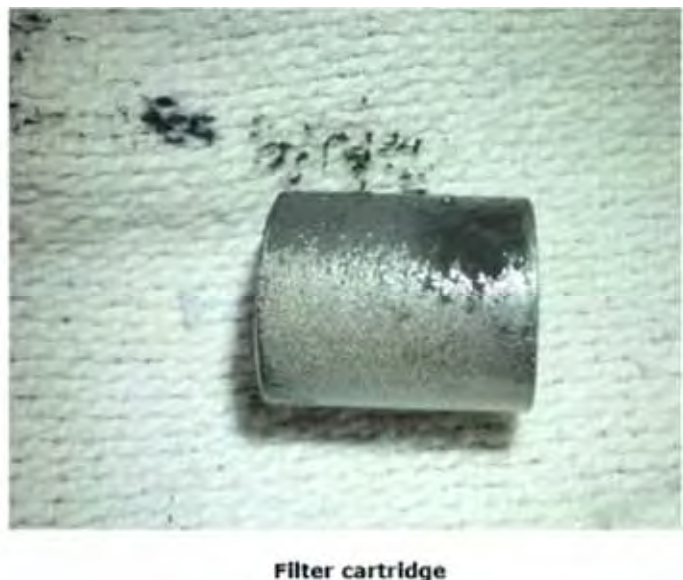


Figure 46: Contamination of the refrigerant filter after failure of compressor no. 1

In agreement with OBR another identical compressor, named no. 2, was installed in the system. Even if it had been done before several times, the entire system was again evacuated, carefully cleaned and flushed to ensure that absolutely no substances or particles could remain. To make sure that the compressor no. 2 will not be damaged as well, it was agreed with OBR to only apply a very low load for one to two hours onto the system after re-installation to let the compressor run-in.

The compressor acted as expected and led to reasonable measurement data. After approx. 30 min of run-in operation the first oil sample was taken from the system. It again showed already a slight blackening, but definitely less than after the failure of compressor no. 1.

This project has received funding from the European Union's Horizon 2020 research and innovation programme under grant agreement No. 769826. The content of this publication is the sole responsibility of the Consortium partners listed herein and does not necessarily represent the view of the European Commission or its services.



Figure 47: Oil drained from refrigerant circuit after 30 min of operation of compressor no. 2

The problems were discussed with OBR the supplier of this component to prevent the damage of compressor no. 2. It was mutually agreed to unmount compressor no. 2 and to send it to OBR for inspection as well. In Figure 47 a sample of the oil drained from compressor no. 2 before dismounting by OBR is shown.

5.6.3. Analysis of oil drained from system after failure of compressor no. 1 (AVL)

While OBR inspected compressors no. 1 and no. 2, a detailed analysis of the used oil was performed (*Fuchs POE-236*) drained from the system after failure of compressor no. 1. It was found that no soot was present in the oil, also no solid particles were present, and the water content of the used oil was slightly less than for the fresh oil (see Figure 48). So, it could be excluded that the oil / Propane mixture, which generally is seen to be hygroscopic, had joined with water from ambient air and lost its lubricative properties. Additionally, the entire refrigerant circuit is sealed and should anyway prevent that refrigerant or oil would get in contact with the ambience.

Soot content				Water content		
Probe:		Quiet-Öl		Probe:	Frischöl Quiet	Gebrauchtöl Quiet
Datum:		11.12.2019		Datum Probenahme:	11.12.2019	11.12.2019
Kunde:		Hr. Leopold Michael		Datum Analyse:	14.01.2020	14.01.2020
Motor:		-		Kunde:	Leopold Michael	Leopold Michael
Laufzeit /entnommen bei [h]:		-		Motor:	-	-
Bemerkung:		-		Laufzeit /entnommen bei [h]:	-	-
	Norm	Ergebnis	Einheit	Bemerkung:	-	-
Rußgehalt	DIN51452	0,01	wt. %	Wassergehalt [ppm]	194	177

Figure 48: Soot and water content of oil drained from refrigerant circuit

This project has received funding from the European Union's Horizon 2020 research and innovation programme under grant agreement No. 769826. The content of this publication is the sole responsibility of the Consortium partners listed herein and does not necessarily represent the view of the European Commission or its services.

The analysis of the material fractions (see Figure 49) of the drained oil showed that mainly aluminium was present (25,4%). The next big fraction was Silicium (12,4%), all others were of minor significance.

A discussion and assessment of these results together with OBR showed that the other material fractions in the drained oil belong to the coating present at the compressor scroll. So, no additional materials, likely belonging to foreign particles or materials inside the refrigerant circuit were present. This was seen as sign that the circuit should be free of unexpected materials.

Prober:		Quiet Frischöl	Quiet Sample
Datum:		-	11.12.2019
Kunde:		-	-
Motor:		-	-
Laufzeit / entnommen bei [h]:		-	-
Bemerkung:		-	-
Element		mg/kg	mg/kg
Aluminium	Al	< 0,1	25,4
Barium	Ba	0,2	0,3
Blei	Pb	< 1	< 1
Bor	B	< 0,1	0,5
Calcium	Ca	17,0	16,9
Chrom	Cr	< 0,1	< 0,1
Eisen	Fe	< 0,1	0,8
Kalium	K	1	1
Kupfer	Cu	< 0,1	0,4
Magnesium	Mg	< 0,1	0,3
Mangan	Mn	< 0,1	0,3
Molybdän	Mo	< 0,1	< 0,1
Natrium	Na	< 1	< 1
Nickel	Ni	< 1	7
Phosphor	P	860	785
Schwefel	S	<< 1000	<< 1000
Silber	Ag	0,1	0,1
Silizium	Si	< 0,1	12,4
Titan	Ti	< 0,1	< 0,1
Vanadium	V	< 0,1	< 0,1
Zink	Zn	< 0,1	0,5
Zinn	Sn	< 1	1

Figure 49: Material fractions found in oil after failure of compressor no. 1

Another question was if the molecular structure of the drained oil could be distorted (molecular bindings broken), which would negatively influence the lubricative properties. To get a sign if this could have happened a gas-chromatographic analysis of the fresh and the used oil was done. An *Agilent Technologies 7890B GC-System* with FID was used for this investigation. The supplied oil was diluted with Carbon Disulfide and investigated in the gas-chromatograph. In Figure 50 the results for fresh and used oil are overlain. The diagram shows that there is almost no difference between fresh and used oil, which was seen as prove that the oil lubricative properties are fine. For peaks which are slightly different in fresh and used oil the area below the curve is minor, the major part of the Chromatogram is identical.

This project has received funding from the European Union's Horizon 2020 research and innovation programme under grant agreement No. 769826. The content of this publication is the sole responsibility of the Consortium partners listed herein and does not necessarily represent the view of the European Commission or its services.

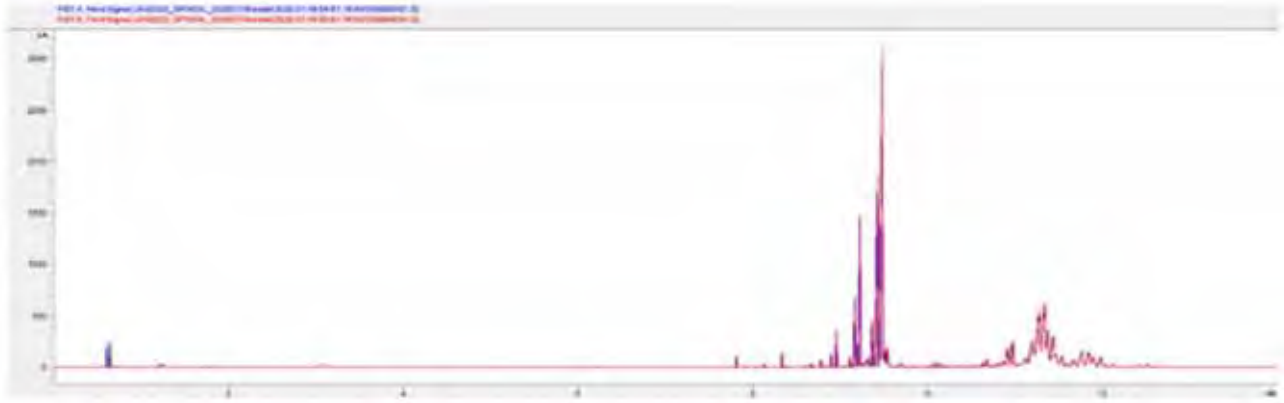


Figure 50: Results of gas-chromatography analysis of oil - excerpt

5.6.4. Failure Analysis of compressor no. 1 (OBR)

OBR inspected compressor no. 1 in detail and found that the bearings were fine and there was enough oil inside the compressor. Although heavy damage of the scroll in axial direction was found (see Figure 51 to Figure 52). The part looked like the scrolls had axially touched and so the massive abrasion and break-out of material happened. The exit of the backpressure system was closed by smeared / glazed material.

Due to the massive damage of the scroll it was impossible for OBR to distinguish the reasons for the failure of compressor no. 1. The overall conclusion was that either the compressor was operated in load conditions where liquid refrigerant enters the compressor on the suction side for a too long time, this would have washed out lubricant and led to heavily increased mechanical friction. Or that the backpressure was too high during operation, which also would lead to an axial touching of the scrolls. This case was prevented by stopping criteria in the testbed control system. Foreign solid particles from the system were identified as another possible reason, but unfortunately it finally could not be verified what exactly was the cause of the failure (see Figure 53). The particles present in the system after the failure could also be abrasion of compressor material or coating due to the massive damage.



Figure 51: Compressor no. 1 - Bearings after failure

This project has received funding from the European Union's Horizon 2020 research and innovation programme under grant agreement No. 769826. The content of this publication is the sole responsibility of the Consortium partners listed herein and does not necessarily represent the view of the European Commission or its services.



Figure 52: Compressor no. 1 - Scrolls after failure

Conclusion

No reliable statement can be made regarding the cause of the failure of the compressor as the damage of the machine is too severe

Possible failure reasons;

1. Foreign particles from system
2. Insufficient lubrication , e.g. longer operation of the compressor while sucking liquid refrigerant and therefore washing out the oil
3. Axial Compliance of Scroll is broken (Backpressure was too high), one indicator for that failure reason is that O-Scroll has blocked Backpressure bore

Figure 53: Compressor no. 1 – Conclusions on failure reasons

After inspection all the damaged parts were exchanged, the entire compressor was carefully cleaned and rebuilt. It was tested for approx. 40 h at the OBR compressor testbed and showed the efficiency expected from a new part. No oil blackening was experienced during this test run. OBR therefore gave approval that the renewed compressor no. 1 can be used for the QUIET measurements again. It was re-sent to AVL.

5.6.5. Failure Analysis of compressor no. 2 (OBR)

OBR also inspected compressor no. 2 in detail. Again, it was found that the bearings were fine and there was enough oil inside the compressor. On the scrolls marks were found which were indications for solid particles inside the system (see Figure 54). At scroll inlet an indication for external particles like resin, polymer or adhesive was present. Generally, the scroll was full of external particles (see Figure 55 and Figure 56).

The abrasion / wear was too high for the short period of operation, but the compressor no. 2 in general was in a condition that it could be re-used for continuation of the measurements. The backpressure system of compressor no. 2 was fine, no damage was found in this region.

This project has received funding from the European Union's Horizon 2020 research and innovation programme under grant agreement No. 769826. The content of this publication is the sole responsibility of the Consortium partners listed herein and does not necessarily represent the view of the European Commission or its services.



▪ Indication for external „hard“ particles

▪ In general, too high abrasion/wear for that short time of running



Figure 54: Compressor no. 2 – Wear marks at scroll after 30 min operation



▪ Indication for external particles like polymer, resin or adhesive at Scroll Inlet



Figure 55: Compressor no. 2 – Indication for external particles at scroll inlet after 30 min operation

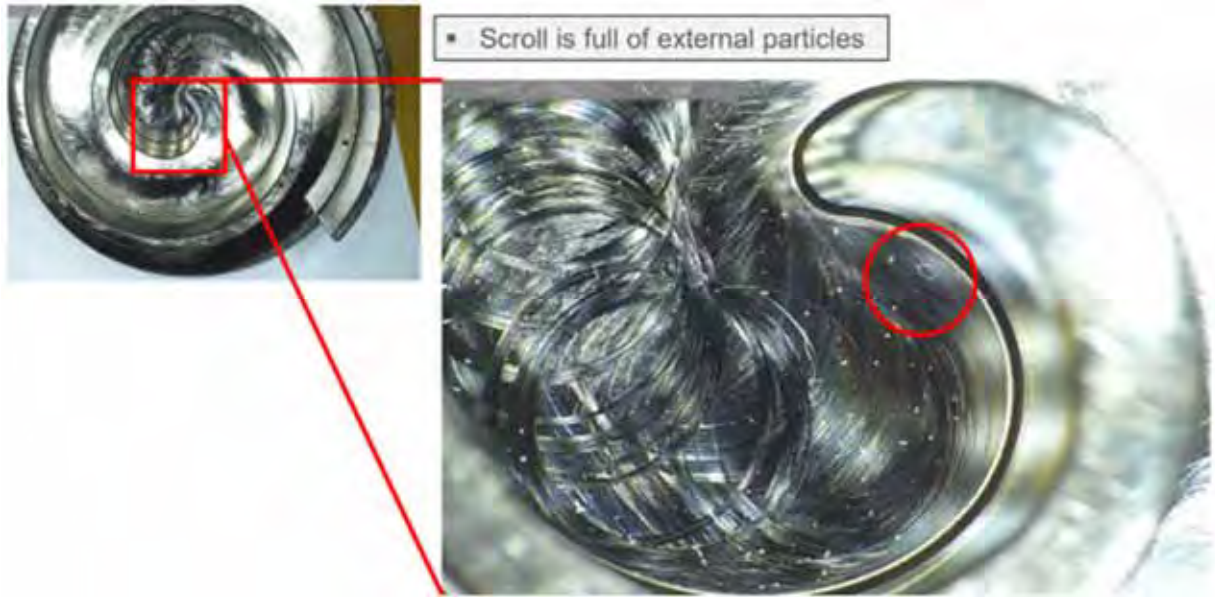


Figure 56: Compressor no. 2 –External particles at scroll inlet after 30 min of operation

After inspecting compressor No. 2 OBR stated that most probably particles (likely abrasion of compressor material or coating), remaining in the system after failure of compressor no. 1 are seen to be the reason for the relatively high wear of compressor no. 2. It was mutually agreed to again clean and flush the system several times until no more particles or blackening is found in the oil. Additionally, a special refrigerant filter, to be supplied by OBR, should be installed in front of the compressor to ensure that no particles will reach the compressor. OBR supplied this filter, which was then installed at the testbed set-up by AVL in the desired direction and position (see Figure 57). Additionally, a careful run-in and re-commissioning of the testbed should be done where OBR participates.



Figure 57: Refrigerant filter installed before the compressor on testbed

This project has received funding from the European Union's Horizon 2020 research and innovation programme under grant agreement No. 769826. The content of this publication is the sole responsibility of the Consortium partners listed herein and does not necessarily represent the view of the European Commission or its services.




After inspection all the damaged parts were exchanged, the entire compressor no. 2 was carefully cleaned and rebuilt. It was tested for approx. 40 h at the OBR compressor testbed and showed the efficiency was only slightly decreased. The difference was found to be in the range of 1 to 2 %, which was seen to be allowable. expected from of new part. No oil blackening was experienced during this test run. OBR therefore gave approval that the renewed compressor no. 2 can be used for the QUIET measurements again. It was re-sent to AVL.

5.6.6. Compatibility check of materials used in refrigerant circuit

No clear reason for the failure of compressor no. 1 could be found by OBR, and compressor no. 2 already showed too high wear after 30 min of low load operation due to particles probably remaining in system after compressor no. 1 failure. To exclude problems due to incompatibility of materials with Propane and / or the used *Fuchs POE-236* oil, which could lead to unexpected particles, the materials present in the refrigerant circuit were analysed and checked in terms of their compatibility. According to OBR, who discussed this topic with the supplier of the used oil, the following compatibilities and incompatibilities exist for *Fuchs POE-236*:

Compatible:	Neopren	Incompatible :	EPDM
	FKM / FPM		CR
	NBR		SI
	HNBR		
	PTFE		
	PA		

After checking all used components, no material incompatibilities with the used *Fuchs POE-236* were found (see Figure 58). Fuchs also stated that their oil is able and suited to be used with Propane as refrigerant.



Materials used in system components

Refrigerant hoses:	PA material inside EPDM material outside	EXV:	<ul style="list-style-type: none"> • PEEK mit Kohle • Edelstahl 1.4305 • Iglidur J350 • MS 58 • EN-AW6082-T6 • EN-AW6082-T6 eloxiert • NS42 • 17-7 PH Stainless Steel • PA66 30%GF
Refrigerant pipes:	Aluminium	PVR:	material not known, but developed by VENTREX under the premise to be used with Propane and for automotive application
Sealings:	no detailed information, but automotive parts used	Compressor:	stainless steel and Aluminium
Used sealing glue:	no detailed data available		
Evaporator:	AISI-316-stainless steel (X3CrNiMo17-13-3) Cu soldered		
Condenser /iCond:	AISI-316-stainless steel (X3CrNiMo17-13-3), stainless steel soldered		
IWT:	Aluminium		
Receiver:	Aluminium		
Measurement devices:	Stainless steel and other metals, no plastic materials		
Sensor mountings, sealings:	no detailed information, but automotive parts used		

Figure 58: Materials used in the R290 micro AC refrigerant circuit of QUIET (Step-1)

Because there were slight doubts about the glue used for sealing at some sensors it was decided to avoid this glue and to seal with Teflon ribbon and compression fittings only.

5.6.7. Re-commissioning of R290 refrigerant circuit after compressor failures

When both compressors were refurbished the entire system was very carefully cleaned again. It was not just flushed with refrigerant, but pipes and hoses were also inside mechanically cleaned with brushes wherever possible. Afterwards all parts were blown through with compressed air to make sure no particles nor liquids remain inside. All components, except IWT and iCond were exchanged with new parts. For the two mentioned ones no spare parts were present so they could not be exchanged, but they were of course internally cleaned as good as possible. The EXV and PRV were also not exchanged but visibly inspected, eventually found particles were removed.

As agreed with OBR the compressor (now no. 2) was re-installed in the system, the special refrigerant filter supplied by OBR was installed in front of the compressor. When all testbed measurement devices and analysis systems were running correct again, OBR and AVL did a joined re-commissioning.

In the course of that process the compressor was first run-in at low to medium load and all resulting measurement values were checked very carefully. After doing so for several hours an oil sample was drained, it was still slightly blackened. The refrigerant filter was checked several times during that period. After the run-in period, still some very small particles were found. So, the run-in process was continued for some more hours. After that the refrigerant filter did not show any more particles and the oil sample was not blackened. Mutually it was agreed to now As next step reference measurements have been performed to make sure that the compressor is still okay and delivers the expected performance and efficiency.

This project has received funding from the European Union's Horizon 2020 research and innovation programme under grant agreement No. 769826. The content of this publication is the sole responsibility of the Consortium partners listed herein and does not necessarily represent the view of the European Commission or its services.

The reference measurements showed values almost identical to the measurement data gained at the OBR approval testbed. Therefore, OBR gave approval to continue with the measurements. During this re-commissioning OBR also supplied rules and guide lines to AVL how the compressor shall be operated for save operation AVL implemented ramps and additional stopping criteria into its testbed control and operating system to ensure safe operation.

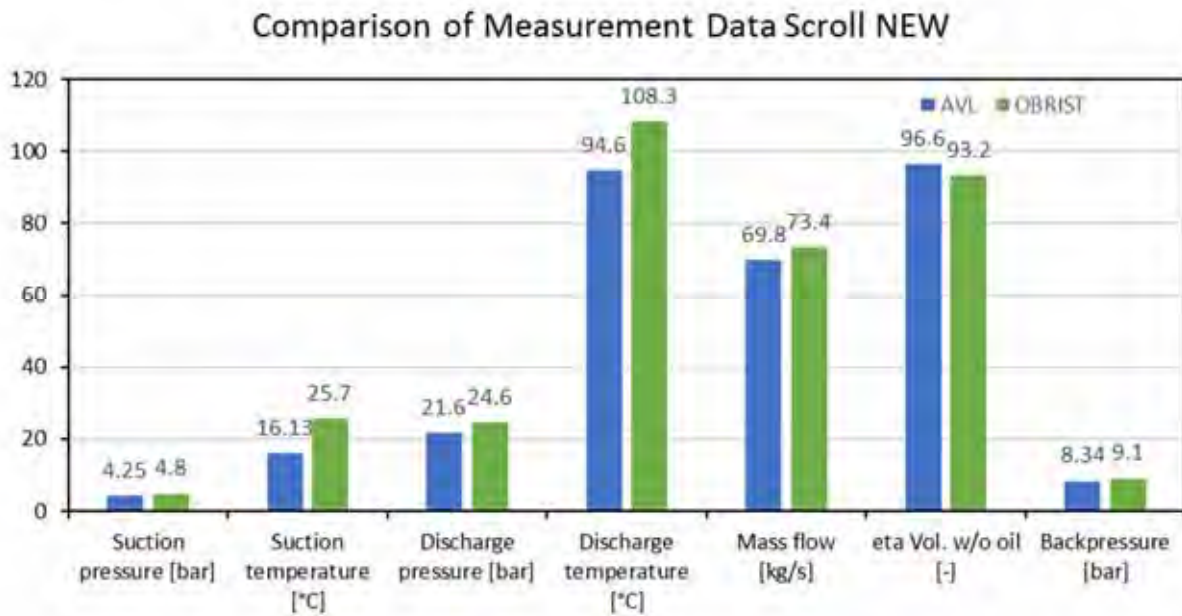


Figure 59: Reference measurement data for rebuilt compressor no. 2 (Step-1)

The entire sequence of failures of compressors no. 1 and no. 2 and the actions to understand the reasons and prevent future damages led to a delay of measurements of 2 ½ months.

5.6.8. Second failure of EXV no. 2

At the end of the reference measurements with the rebuilt compressor no. 2 again issues with the EXV (EXV no. 2 installed) appeared. The EXV showed problems in control and positioning. Immediately VEN was informed, the EXV was unmounted and handed over to VEN for inspection. VEN found particles at the entry and inside the EXV which were identified as reason for these problems (see and Figure 61). The largest particle was a polymer material with a length of approx. 6 mm and a width of less than 0.5 mm). Intense discussions were done within AVLs testbed build-up team and also with VEN and OBR, a reasonable explanation for the presence of this polymer part could not be found.

To prevent further contamination of the EXV, in agreement with VEN, a fine refrigerant filter (HyLok FI3H, with a mesh width of 15 µm) was installed in front of the EXV. During the subsequent measurements it was found that the 15 µm filter element got stuffed very quickly and led to a too big pressure drop of. Therefore, a filter element with a mesh width of 60 µm was used from then on. The spare part EXV was installed and the measurements were continued. The contaminated EXV no. 2 was cleaned / reassembled. The delay caused by this problem was 5 days.

This project has received funding from the European Union’s Horizon 2020 research and innovation programme under grant agreement No. 769826. The content of this publication is the sole responsibility of the Consortium partners listed herein and does not necessarily represent the view of the European Commission or its services.



Figure 60: 2nd failure of EXV no. 2 – particles in EXV no. 2



Figure 61: 2nd failure of EXV no. 2 – particles found

This project has received funding from the European Union’s Horizon 2020 research and innovation programme under grant agreement No. 769826. The content of this publication is the sole responsibility of the Consortium partners listed herein and does not necessarily represent the view of the European Commission or its services.

5.6.9. Continuation of heat pump modes measurement

While all the investigations on compressor failure, used oil analysis etc. were done, it was decided that the entire VTMS (Step-2) incl. the refrigerant circuit was build-up at the AC system testbed. Here the refrigerant circuit, the two coolant circuits, the HVAC unit, the radiators and the fan are present (see Figure 65 and Figure 66).

The main reason for this decision was not to lose too much time in the development process. The Step-1 build-up is part of the Step-2 build-up. For the remaining tests and the measurements of heat pump modes of Step-1 it was possible to disconnect the two coolant circuits and to connect the coolant lines of chiller and iCond to two separate conditioning units instead, which then again represents the Step-1 build-up. By re-connecting the coolant circuits to chiller and iCond the build-up afterwards will again represent Step-2.

After the compressor and EXV failures, exchange of the particular components and application of filters in front of EXV and in front of compressor the measurements with Step-1 were continued. To make sure that the results fit to the measurements performed in late 2019, first an air conditioning measurement point already measured in 2019 was re-investigated. The results were comparable to that from late 2019 (see Figure 62) and no more contamination was found in the two applied filters, therefore it was decided to continue the heat pump measurements.

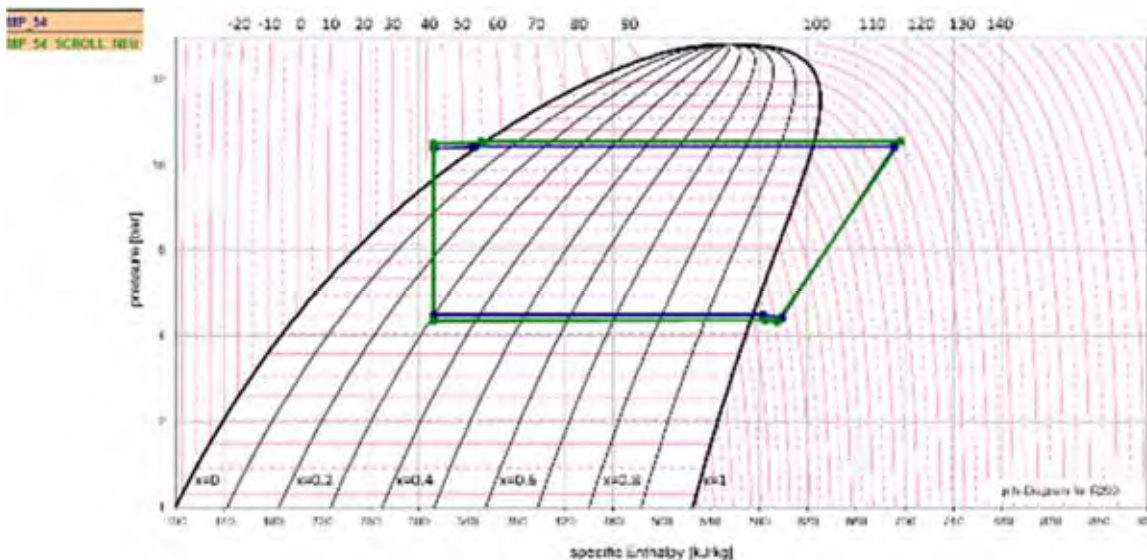


Figure 62: Comparison of AC measurement point before and after the failures

During the heat pump mode measurements of Step-1 no problems with compressor, nor with EXV were experienced. All components of the investigated system behaved as expected. After the heat pump mode measurements were finished, the analysis of the gained data was done. During these measurements it was experienced that the refrigerant exit temperature from compressor needed to be quite close to the upper temperature limit of the compressor to be able to achieve good performance and efficiency (good COP values) of the system.

As expected, the reached COP value of course also depends on the boundary conditions. Exemplary results are shown in Figure 63 and Figure 64.

This project has received funding from the European Union's Horizon 2020 research and innovation programme under grant agreement No. 769826. The content of this publication is the sole responsibility of the Consortium partners listed herein and does not necessarily represent the view of the European Commission or its services.

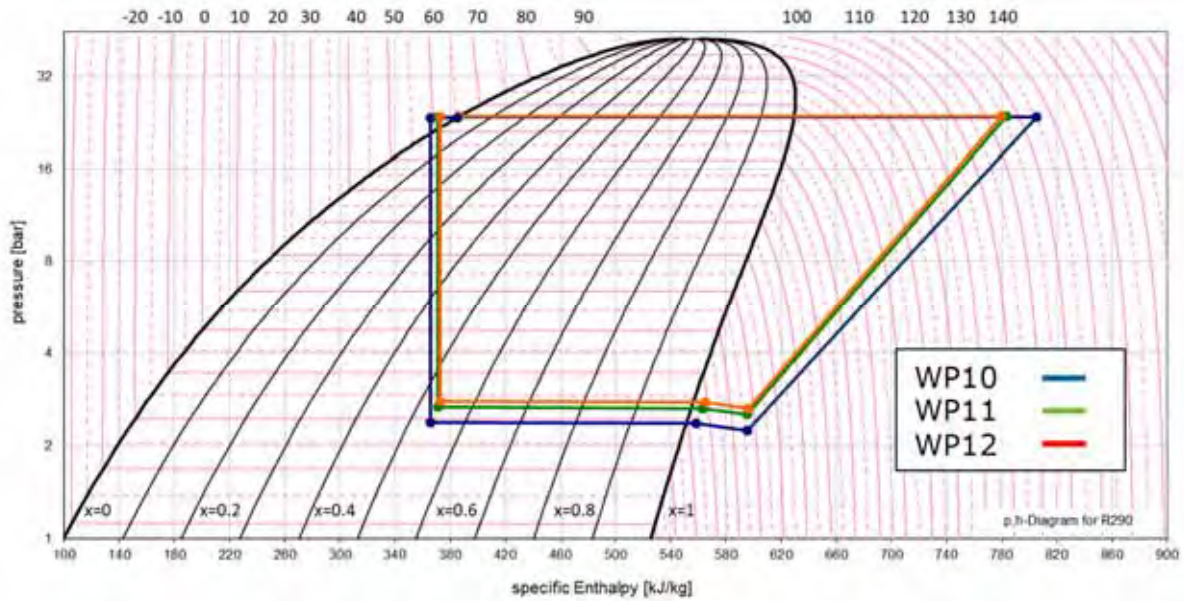


Figure 63: Result for different operational conditions in heat pump mode measurements

MP	Comp_in		Comp_out		n_Comp rpm	mdot_ges kg/h	sh_Chiller_out K	P_el_comp W	Q_c_iCond W	COP [-]
	bar	°C	bar	°C						
WP04	2.00	-1.5	23.98	138.5	7998	43.94	0.14	2823	4678	1.66
WP05	2.14	4.4	24.30	138.9	7998	47.05	4.28	2899	5187	1.79
WP06	2.20	5.5	24.30	137.8	7998	48.88	5.60	2936	5357	1.82
WP08	2.53	7.1	23.57	126.0	3996	25.96	5.37	1557	2775	1.78
WP09	2.65	7.4	23.57	124.2	3996	26.86	5.27	1581	2874	1.82
WP10	2.24	6.4	23.56	135.1	3996	24.18	4.89	1489	2602	1.75
WP11	2.53	6.9	23.67	126.3	3996	26.53	5.39	1558	2841	1.82
WP12	2.64	7.6	23.70	124.7	3996	27.74	5.40	1587	2973	1.87
WP14	2.91	11.6	23.29	137.0	1996	13.96	4.42	907	1582	1.74
WP15	2.97	12.1	23.31	135.3	1996	14.75	4.87	907	1602	1.77
WP17	2.91	12.0	23.40	138.9	1996	14.43	5.03	943	1681	1.78
WP18	2.99	11.7	23.38	137.0	1996	14.77	4.05	943	1719	1.82

Figure 64: COP values achieved during heat pump mode measurements for different operational conditions

The measurement results of Step-1 show that the present newly developed HVAC system using R290 as refrigerant is able to achieve good COP values in heat pump mode, even with the very compact layout used in the present project. It can and should therefore be used to achieve remarkable energy savings in the passenger cabin climatization of future electrified vehicles and to increase their driving range.

This project has received funding from the European Union’s Horizon 2020 research and innovation programme under grant agreement No. 769826. The content of this publication is the sole responsibility of the Consortium partners listed herein and does not necessarily represent the view of the European Commission or its services.

6. Set-up, instrumentation and commissioning of the entire VTMS (Step-2) (AVL)

For the measurements of this work step the entire VTMS incl. the refrigerant circuit was necessary. As described in 5.6.9 it was build-up at the AC system testbed while the investigations on compressor and used oil analysis were done. Here now the refrigerant circuit, the two coolant circuits, the HVAC unit, the radiators and the fan are present (see Figure 65 and Figure 66). By re-connecting the coolant circuits to chiller and iCond, instead of using two conditioning units as in Step-1, the build-up represented the entire VTMS. The air going through radiators and HVAC unit was supplied by two separate conditioning units, where the particular air volume flow and temperature were controlled.

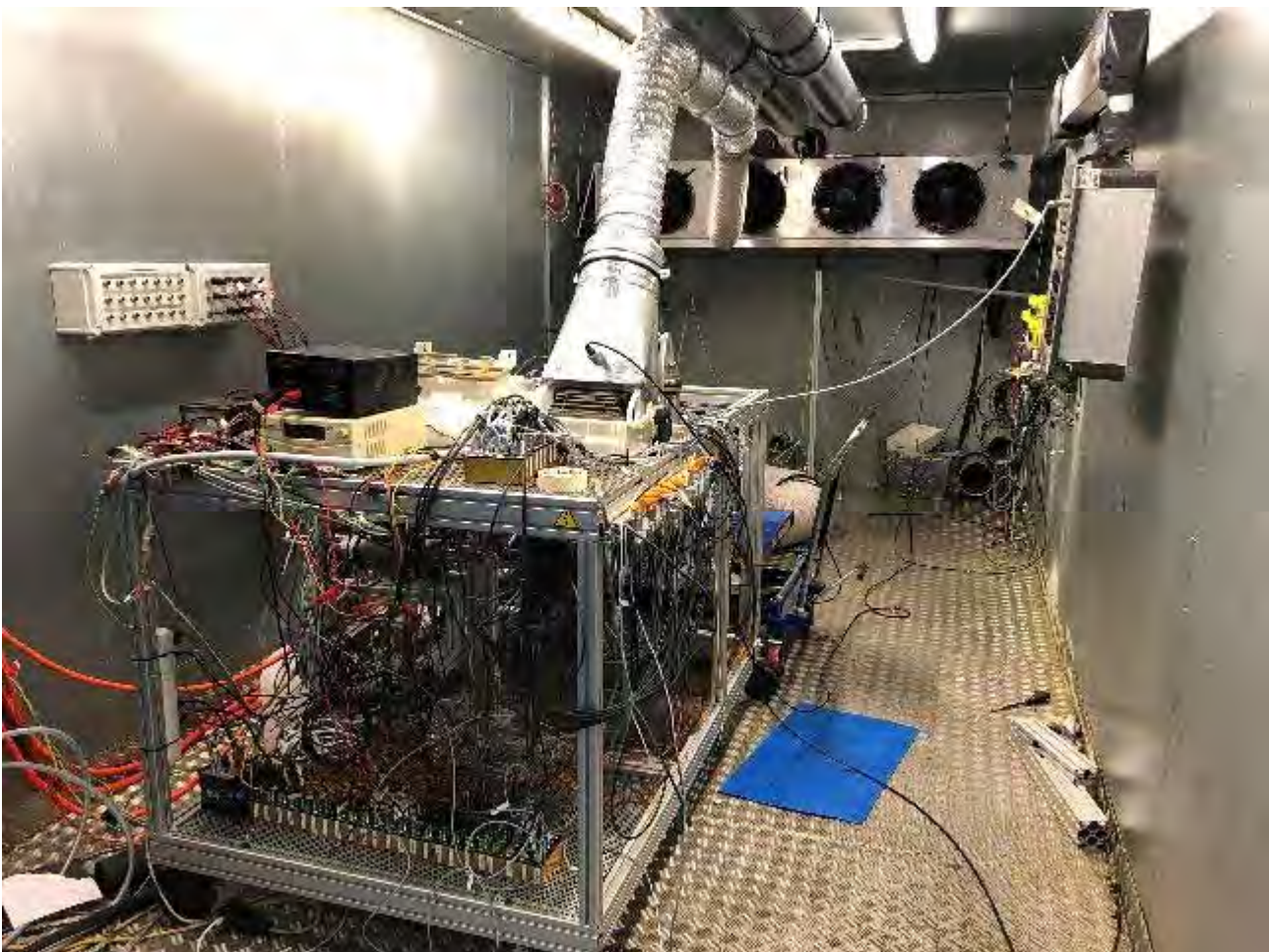


Figure 65: Build-up and instrumentation of Step-2 (entire VTMS) at AC system testbed

This project has received funding from the European Union's Horizon 2020 research and innovation programme under grant agreement No. 769826. The content of this publication is the sole responsibility of the Consortium partners listed herein and does not necessarily represent the view of the European Commission or its services.

D4.2: ASSESSMENT REPORT FOR ENHANCED ENERGY EFFICIENCY AND COMFORT (PU)



Figure 66: Build-up and instrumentation of Step-2 (entire VTMS) at AC system testbed

The built-up system of Step-2 was instrumented with numerous temperature, pressure and mass flow (turbines and MIDs) sensors (see Figure 67) to be able to gain all the data necessary for assessment and control optimization of the entire VTMS. The radiators were all instrumented with a net of temperature sensors before and after as well. So, also the air temperature and temperature delta could be measured.

All the LIN/CAN control functions of coolant valves, coolant pumps etc. were implemented into the control system of the AC system testbed. Not to confuse the LIN/CAN control system care had to be taken that e.g. the LIN/CAN numbering of valves and pumps is correct.

This project has received funding from the European Union's Horizon 2020 research and innovation programme under grant agreement No. 769826. The content of this publication is the sole responsibility of the Consortium partners listed herein and does not necessarily represent the view of the European Commission or its services.

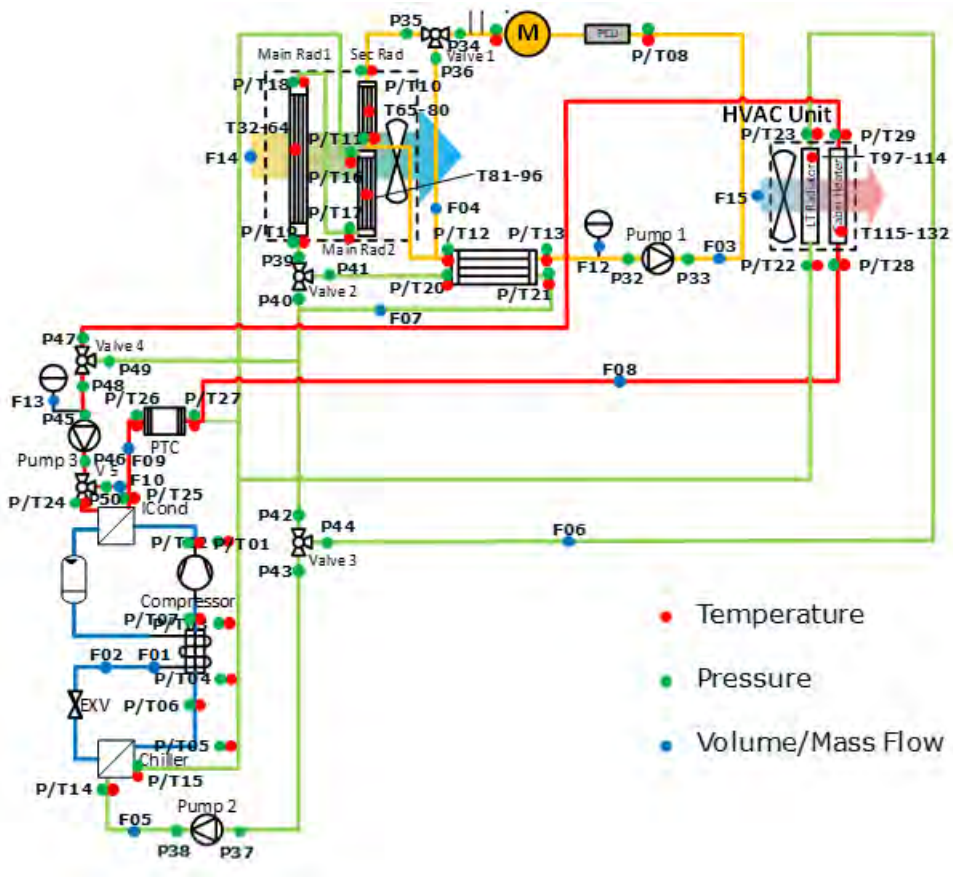


Figure 67: Instrumentation of testbed build-up for Step-2 (entire VTMS)

This project has received funding from the European Union’s Horizon 2020 research and innovation programme under grant agreement No. 769826. The content of this publication is the sole responsibility of the Consortium partners listed herein and does not necessarily represent the view of the European Commission or its services.

7. Development of control strategy for entire VTMS (AVL)

In parallel to the set-up, commissioning and measurements of Step-1 and Step-2 on the testbed the control strategy for the entire VTMS was developed (see Figure 68) and distributed to AIT and UoZ. It is based on high sophisticated HVAC + VTMS systems and strategies to reach high energy efficiency. Within the QUIET consortium, corresponding boundary conditions for the control strategy optimization were developed and agreed by all involved partners (see Figure 69). This data was handed over to UoZ for further processing as well. For further information on these topics it is referred to deliverable D5.3.

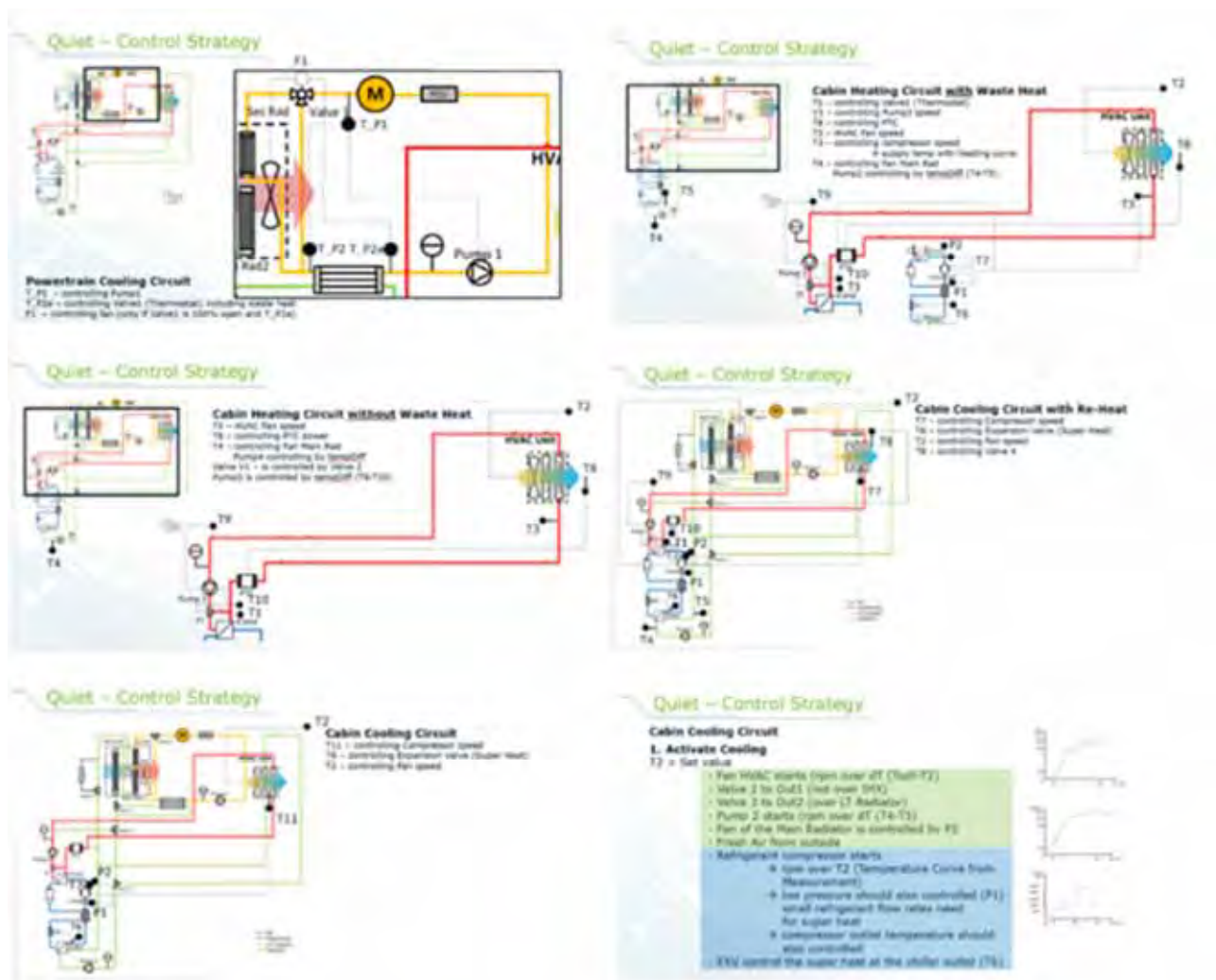


Figure 68: Control strategy for entire VTMS

(excerpt, for details see Deliverable D5.3)

This project has received funding from the European Union's Horizon 2020 research and innovation programme under grant agreement No. 769826. The content of this publication is the sole responsibility of the Consortium partners listed herein and does not necessarily represent the view of the European Commission or its services.

	Test & Evaluation conditions			
	Hot		Cold	
	Energy benchmark	Comfort evaluation	Energy benchmark	Comfort evaluation
Temperature	+40°C	+32°C	-10°C	+5°C
Humidity	High	Moderate	n/a	n/a
Solar load	High	Moderate	None	None
Passengers	2			
Recirculation mode	Same as baseline			
Air flow distribution mode	Same as baseline			
Speed profile	WLTC CCT	50..70 km/h	WLTC CCT	50..70 km/h
	Unit	Parameter range for optimisation		
		Heating	Cooling	Cooling& reheat
Speed pump 2	[1/min]	1600..8000	←	←
Speed pump 3	[1/min]	1600..8000	←	←
Blower flow rate	[m³/h]	250	380	←
Compressor speed	[1/min]	1500..8000	←	←
Compressor speed gradient	[u/min/s]	200		
EXV opening	[mm²]	0...8	←	←
Cabin inlet temp	[°C]	40..65	5..30	←
LTR temp setpoint	[°C]	N/A	=Cabin inlet	(5-8)
HC temp setpoint	[°C]	= Cabin inlet.	N/A	5..30
Main radiator fan mass flow rate*	[kg/s]	0.5 .. 0.75	←	←
Speed pump 1***	[1/min]	1600..8000	←	←
Main Radiator mass flow rate without fan	[kg/s]	0 ... 0.6	←	←
IR panel temperature	[°C]	20..60	N/A	N/A

Figure 69: Boundary conditions for control strategy of entire VTMS

(excerpt, for details see Deliverable D5.3)

In addition to the development of the control strategy, support was given in development of safety features and procedures to start, control and shut-down the AC and VTMS. Here information available on min/max range, temperature and pressure limits, speed ramps etc. for the compressor were exchanged. Of course, this was done in agreement with OBR the developer of this component. Parameter settings (start pump speeds at coolant circuits, compressor start speed and speed ramps, and EXV start / shutdown openings) for safe starting, operation and shutdown were defined. This was done based on the experiences from the Step-1 and Step-2 measurement campaigns. These safety features were implemented into the HVAC control unit by AIT (see deliverable D5.3)

This project has received funding from the European Union's Horizon 2020 research and innovation programme under grant agreement No. 769826. The content of this publication is the sole responsibility of the Consortium partners listed herein and does not necessarily represent the view of the European Commission or its services.

8. Commissioning of the control board for the entire VTMS (Step-2) on testbed

Based on the control strategy developed by AVL, the VTMS control functions for all valves, pumps, HVAC unit, etc. will be implemented into a corresponding control board /control unit, developed by AIT. This CU should also communicate with the already existing HVAC-CU and the VCU. The optimization of the control functions and parameter sets was done by UoZ

When the control board was as ready as necessary, AVL and AIT did a joined commissioning of the control board (see Figure 70 and Figure 71) at the AC system testbed to make sure all functions can be controlled as desired when performing the Step-2 measurements. Additionally, this was a good opportunity for AIT to test the developed control board hardware and software on the real VTMS hardware before it will be implemented into the demonstrator vehicle. Of course, the board was connected to the testbed system via standard plugs and connectors, but not with a connector later used in the demonstrator vehicle. Before implementing it into the vehicle this will be updated accordingly. After finishing the Step-2 measurements this control board was be given back to AIT, where further programming will take place. Finally, it will be implemented into the demonstrator vehicle.

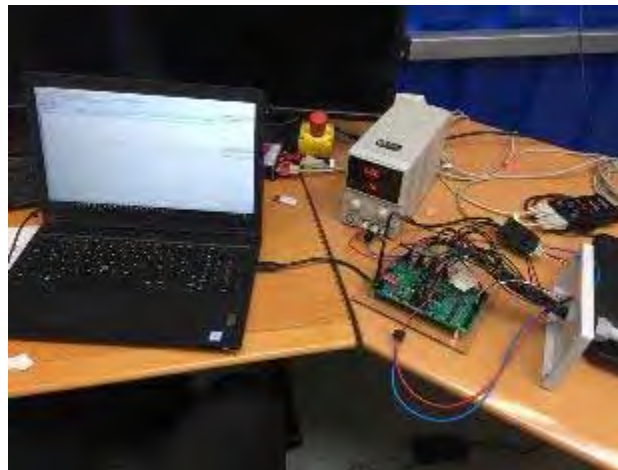


Figure 70: Commissioning of control board for entire VTMS at AC system testbed

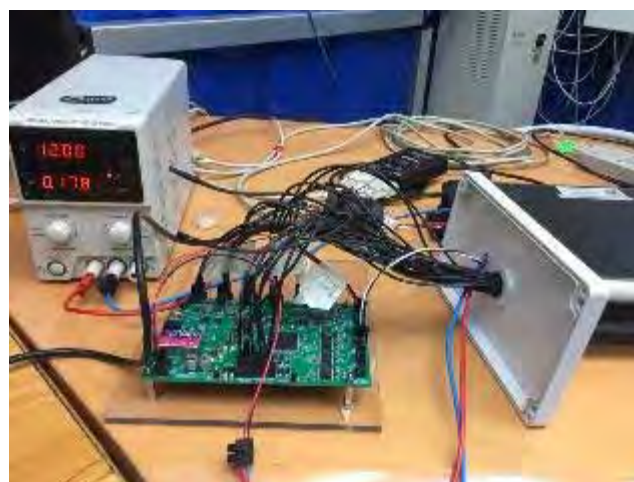


Figure 71: Control board for entire VTMS

This project has received funding from the European Union's Horizon 2020 research and innovation programme under grant agreement No. 769826. The content of this publication is the sole responsibility of the Consortium partners listed herein and does not necessarily represent the view of the European Commission or its services.



9. Measurements of the entire VTMS (Step-2) (AVL)

After the measurements of Step-1 had been finished the coolant circuits were re-connected to chiller and iCond to represent the Step-2 build-up. Now the R290 refrigerant circuit, the two coolant circuits, the HVAC unit, the radiators and the fan were present at the AC system testbed. Therefore, the entire VTMS was build-up to be able to perform measurements of Step-2. The waste heat of e-motor and power electronics is represented by an electric heater (PTC) implemented instead. In agreement with the partners, no measurements using waste heat were done within the present measurement campaign.

Before starting measurements for Step-2 all applied instrumentation, the control functions and the entire testbed system were re-checked in terms of correct function. When all tests were passed, the measurements for Step-2 were started. Here the build-up were tested in terms of its ability to fulfil the needs of cooling and heating modes under defined conditions (summer and winter load cases). The main target of these measurements was to derive and optimize the parameters for an energy efficient VTMS control. Of course, they also serve to check the ability of the VTMS to achieve the desired energy savings and efficiency targets.

As starting point for the Step-2 measurements performed at the testbed, parameter sets derived from simulations done by UoZ were used (see deliverable D5.3). This was done to save time by not trying parameter combinations leading to undesired behaviour and results.

In the project consortium, and in agreement with HRE who will supervise the later vehicle tests, it was agreed to investigate one summer load case and one winter load case in order to check the system ability to reach the desired performance and to support energy savings and driving range increase in future electric vehicles.

9.1. Measurements of summer load case

In agreement with the project partners the following boundary conditions were used for the summer load case (see Table 13):

Table 13: Summer load case, boundary conditions

Mode	T_amb	mdot_Cooling Package	rH_amb	HVAC Blower Flow Rate	Modus HVAC	Comp_Speed	EXV	Pump 2	Pump 3	Valve 2	Valve 3	Valve 4	Valve 5	super heat chiller out	PTC Heater	Simulation
	°C	kg/s	%	m³/h		rpm	steps	rpm	rpm	%	%	%	%	K	%	
Cooling Circuit	40	0,55	60	380	0 VENT	3600		1800	1800	0% to WT	100% back to Pump2	100% from Cooling Package	100% over iCond	5	0	In Simulation Air Cabin Inlet 20°C

During summer load case measurements of Step-2 no problems with compressor, nor with EXV were experienced. All components of the investigated system behaved as expected. For results and parameters achieved from summer case measurements see Table 14.

This project has received funding from the European Union's Horizon 2020 research and innovation programme under grant agreement No. 769826. The content of this publication is the sole responsibility of the Consortium partners listed herein and does not necessarily represent the view of the European Commission or its services.

Table 14: Parameters gained from summer case measurement

	Air	Air	Air	Air	Air	Air	Air							Ref	EL	Air
	LTR in	MR 2 in	MR 2 in	MR 2 in	LTR in	LTR in	HVAC	Comp	EXV	Pump 2	Pump 2	Pump 3	Pump 3	Chiller out	PTC	HVAC out
	temp	temp	vdot	mdot	relH	vdot	Mode	rpm	steps	rpm	vdot	rpm	vdot	sh	Q	temp
	°C	°C	m³/h	kg/s	%	m³/h		rpm	steps	rpm	l/min	rpm	l/min	K	W	°C
S_WP1	39,7	40,0	1776	0,54	60,5	240	2	3595	1370	6000	20,3	3000	6,5	3,8	0	22,1
S_WP2	40,0	40,1	1776	0,54	60,5	186	2	3595	1370	6000	20,2	3000	6,4	2,3	0	19,8
S_WP3	39,8	40,0	1778	0,54	60,0	186	2	3596	1350	4650	15,1	3000	6,4	2,5	0	19,6
S_WP4	39,8	40,0	1777	0,54	60,4	182	2	3595	1331	3400	10,3	3000	6,4	2,3	0	19,9
S_WP5	39,7	40,0	1777	0,54	59,7	164	2	3595	1280	1800	4,5	3000	6,4	0,9	0	20,1
S_WP6	40,9	40,1	1777	0,54	56,3	290	2	7698	1279	1800	4,5	3000	6,6	2,8	0	22,3

Unlike the simulation an air leakage is seen in the HVAC unit and around the low temperature radiator (LTR). This is the reason for the here experienced lower air mass flow over LTR. As expected, the reached COP value of course also depends on the boundary conditions. Exemplary results of the summer case measurements are shown in Figure 72 and Figure 73.

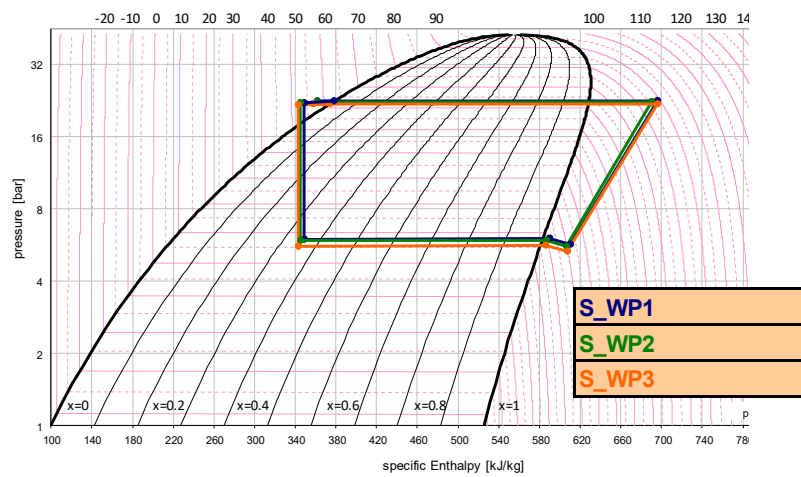


Figure 72: Exemplary results of Step-2 summer case measurements (S_WP1 to S_WP3)

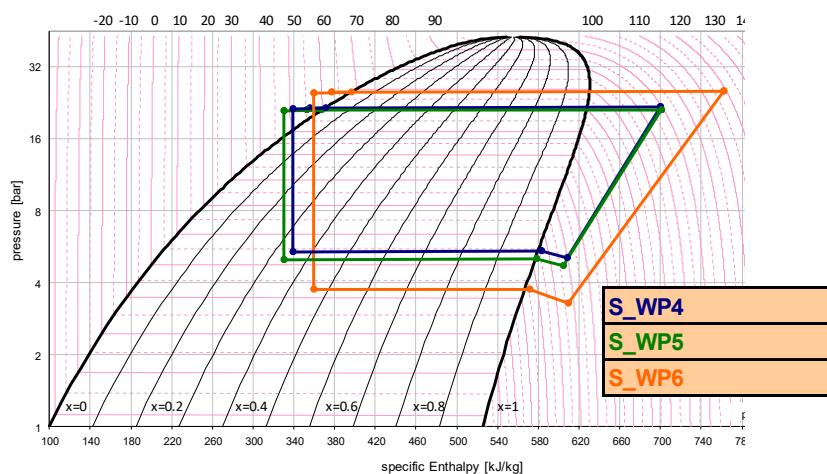


Figure 73: Exemplary results of Step-2 summer case measurements (S_WP4 to S_WP6)

This project has received funding from the European Union’s Horizon 2020 research and innovation programme under grant agreement No. 769826. The content of this publication is the sole responsibility of the Consortium partners listed herein and does not necessarily represent the view of the European Commission or its services.



It was also found that it was difficult to achieve the target HVAC unit air outlet temperature of 20°C. With the applied boundary conditions, the lowest value reached was approx. 22 °C. To reach the desired 20°C the air mass flow over the HVAC needed to be reduced. With increased compressor speed, here almost the max. value was applied, it was possible to reach the desired lower outlet air temperature, even for a higher air mass flow, but of course with reduced efficiency. The results suggest that the limiting component is the low temperature radiator (LTR) installed in the HVAC unit instead of the original evaporator. Due to the limited space inside the HVAC unit this heat exchanger is most likely not thick enough / not capable, to allow the heat transfer necessary to reach the target value. The maximum transferable power at the LTR, for the applied operational conditions, is approx. 4 kW. In the demonstrator vehicle air leakage in the HVAC unit and around the LTR should be carefully considered and reduced as much as possible.

9.2. Second failure of compressor no. 2

At the end of the summer case measurements the compressor no. 2 suddenly failed again. No pressure increase over compressor was possible, and it even could not reach compressor speeds set on the testbed control board. AVL immediately stopped the measurements and informed OBR. Mutually it was agreed to unmount compressor no.2 from the testbed build-up and to send it to OBR for inspection. Additionally, measurement data gained before the failure (last several hours) was supplied to OBR. In order not to delay the measurements too much, the spare part compressor no. 1 was installed into the system to be able to continue. The coloration and the condition of the oil were manually checked and the system was carefully flushed and re-filled with the correct amount of refrigerant before re-starting measurements.

During inspection of the compressor by OBR, a massive damage was found. The reason for this is an event in which a remarkable amount of liquid refrigerant has entered the compressor. This led to an unexpectedly high axial movement of the scroll and to mechanical damage (see Figure 74). First it was suspected that this fatal event was caused by maloperation of the testbed system by the operator. A detailed investigation of the measurement data before the failure (several hours measurement period) showed that this was definitely not the case.

This project has received funding from the European Union's Horizon 2020 research and innovation programme under grant agreement No. 769826. The content of this publication is the sole responsibility of the Consortium partners listed herein and does not necessarily represent the view of the European Commission or its services.

OE eR290 01-02 failure analysis

- Backside of O-Scroll is completely deformed and destructed, a lot of abrasion is visible
- Deformation and abrasion is caused by break outs from O-Scroll



Figure 74: Damage of compressor no. 2 (Source OBR)

After inspecting the damaged EXV (see 9.3), which happened right after installation of the spare part compressor no. 1, it was found that a failure of the EXV, especially the self-acting movements, was most likely also the reason for the failure of the compressor no. 2.

Although the reason of the failure was seen in a failure of the EXV, OBR recommended to slightly internally rework the compressor to make it less sensitive to such events. Because the remaining Step-2 measurements would only need 1 to 2 more days, it was agreed between AVL and OBR to proceed and finish without the modification. For the compressor applied for the later demonstrator vehicle tests this modification was highly recommended. Therefore, this information was passed on to the team responsible for the construction of the demonstrator vehicle. The compressor used there was sent to OBR to be reworked as well. After this process it will be re-installed into the demonstrator vehicle.

9.3. Third failure of EXV no.1

After the compressor no. 1 was installed into the system all filters present in the system were inspected. While system tests were performed suddenly the EXV started to react unexpectedly. It started to move and to change its position / opening cross section without setting values at the testbed control board. Inputs did not lead to expected changes and most likely wrong positioning information was replied by the EXV.

The testbed was stopped immediately, the EXV was unmounted and VEN was informed about the problems. In agreement the spare part EXV was installed and the damaged EXV was sent to VEN for inspection. While AVL installed the spare part EXV and prepared the system for re-start of measurements, VEN already inspected the damaged EXV. It was found that corrosion had happened at an electric connection, leading to wrong internal signal processing. The corrosion was most likely caused by the high air humidity present in the test chamber for the summer load case.

This project has received funding from the European Union's Horizon 2020 research and innovation programme under grant agreement No. 769826. The content of this publication is the sole responsibility of the Consortium partners listed herein and does not necessarily represent the view of the European Commission or its services.



The corrosion problem of the EXV, especially the unexpected behavior of closing and opening the EXV cross section without changing values on the test bed control board, was most likely already the reason for the failure of the compressor.

VEN asked AVL to wait with re-starting measurements until the EXV was repaired / sealed and tested. This was done in order to prevent another EXV failure and a possible resulting compressor failure. After the sealing and leakage tests were passed properly the EXV was re-installed into the testbed. All tests now showed proper behavior, so the remaining measurements were continued.

The information about the corrosion problems / leakage of the EXV was also given to the team responsible for building-up of the demonstrator vehicle. The EXV used there was sent to VEN to be sealed and leak tested as well. After this process it will be re-installed into the demonstrator vehicle.

9.4. Measurements of winter load case

When the entire system was back in operation and appropriate tests were carried out, the measurements of the winter load case were performed.

In agreement with the project partners the following boundary conditions were used for the winter load case (see Table 15):

Table 15: Winter load case, boundary conditions

Mode	T_amb	m _{dot} _Cooling Package	rH_amb	HVAC Blower Flow Rate	Modus HVAC	Comp_Speed	EXV	Pump 2	Pump 3	Valve 2	Valve 3	Valve 4	Valve 5	super heat chiller out	PTC Heater	Simulation
	°C	kg/s	%	m ³ /h		rpm	steps	rpm	rpm	%	%	%	%	K	%	
Cabin Heating Circuit without Waste Heat (winter load case)	-10	0,15	n.n.	200	2 HEAT	3600		1800	1800	0% to WT	0% from LT Radiator	100% from Cabin Heater	100% over iCond	5	0-100	In Simulation Air Cabin Inlet 40°C

During winter load case measurements of Step-2 no problems or hardware failures were experienced throughout these measurements. All components behaved as expected. For results and parameters achieved from winter case measurements see Table 16. As expected, the desired HVAC outlet air temperature could not be reached by pure heat pump operation. Additional energy had to be brought into the system by the included PTC heater.

This project has received funding from the European Union’s Horizon 2020 research and innovation programme under grant agreement No. 769826. The content of this publication is the sole responsibility of the Consortium partners listed herein and does not necessarily represent the view of the European Commission or its services.



Table 16: Parameters gained from winter case measurement

	Air	Air	Air	Air	Air	Air	Air							Ref	EL	Air
	LTR in	MR 2 in	MR 2 in	MR 2 in	LTR in	LTR in	HVAC	Comp	EXV	Pump 2	Pump 2	Pump 3	Pump 3	Chiller out	PTC	HVAC out
	temp	temp	vdot	mdot	relH	vdot	Mode	rpm	steps	rpm	vdot	rpm	vdot	sh	Q	temp
	°C	°C	m³/h	kg/s	%	m³/h		rpm	steps	rpm	l/min	rpm	l/min	K	W	°C
W_WP1	-9,2	-12,1	485	0,17	67,2	120	0	3596	461	5500	2,2	1850	3,8	0,4	0	27,8
W_WP2	-9,1	-12,2	485	0,17	68,4	120	0	3595	461	5500	2,2	1850	3,8	0,4	250	28,3
W_WP3	-8,4	-12,2	485	0,17	67,0	121	0	3596	440	5500	2,3	1850	4,1	0,2	300	34,4
W_WP4	-9,0	-12,2	485	0,17	51,1	126	0	3595	380	5500	2,5	1900	4,4	0,4	500	34,9
W_WP5	-9,3	-12,3	486	0,17	59,0	128	0	3595	371	5500	2,5	1700	3,9	0,5	500	36,8
W_WP6	-8,7	-12,3	485	0,17	69,2	128	0	3595	350	5500	2,4	1700	4,1	0,4	650	39,7

As could already be seen in the summer case measurements, air leakage occurs in the HVAC unit in contrast to the simulation. This is the reason for the lower air mass flow over LTR. As expected, the reached performance of course also depends on the boundary conditions. Exemplary results are shown in Figure 75 and Figure 76.

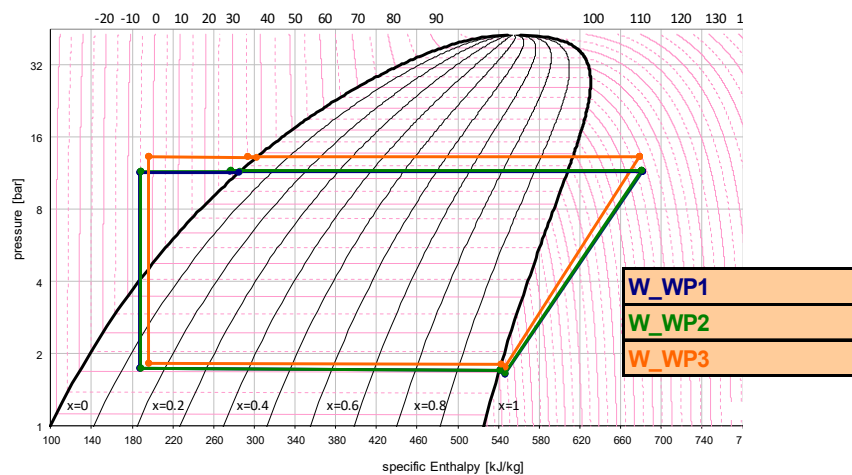


Figure 75: Exemplary results of Step-2 winter case measurements (W_WP1 to W_WP3)

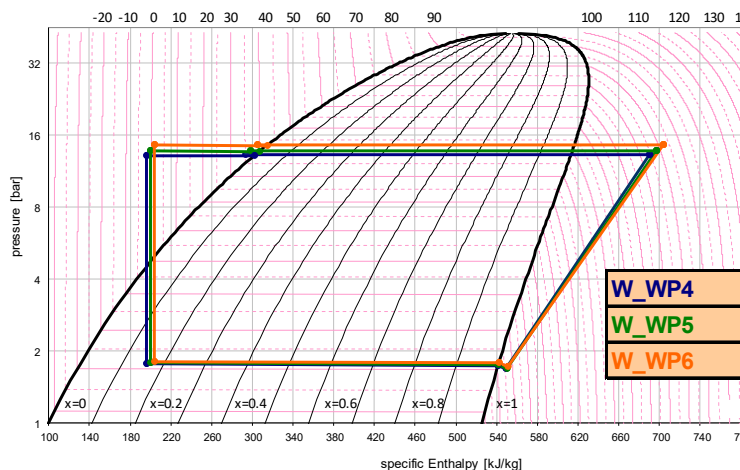


Figure 76: Exemplary results of Step-2 winter case measurements (W_WP4 to W_WP6)

This project has received funding from the European Union’s Horizon 2020 research and innovation programme under grant agreement No. 769826. The content of this publication is the sole responsibility of the Consortium partners listed herein and does not necessarily represent the view of the European Commission or its services.



The results of the measurements show a high subcooling under all conditions. The target to superheat 5K after the chiller is not always possible. The need to superheat at the compressor inlet limits the compressor speed. A possible improvement could be to lower the filling amount of refrigerant. On the demonstrator vehicle this will anyway be the case because the additional measurement devices and corresponding piping will not be present. Therefore, a measurement for derivation of correct refrigerant filling amount is recommended for the demonstrator vehicle system, which is slightly different due to the absence of several measurement devices, before starting the measurement series on the dyno. The desired air outlet temperature could, under the applied boundary conditions, only be reached by support from the electric heater (PTC). This is of course possible, but on the other hand, slightly reduces the overall efficiency of the system. HVAC air leakage should be carefully considered and reduced as much as possible.

This project has received funding from the European Union's Horizon 2020 research and innovation programme under grant agreement No. 769826. The content of this publication is the sole responsibility of the Consortium partners listed herein and does not necessarily represent the view of the European Commission or its services.



10. Conclusions

The R290 safety concept from VEN was already presented in detail in Deliverable D4.1. It contains a special PRV to be installed either in the low-pressure or the high-pressure part of the Propane (R290) refrigerant circuit. VEN developed this PRV and ensured to lead the flammable R290 away from any potential source of ignition in case of an accident. To ensure this is the case, a piping can be attached at the outlet side of the pressure relief valve. According to the developed safety concept the PRV was implemented into the testbed set-up and the demonstrator vehicle, it was placed in the high-pressure part of the R290 refrigerant circuit. Without any safety instance the safety concept is seen to be functional and suitable for safe operation of the refrigerant circuit using R290. To get type approval for usage of R290 refrigerant circuits in automotive applications now this topic needs to be brought to the standardization institutes (ISO, European parliament standardization, SAE, etc.) responsible for the different markets. A possible roadmap on how this process should be done is also described in deliverable D4.1.

The thermal storage tank based on PCM showed promising results on the approval tests of RUB / IFAM. Detailed assessment will only be possible after the tests on the demonstrator vehicle. RUB is in the experimental and planning phase to create conditions for producing high-performance PCM storages. The specifications of the components place high demands on the new systems, which require considerable investment.

The radiative heating surfaces (so-called *powerfilms*) to be developed and adapted for the demonstrator vehicle by ATT have already proven their ability to increase vehicle heating efficiency and to save heating power in the past reporting period. The assessments were done by means of simulations. In the present reporting period the *powerfilms* and the corresponding control unit were manufactured and are currently prepared to be installed into the demonstrator vehicle. This installation will take place most likely within the next month. When this is done they will show their potential in the following demonstrator vehicle tests.

The activities within WP4 focused on the evaluation of the different technological solutions as well as the assessment of the HMI framework with respect to the thermal comfort. The assessment of the thermal comfort in confined space, such as a vehicle cabin, is a complex task and a well-known index used to estimate global thermal comfort of people is the Predicted Mean Vote (PMV) Index is used.

Various realistic scenarios have been developed and evaluated with the simulation approach described in deliverable D2.2. The results from the scenarios show that in steady state conditions the HVAC system and the heating panels are able to give to the passengers a comfortable thermal state, with small differences between passengers which space between slightly cold thermal state (PMV ~ -0.5) and slightly warmer thermal state (PMV ~ +0.5).

Additionally, a use case has been developed to compare the heating panel solution with the standard HVAC system solution. The standard concept consists of the HVAC system keeping the cabin temperature to 20°C while in the alternative solution the cabin temperature is reduced to 15°C and the heating panels are turned on to achieve a neutral thermal state. The heating panel solution is able to achieve at steady state similar thermal state conditions. Moreover, the solution with the heating panels enables to achieve energy reduction of about 11% and to increase the thermal comfort (faster heat up response).

The refrigerant circuit (Step-1) and the entire VTMS (Step-2) of the QUIET vehicle were built-up, instrumented and commissioned at the AVL AC system testbed. Different problems with the used prototype parts, with contamination of the refrigerant circuit etc. occurred during commissioning the testbed build-up

This project has received funding from the European Union's Horizon 2020 research and innovation programme under grant agreement No. 769826. The content of this publication is the sole responsibility of the Consortium partners listed herein and does not necessarily represent the view of the European Commission or its services.



and performing the measurements. They were the reasons for the delay. An important part of the QUIET work package WP4 content is the development of a new refrigerant circuit based on refrigerant R290 (Propane). Here several new parts, suited to this special refrigerant, needed to be developed and tested. In highly sophisticated development projects, unfortunately, such problems may occur but are of course not desired. All involved project partners invested a huge effort to inspect damaged parts in detail, to analyze the oil, material compatibilities, etc., find the reasons for particular problems and to provide possible solutions as soon as possible.

Although a relatively huge delay happened in the testing schedule of the current reporting period, finally the planned measurements were started and until delivery of the present final version of the deliverable D4.2 they are finished. As mentioned above, the reasons for the delay are to see in 1.) late delivery of parts which led to delays on testbed build-up, see deliverable D4.1, and 2.) in several, different hardware failures during measurement campaigns.

The measurements of Step-1 (micro AC circuit using R290 (Propane) as refrigerant) showed that the developed system is able to provide good cooling performance. In heat pump mode also good COP values can be achieved. Therefore, this kind of system is valid to be applied in future hybrid / electric vehicles to support the desired energy savings and driving range extension.

The results of the measurements of Step-2 (micro AC circuit using R290 as refrigerant, combined with the coolant circuits of the VTMS) led to parameters which can be used to update and calibrate the simulation models of AIT and UoZ. These results were handed over to these partners. The results also proved the entire systems ability to provide desired energy savings. Findings from the summer and winter load point tests were provided to the developers of the used prototype hardware (OBR and VEN) and the partners who build-up the demonstrator vehicle.

According to the results achieved in the performed testbed measurements it can be concluded, that the AC / VTMS system, featuring R290 as refrigerant and developed within the QUIET project is able to provide the desired performance. Based on the testbed measurements the expected energy savings seem to be achievable in the vehicle application.

The HVAC control strategy was developed by AVL and handed over to AIT for implementation into a holistic simulation model and into the control unit and to UoZ for further optimization. The strategy is based on experience in HVAC control development and on newest findings on holistic, sustainable and energy efficient vehicle thermal management systems. The boundary conditions for the HVAC control optimization were developed by AVL and HRE, again here most possible energy efficient application of the applied components and VTMS system was the focus. Additionally, min/max parameters and procedures for safe operation of AC circuit and coolant circuits were provided to AIT, these data will also be used to implement safety measures into the new HVAC / VTMS control unit (see deliverable D5.3).

Outlook: As a next step the validation of the resulting energy saving potential in real vehicle application will be performed. This will be done by chassis dyno test of the demonstrator vehicle which currently is build-up and prepared. The corresponding results will be presented in deliverable D5.4.

This project has received funding from the European Union's Horizon 2020 research and innovation programme under grant agreement No. 769826. The content of this publication is the sole responsibility of the Consortium partners listed herein and does not necessarily represent the view of the European Commission or its services.



11. Bibliography

- [1] DIN EN ISO 7730. 2003. “Analytische Bestimmung und Interpretation der thermischen Behaglichkeit durch Berechnung des PMV- und des PPD Indexes und der lokalen thermischen Behaglichkeit”.
- [2] H., Zhang. Human Thermal Sensation and Comfort in Transient and Non-Uniform Thermal. Berkley: University of California, 2003.
- [3] American Society of Heating, Refrigerating and Air-Conditioning Engineers, Chapter 8, Thermal Comfort. In *ASHRAE Handbook Fundamentals (SI Edition)* (pp. 8.1-8.26). Atlanta, USA: ASHRAE.

This project has received funding from the European Union’s Horizon 2020 research and innovation programme under grant agreement No. 769826. The content of this publication is the sole responsibility of the Consortium partners listed herein and does not necessarily represent the view of the European Commission or its services.

D4.2: ASSESSMENT REPORT FOR ENHANCED ENERGY EFFICIENCY AND COMFORT (PU)



12. Acknowledgment

European Union's Horizon 2020 research and innovation program

This project has received funding from the European Union's Horizon 2020 research and innovation program under **grant agreement No. 769826**. The content of this publication is the sole responsibility of the Consortium partners listed herein and does not necessarily represent the view of the European Commission or its services.

Project Partners:

The author(s) would like to thank the partners in the project for their valuable comments on previous drafts and for performing the review.

Participant No	Participant short name	Participant organisation name	Country
1 Coordinator	AIT	AIT Austrian Institute of Technology GmbH	Austria
2	HRE	Honda R&D Europe (Deutschland) GmbH	Germany
3	AVL	AVL List GmbH	Austria
4	QPD	AVL Thermal & HVAC	Germany
5	VEN	VENTREX Automotive GmbH	Austria
6	UOZ	University of Zagreb	Croatia
7	IFAM	Fraunhofer Institute for Manufacturing Technologies and Advanced Materials IFAM	Germany
8	ATT	ATT advanced thermal technologies GmbH	Austria
9	ECON	eCon Engineering Kft.	Hungary
10	RUB	RUBITHERM Technologies GmbH	Germany
11	STS	SeatTec Sitztechnik GmbH	Germany
12	OBR	OBRIST Engineering GmbH	Austria
13	JRC	Joint Research Centre - European Commission	Italy

This project has received funding from the European Union's Horizon 2020 research and innovation programme under grant agreement No. 769826. The content of this publication is the sole responsibility of the Consortium partners listed herein and does not necessarily represent the view of the European Commission or its services.
